Aalto University
School of Chemical
Technology

CHEM-E1150

BIOMASS PRETREATMENT AND FRACTIONATION

CELLULOSE CHEMISTRY

Herbert Sixta, 2018

Sources of Cellulose

Plants

- Trees
- grasses

Naturally synthesized cellulose

- Heterotrophic bacteria, such as *Gluconacetobacter xylinus* -> bacteria cellulose
- Slime molds, such as *Physarum polycephalum*
- Group of animals, the *tunicates, e.g. Halocynthia roretzi*
- *Valonia ventricosa*, also known as "bubble algae" and "sailors' eyeballs

Wood hierarchical structure

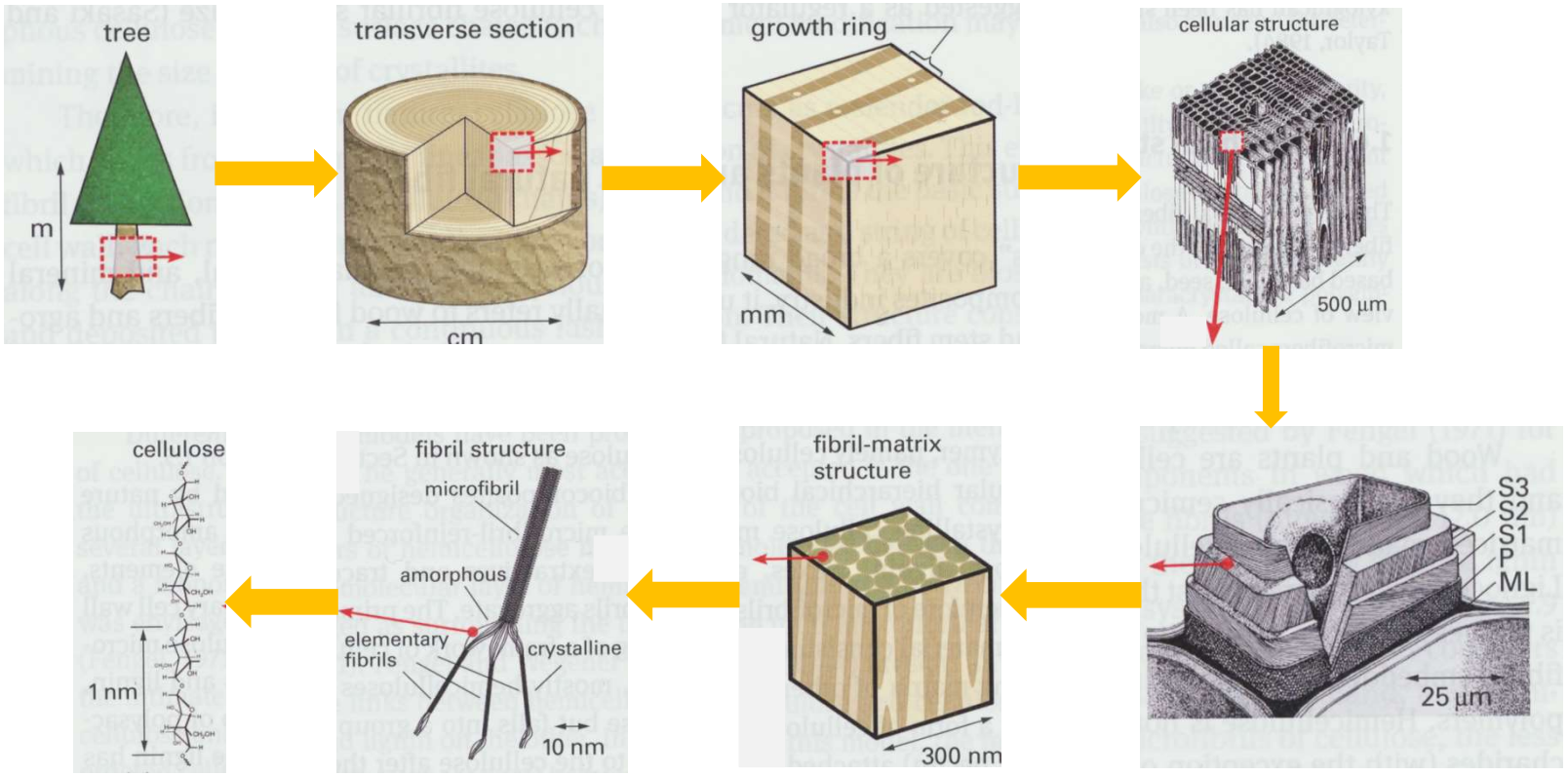

Cellulose Microfibril

- Diameter: 3–4 nm (wood)
- Aggregates: 15 nm (wood)

Individual fibre

- Diameter: 10–30 µm
- Length: 1–4 mm

Dufresne, Alain. Nanocellulose. De Gryter, **2012**

Cellulose Molecule

- Conformation
- Chain length, molecular weight
- H-bonding

Cellulose – molecular structure

Linear homopolymer consisting of D-anhydro-gluco-pyranose units (AHG) connected by β-(1-4)-glycosidic bonds.

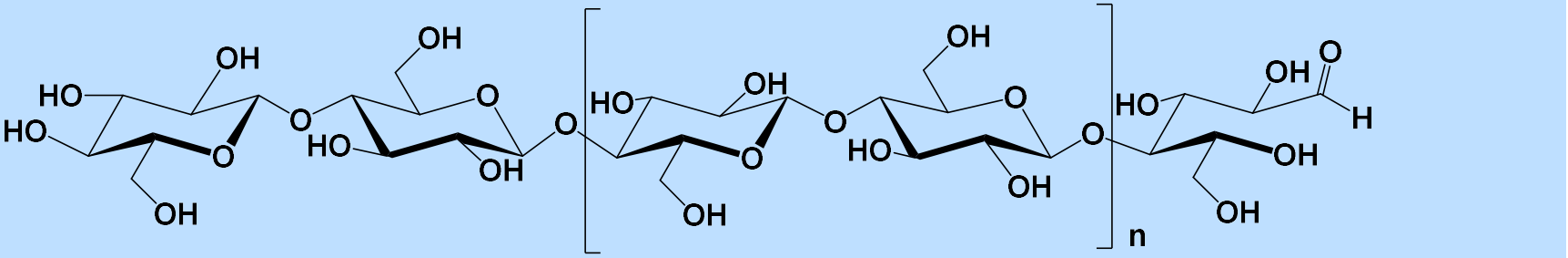

$^4C_1$ chair formation

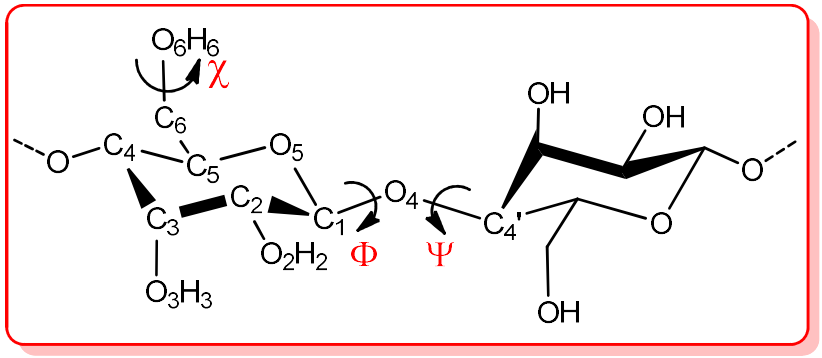

CH_2OH group conformation of C-6

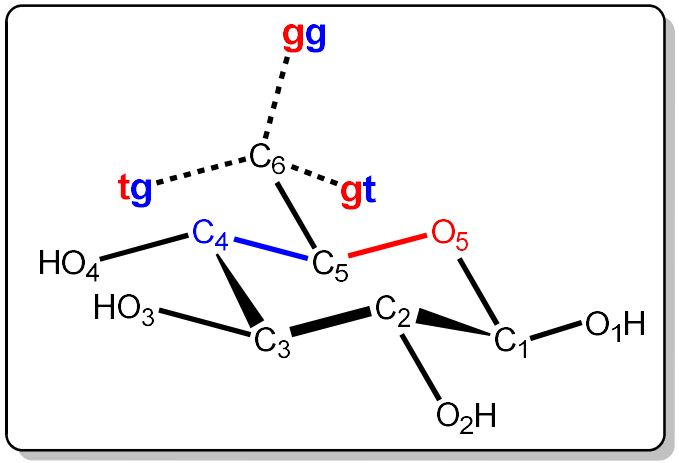

Atomistic toolkit. https://nano-hub.org/tools/ccamt

DPs of different cellulose samples

Substrate	Allomorphie	[η], mL/g	DP_w
Cotton Linters (untreated)	I	>2000	10 000-15 000
Cotton Linters Kier-boiled, bleached	I	2000	7 500
SW-Sulfite ether pulp HV	I	1700	6 000
SW-Sulfite ether pulp MV	I	1200	3 800
Birch Kraft-paper	I	1000	3 000
PHK acetate pulp	I	800	2 250
Sulfite viscosep	I	570	1 450
PHK viscose pulp	I	450	1 050
Lyocell fiber	II	400	950
Modal fiber	II	280	670
Regular viscose fiber	II	190	450

Mark-Houwink: $[\eta] = Q' DP^a$

Gruber and Gruber (1981), SCAN-CM 15:88:

Q' = 0.42, a = 1: DP<950

Q' = 2.28, a=0,76: DP > 950

Molar Mass Distribution

Dissolving Pulps

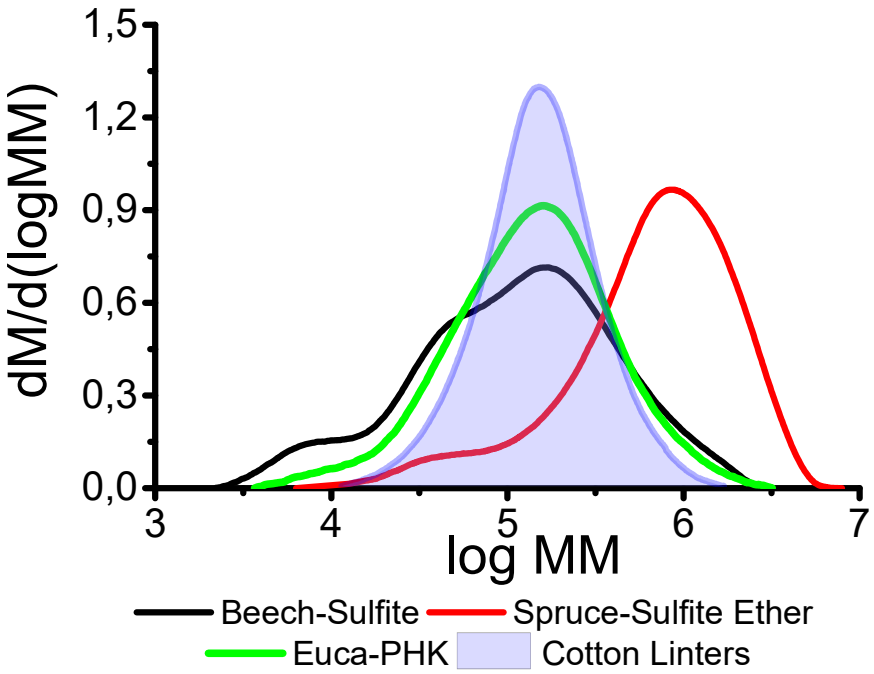

Pulps	DPw GPC	PDI	DP<100 wt%	DP>2000 wt%
HW-PHK	1400	3.0	2.5	20.0
HW-S	1790	6.5	9.0	26.8
SW-S (ether)	4750	10.6	0.5	61.0
CL	**1250**	**1.8**	**0.3**	**15.5**

Paper Pulps

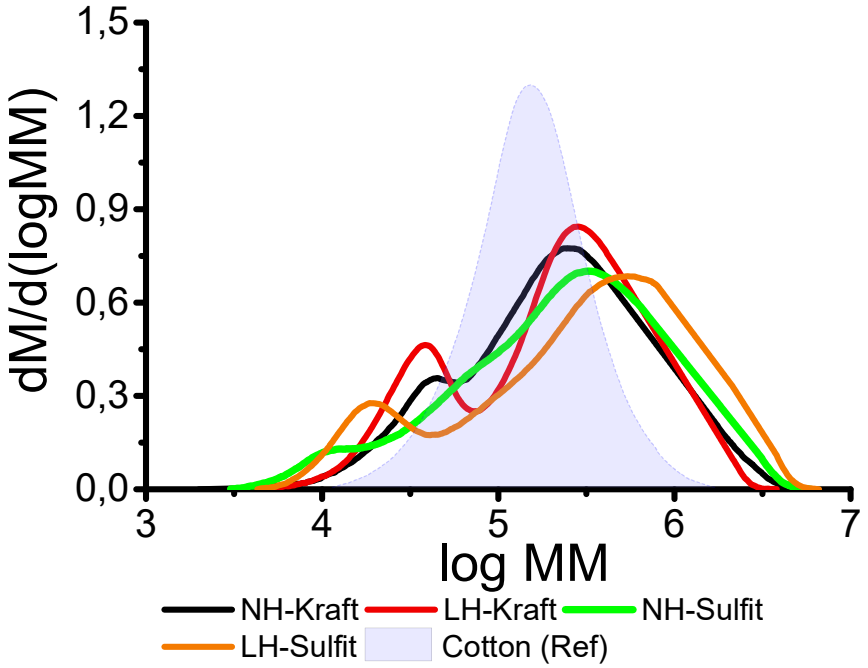

Pulps	DPw GPC	PDI	DP<120 wt%	DP>2000 wt%
NH-K	2825	4.3	3.5	38.7
LH-K	2850	4.6	3.0	40.5
NH-S	3150	6.2	6.3	44.0
LH-S	4050	7.8	7.4	53.4

Molar Mass Distribution

The higher the **amount of short chains, DP < 100**, the lower is the strength potential of viscose fibers.

Viscose fibers made under constant conditions from different pulps:

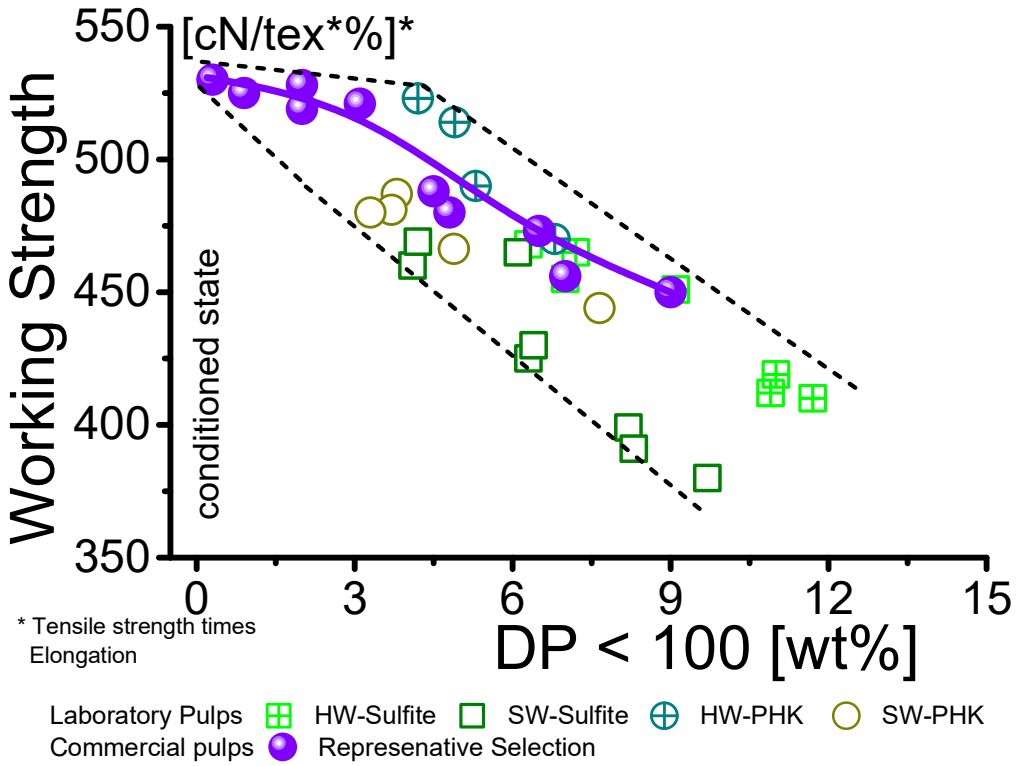

H. Sixta et al., *Handbook of Pulp*, 2006

Cooperative networks of H-bonds in Cellulose Iβ

H-bonding system represented by two exclusive H-bonding schemes A and B

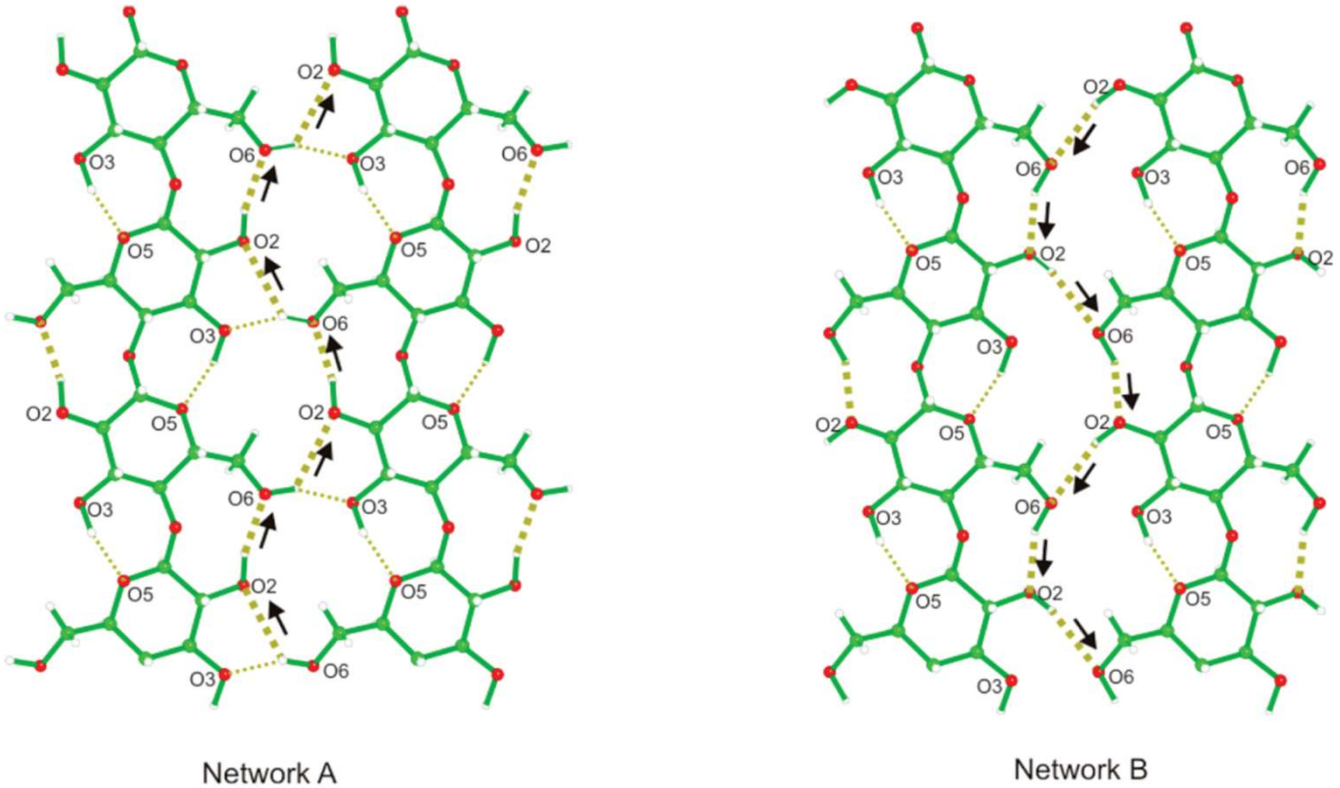

Within the Hydrogen-bonded planes $(110)_t$ and $(200)_m$
Arrows show the donor-acceptor-donor directions

Nishiyama, Y., et al., Biomacromolecules, 2008. **9:** p. 3133-3140.

Cellulose Structure

- Crystal Structure
- Fibrillar Structure
- Morphological Structure
- Pore structure and inner Surface

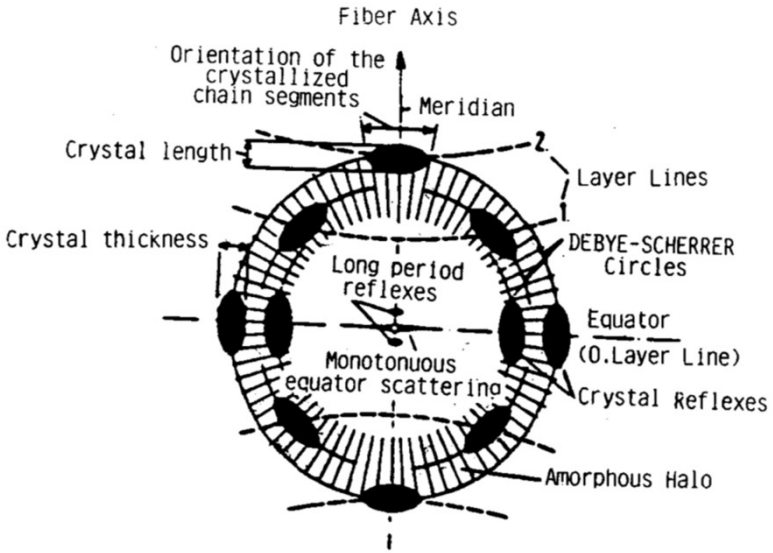

X-ray diffractogram, *Krässig 1993*

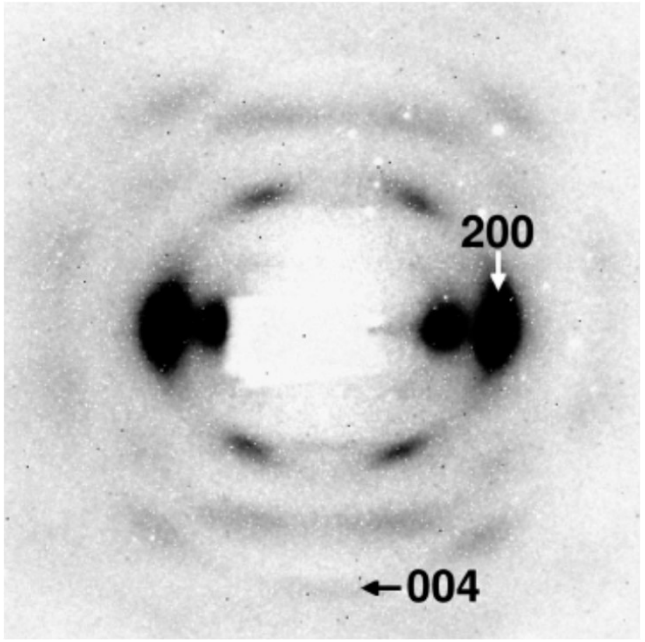

Cellulose I (flax)

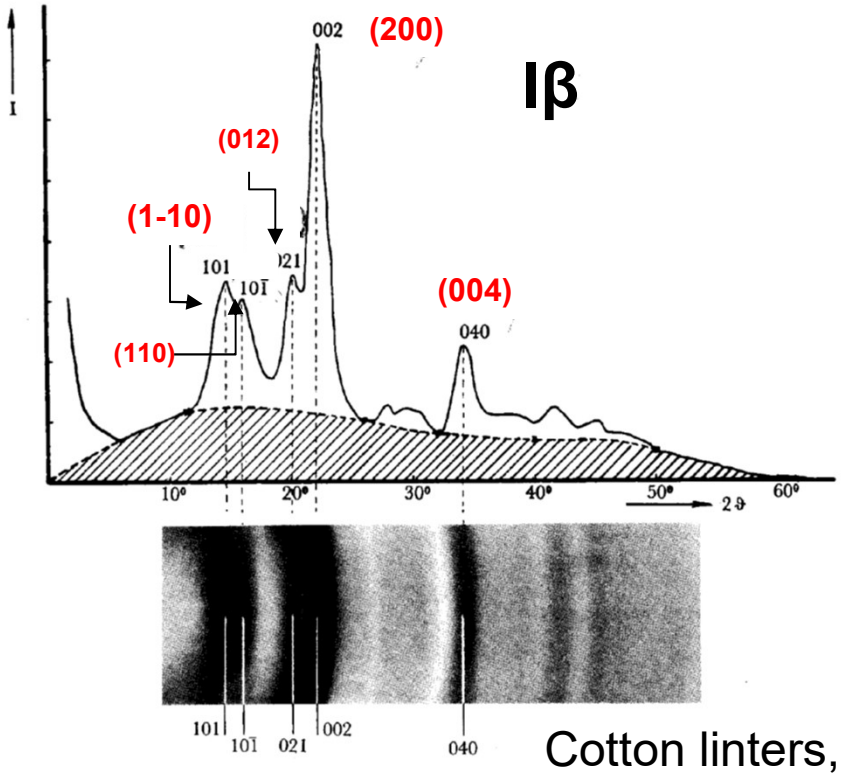

Cotton linters, Temming, p160

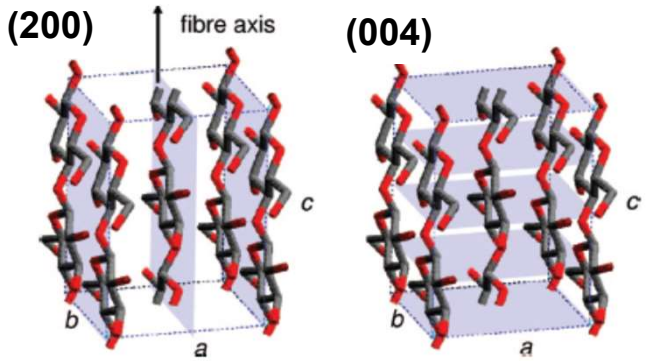

Diddens, I., et al., Macromolecules 2008: **41** p. 9755-9759.

Cellulose polymorphs

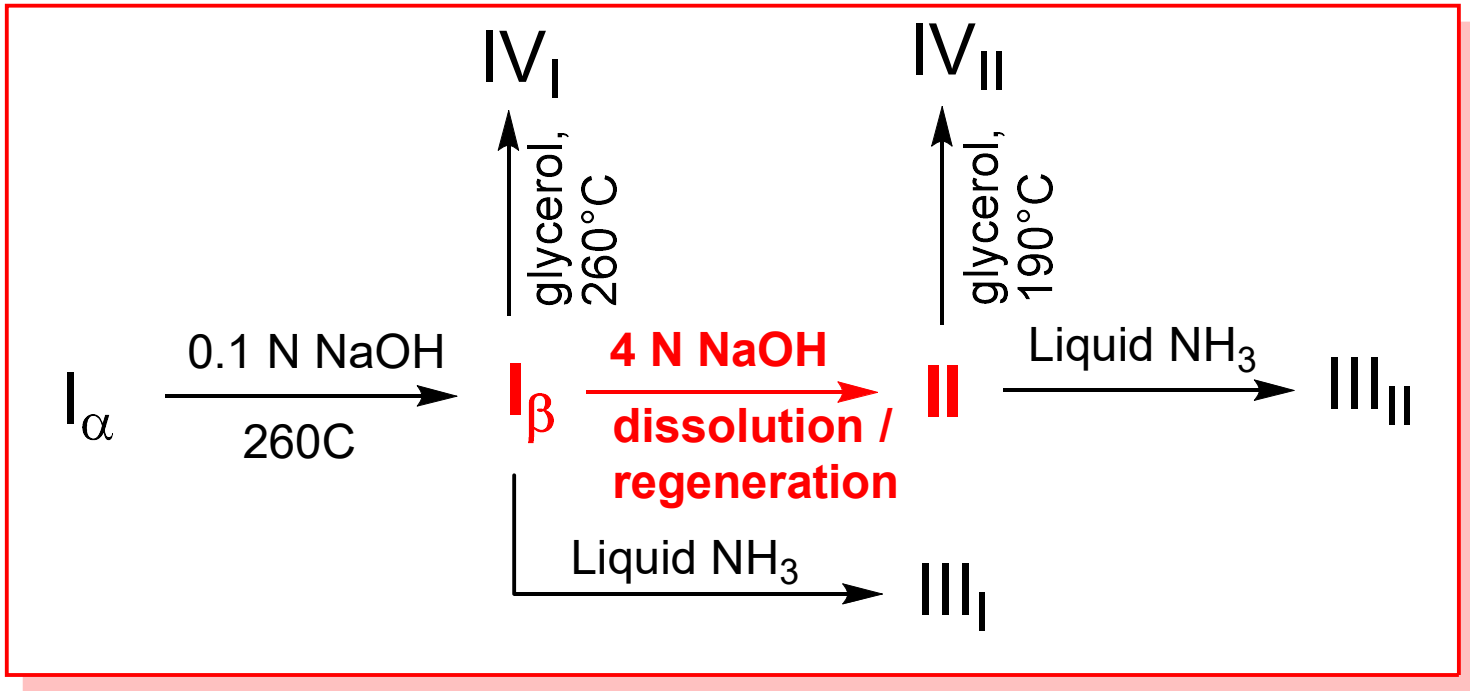

Kono, H., et al., Macromolecules, 2004. **37** p. 5310-5316.

- Cellulose I: naturally produced:
  - **Iα allomorph**, higher plants (tunicates) mostly the
  - **Iβ allomorph**. Thermodynamically metastable
- Cellulose II: stable structure from dissolution/regeneration and mercerization.
- Cellulose III: formed through liquid ammonia treatment
- Cellulose IV: formed through thermal treatment

Unit Cell - Coordinate System

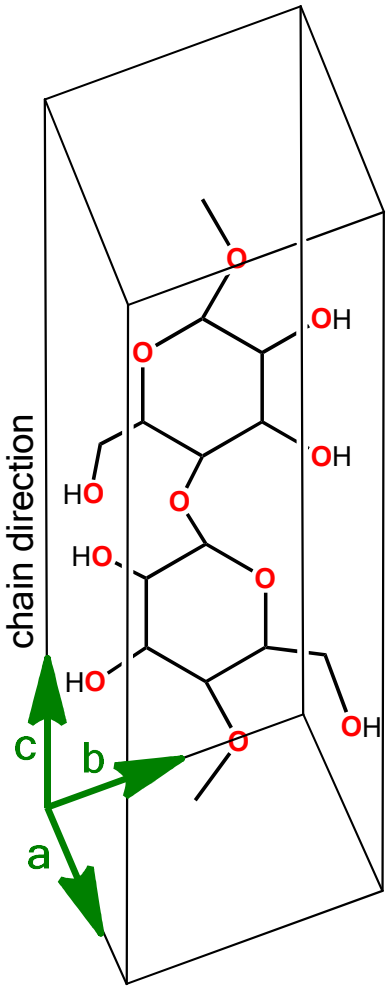

- **Simplest repeating unit in a crystal**, charcterized by
- Vectors: a, b and c form the edges of a parallelepiped
- Angles: α (b/c), β (a/c), **ɣ (a/b)**
- **Convention:**
  c cellulose chain axis;
  b forms the plane with c;
  a forms the distance between the sheets
- Monoclinic: a≠b≠c, α=β=90° ≠ɣ
- Triclinic: a≠b≠c, α≠β≠ɣ

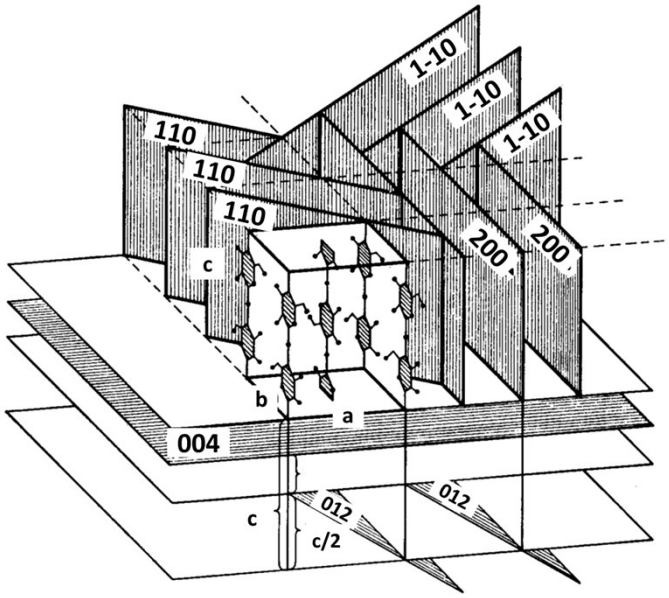

Temming Linters (1973), p 161 revised

Cellulose (2013), 20: 20703-2718. DOI 10.1007/s10570-013-0071-8

Cellulose polymorphs

Polymorph	space group	chains / unit cell	Chain direction	a [Å]	b [Å]	c [Å]	α [°]	β [°]	γ [°]
Iα	triclinic, P1	1	parallel	6.72	5.96	10.40	118.1	114.8	80.4
Iβ	**Monoclinic, 2P1**	**2**	**parallel**	**7.78**	**8.20**	**10.38**	**90.0**	**90.0**	**96.5**
II	**Monoclinic, 2P1**	**2**	**antiparallel**	**8.10**	**9.08**	**10.36**	**90.0**	**90.0**	**117.3**
III_I	Monoclinic, 2P1	1	parallel	4.48	7.85	10.31	90.0	90.0	105.1
IV_I	Triclinic, P1	2	parallel	8.03	8.13	10.4	90.0	90.0	90.0

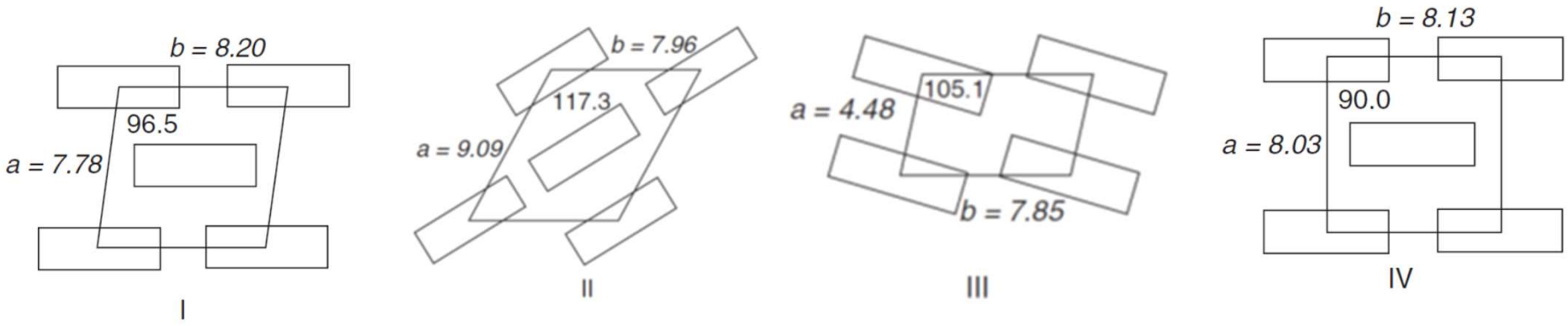

Seong H. Kim et al. *Korean J.Chem.Eng*. (2013), 30(12), 2127-2141
Nishiyama, Y., et al., J. Am. Chem. Soc., 2003. **125** p. 14300-14306.
Nishiyama, Y., P. Langan, and H. Chanzy, J. Am. Chem. Soc., 2002. **124** p. 9074-9082.

Kobayashi, K., et al., Carbohydr. Polym., 2011. **86** (p. 975-981
Bellesia, G., et al., J. Phys. Chem. B, 2012. **116** p. 8031-8037

NMR assignments

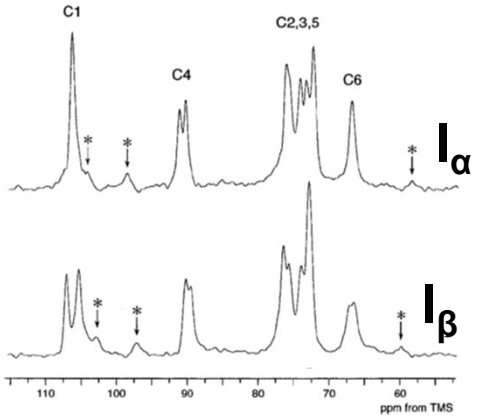

Kono, H., et al., *J. Am. Chem. Soc.*, 2002. **124:** p. 7506-7511.

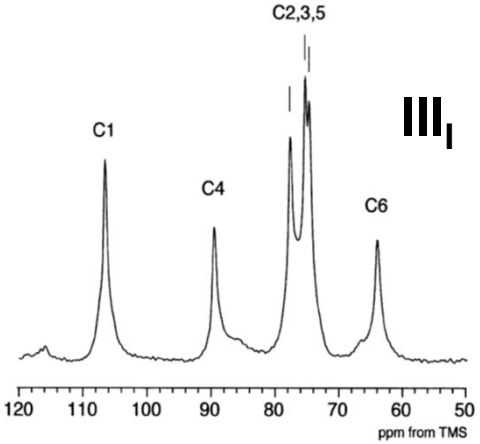

Kono, H., T. Erata, and M. Takai, *Macromolecules*, 2003. **36** : p. 3589-3592.

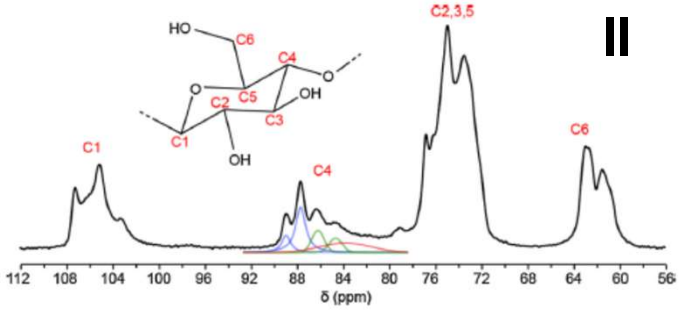

Idstroem, A., et al., *Carbohydr. Polym.*, 2016. **151**: p. 480-487.

Polymorph	^{13}C chemical shifts, ppm C1		C4		C6		Source	Comment
Cellulose Iα	106.9		91.6	90.8	67.1		Kono,H. JACS (2002)	Cladophora sp.
	104.9		89.5					
Cellulose Iβ	**107.6**	**105.9**	**90.6**	**90.0**	**67.5**	**66.9**		Tunicate
	105.6	**103.9**	**88.7 (β+α)**	**88.4 (pc)**			P.T. Larsson et al.	Cotton cellulose
			87.9	**84.9 (am)**			Carboh Res 302 (1997), 19-15	Cotton cellulose
			84.1 (surf)	**83.2 (surf)**				Cotton cellulose
Cellulose II	**107.2**	**105.1**	**87.7**	**88.9**	**62.5**	**63.2**	Idström, I. Carbohydr Polym (2016)	Regeneration of 13C enriched
	106.4	**103.3**	**86.2**	**84.8**	**61.7**	**61.3**	Idström, I. Carbohydr Polym (2016)	bacterial cellulose (EMIMOAc)
Cellulose III_I	106.6		89.6		64.0		Kono, H. Macromolecules (2003)	Ethylenediamine of Cell I
Cellulose IV_I	*105.6*		*84.4*	*83.6*	*63.3*	*63.8*	*Isogai, Macromolecules (1989)*	
Cellulose IV_{II}	*105.5*		*84.6*	*83.5*	*63.7*		*Isogai, Macromolecules (1989)*	
Amorph	104.6		75.8		61.4		Idström, I. Carbohydr Polym (2016)	
	105		84		63		Isogai, Macromolecules (1989)	

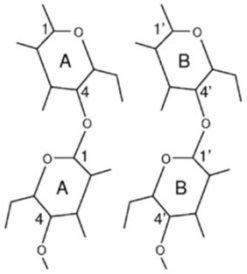

Independent chains (-A-A- and –B-B-

Kono, H. *Polymer* (2004)

Transition Cell I⟶ Cell II

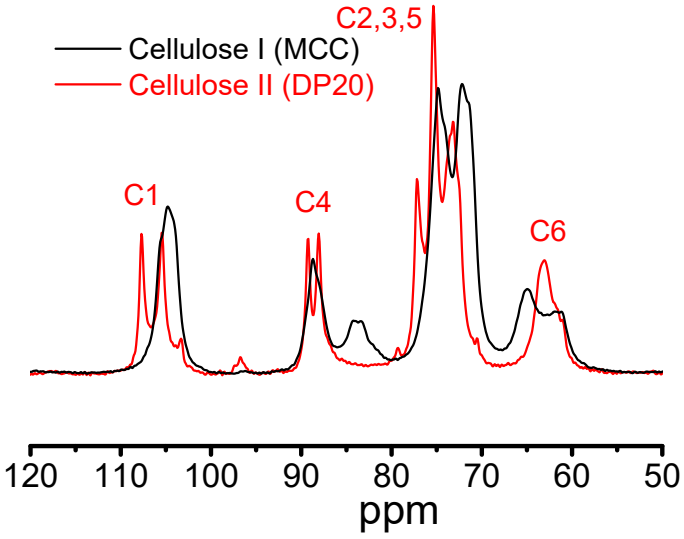

Tolonen, L.; Sixta, H. (2013)

X-ray diffraction

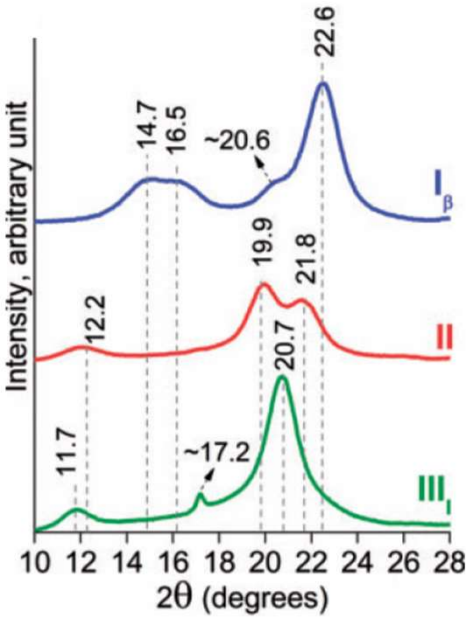

Kafle, K., et al., Text. Res. J., 2014. **84** p. 1692-1699, 8 pp.

Polymorph	Diffraction angle, 2θ, lattice planes (h,k,l) 100	010	*002*	110		Source
Cellulose Iα	14.2	16.9	*21,05*	22.6		Cellulose (2014) 21:885-896
	1-10 (eq)	**110 (eq)**	**102 (eq)**	**200 (eq)**	**004 (mer)**	
Cellulose Iβ	**14.8**	**16.3**	**20.6**	**22.4**	**34.4**	Cellulose (2014) 21:885-896
Polymorph	**1-10 (eq)**	**110 (eq)**	**020 (eq)**	**004 (mer)**		
Cellulose II	**12.2**	**19.9**	**21.8**	**~35**		Cellulose (2014) 21:885-896

Isogai, A., et al., Macromolecules, 1989. **22** p. 3168-72.
Hori, R. and M. Wada, Cellulose, 2006. **13:** p. 281-290.
French 2014

Transition Cell Iα⟶ Cell Iβ

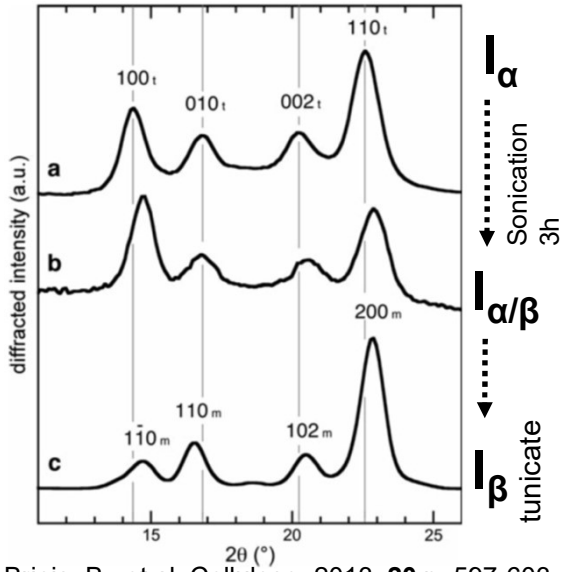

Briois, B., et al. Cellulose, 2013. **20** p. 597-603.

Transition Cell I⟶ Cell II

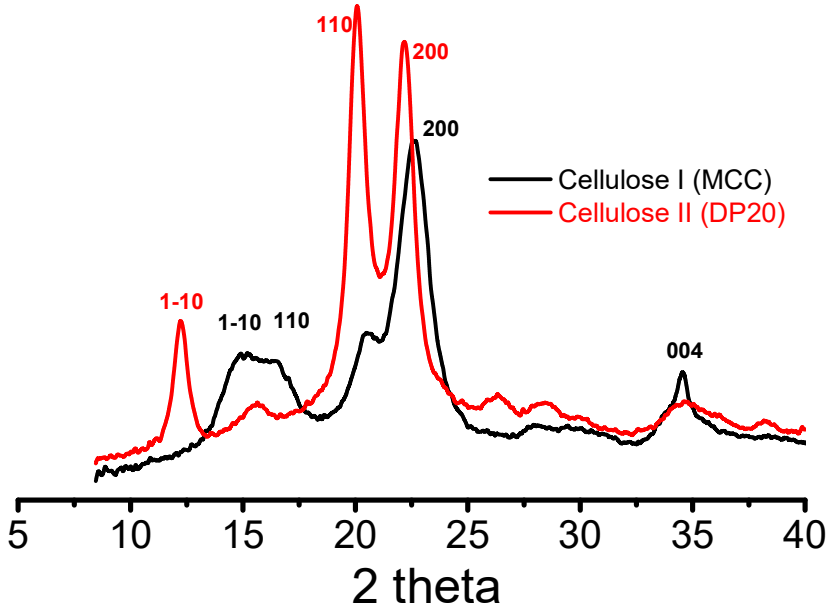

Tolonen, L. et al. Cellulose (**2013**) 20:2731–2744

Cellulose I Family

Unit cells of Cellulose Iα and Iβ

CH_2OH conformation of both crystal forms in tg conformation

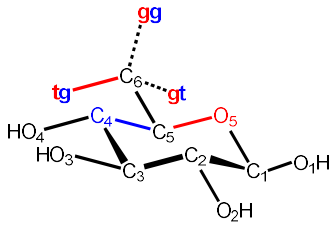

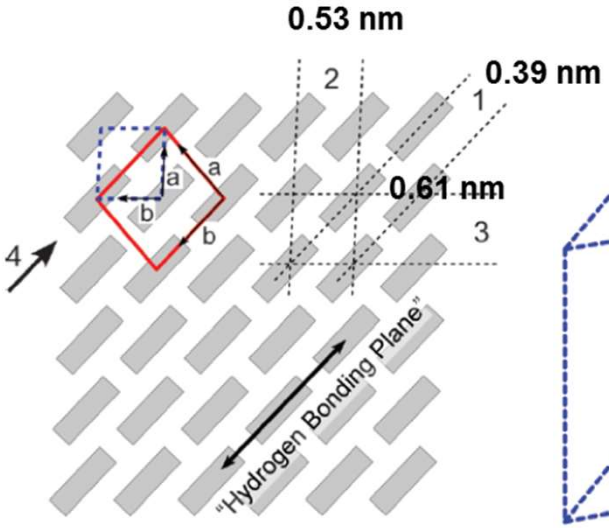

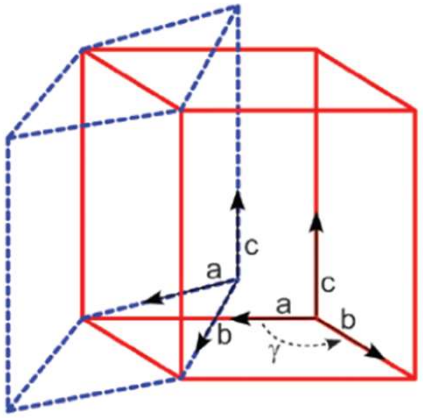

In the plane of the H-bonded sheets

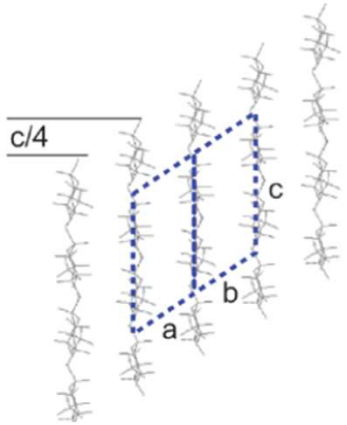

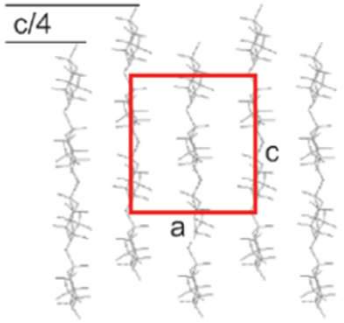

Looking down the chain axis c.
Lattice planes:
1: $(110)_t$, $(200)_m$
2: $(010)_t$, $(110)_m$
3: $(100)_t$, $(1\text{-}10)_m$

Relative configuration of Iα with respect to Iβ unit cell

Sugiyama, J., R. Vuong, and H. Chanzy. *Macromolecules*, 1991. **24**: p. 4168-75.

Displacement of the H-bonding for Iα of +c/4

Displacement of the H-bonding for Iβ alternating +c/4 and –c/4

Moon, R.J., et al., *Chem. Soc. Rev., 2011*. **40** p. 3941-3994.

Unit cell symmetry of cellulose III_I

Obtained through liquid ammonia treatment of cellulose I.
Single-chain unit cell;

All chains are parallel and O6 atom has **gt conformation** which allows 3-dim H-bond network.

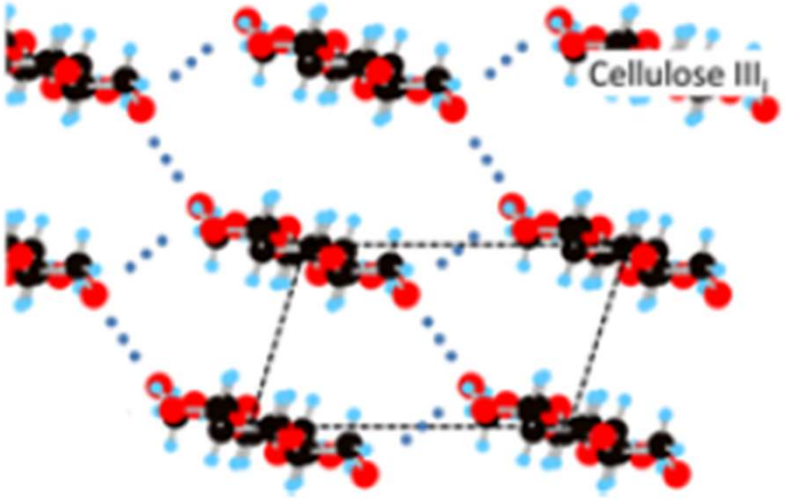

Seong H. Kim et al. *Korean J.Chem.Eng*. (2013), 30(12), 2127-2141

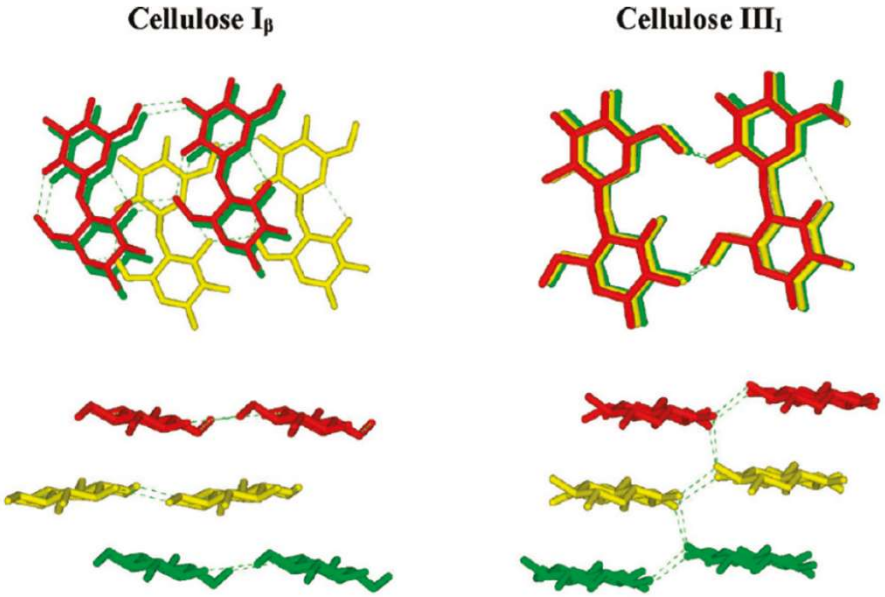

Parthasarathi, R., et al., J. Phys. Chem. A, 2011. **115** : p. 14191-14202

Cellulose II Family

Aalto University
School of Chemical
Technology

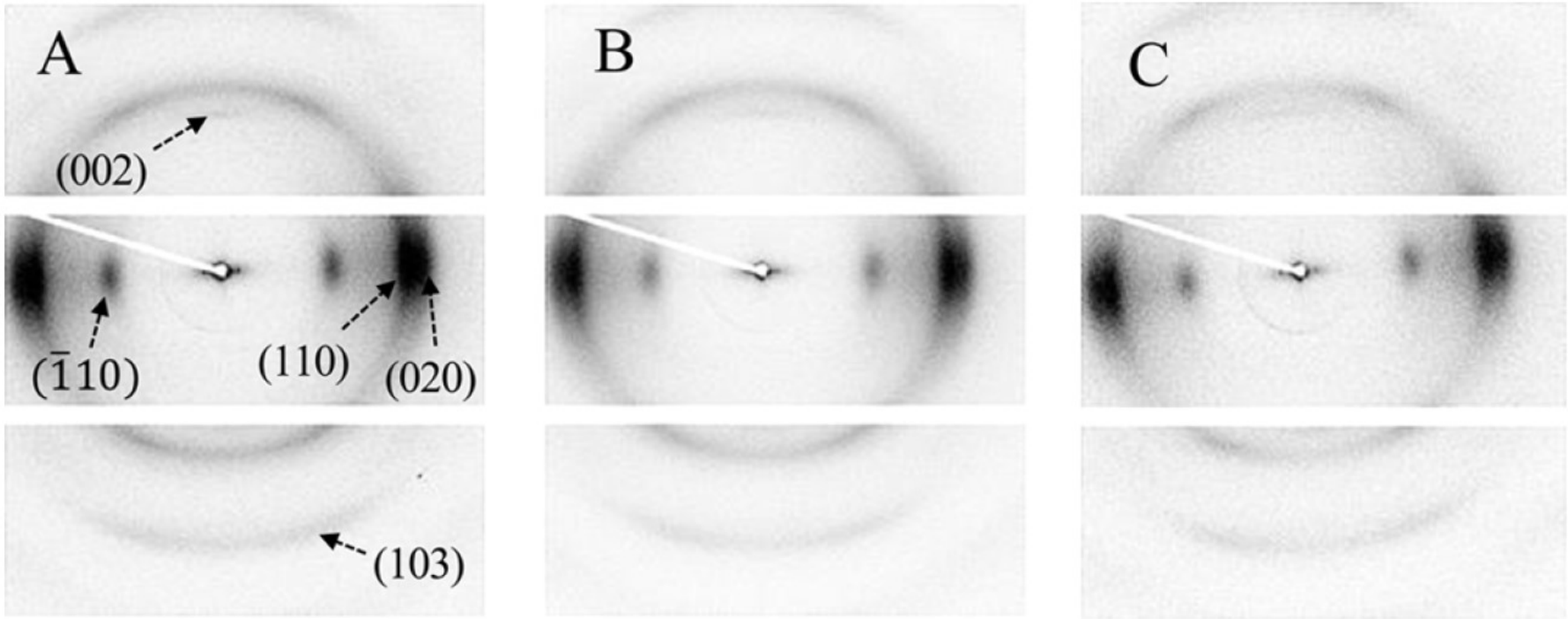

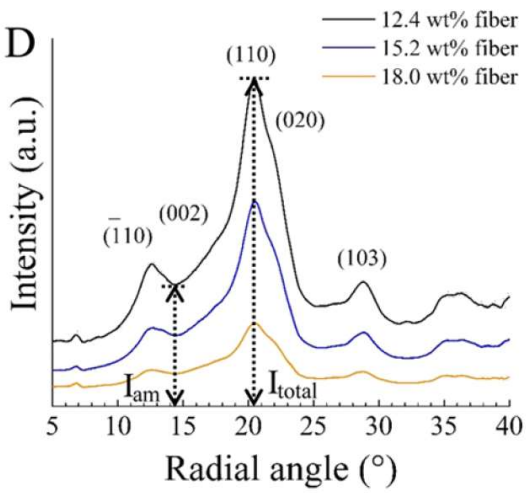

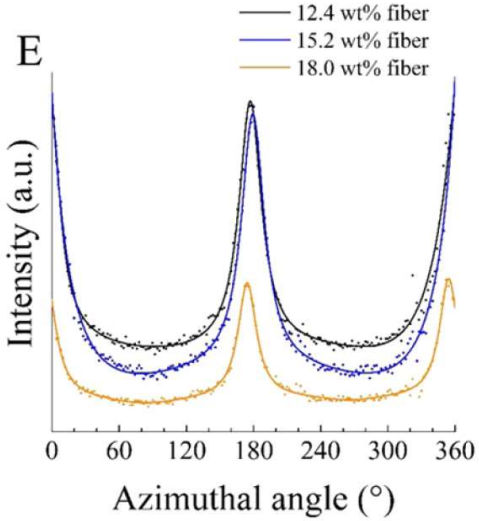

WAXS patterns (A) 12.4, (B) 15.2, and © 18.0 wt% cellulose fibers.
(D) Radial scanning data
(E) Azimutal scanning data
From the (-110) peak

Source: ACS Sustainable Chem Eng 2016, 4, 4545

Conversion of Cellulose I to II

1. **Dissolving the cellulose / regeneration (√)**
2. **Swelling in concentrated alkali (?)**

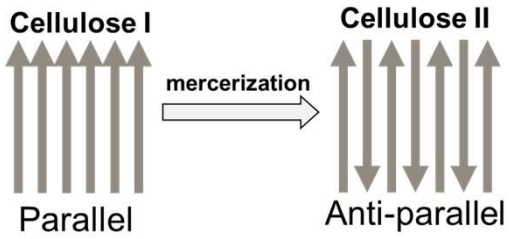

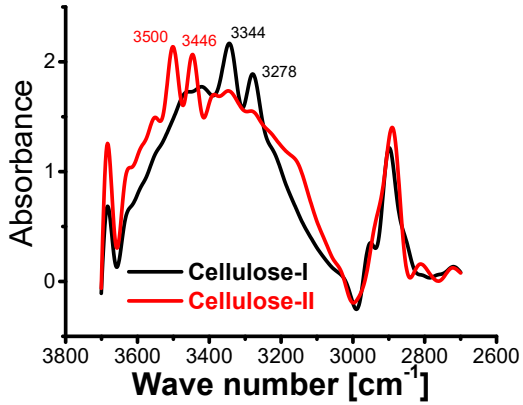

NaOH into noncrystalline region → Na-cellulose I.

Chains from the crystalline regions are *peeled-off* and added to the growing chain (re-arranging).

Washing removes alkali and converts to cellulose hydrate and after drying to Cellulose II.

Na-cellulose I formation

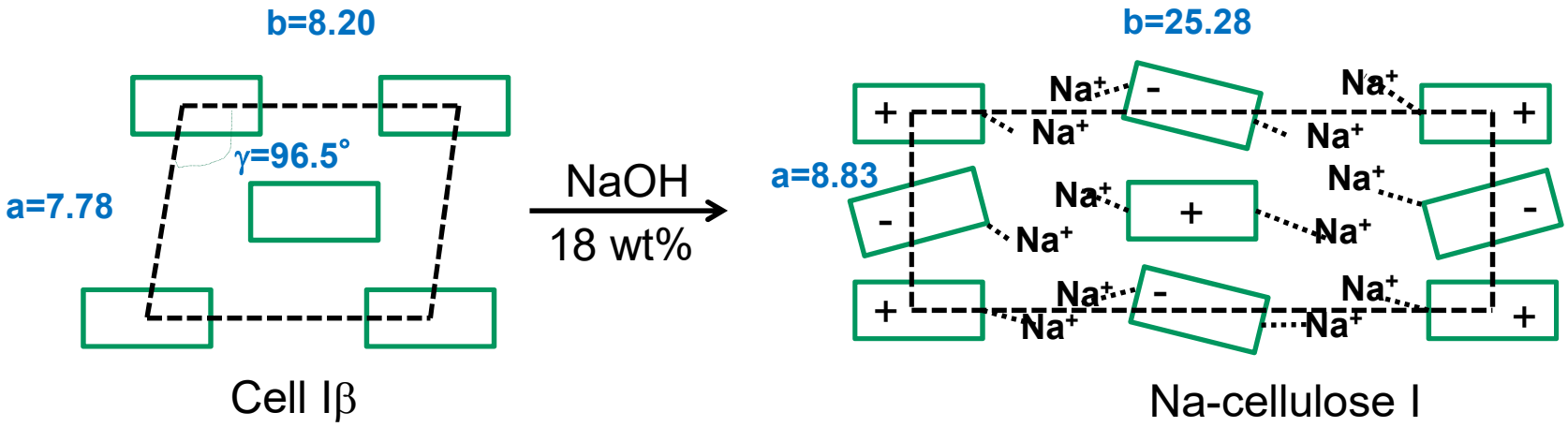

Microfibrils of Cell I are parallel-chain single crystals.

Aggregation of microfibrils into a fiber is a random process.
Equal numbers of ”up” and ”down” pointing microfibrils:

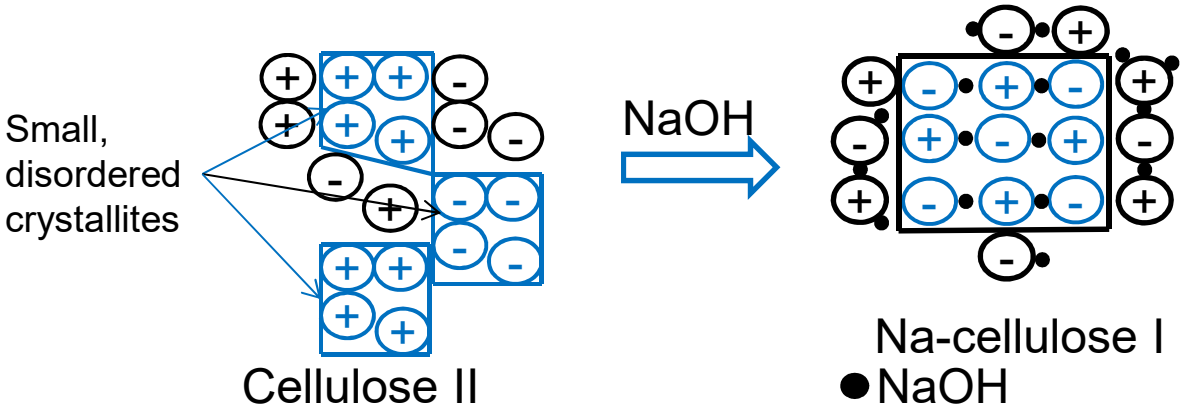

A. Sarko, H. Nishimura, T. Okano, In ACS Series 340, edited by R.H. Atalla, p169pp

Cellulose II formation

Once **all H-bonded cellulose** structure has **disappeared** a more stable threefold helical Na-cellulose IIB structure forms:

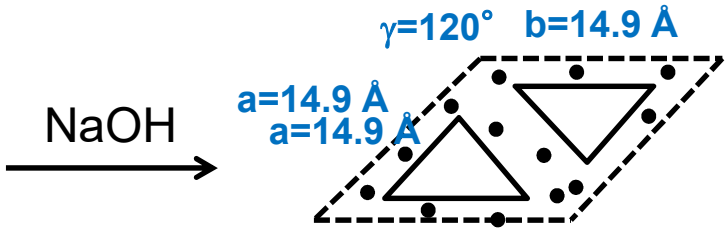

Na-cellulose IIB

Unit cell filled with NaOH and water

Removing NaOH by washing, an X-ray structure similar to that of cellulose II is obtained: two-chain, monclinic unit cell. Difference arises from **2 water molecules in the unit cell.**

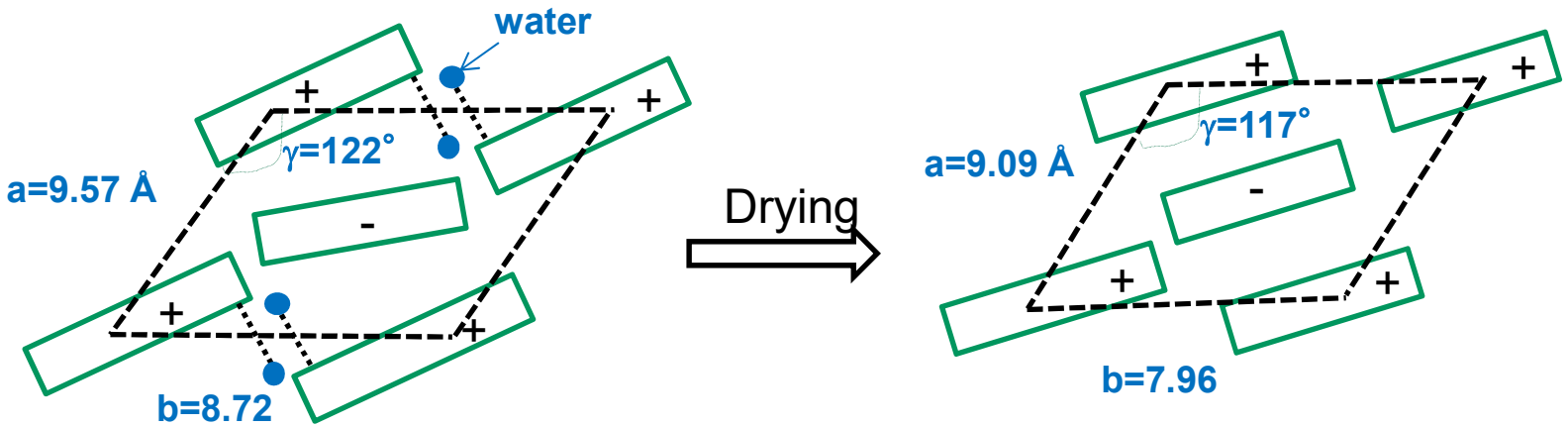

Na-cellulose IV

Cellulose II

O(3)---O(6)-intermol H-bonding Disrupted, therefore corner chain O(6) OHs is present in gt conformation

Antiparallel origin and center chains; CH2OH groups of both chains are near gt conformation. 3 dimensional H-bonds: O3-H…O5 (intra), O2-H…O6 (inter in origin sheet), O6-H..O2 (inter in center sheets) and both O6-H…O6 and O2-H…O2 in sheets containing origin and center chains.

Cellulose-I→II Transfer by Alkali Treatment

CCE treatment of *Eucalyptus Globulus* Kraft Pulp

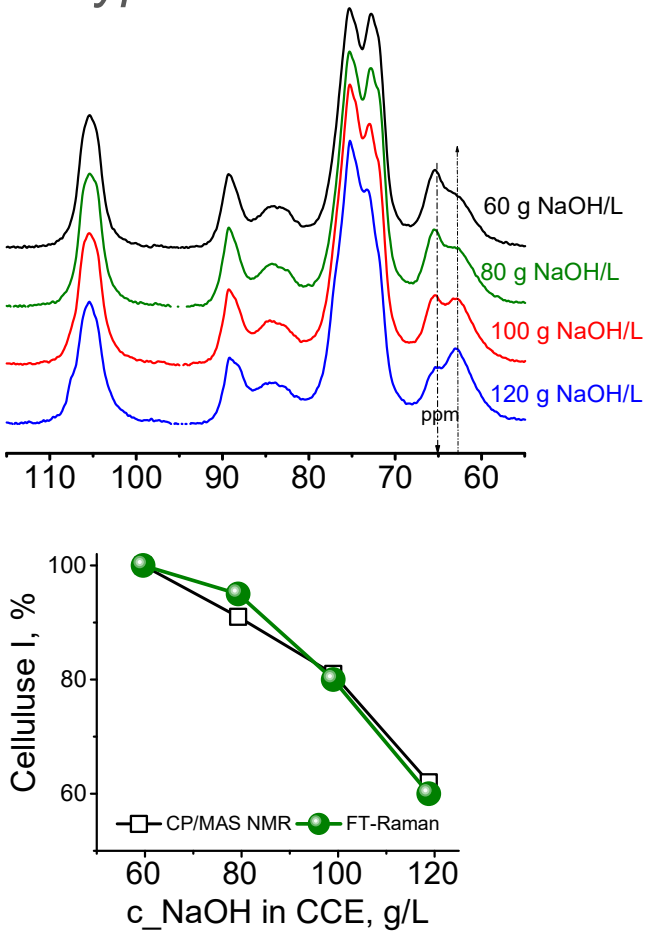

Sixta, H. unpublished (2007)

Mercerization (I) of Euca-PHK

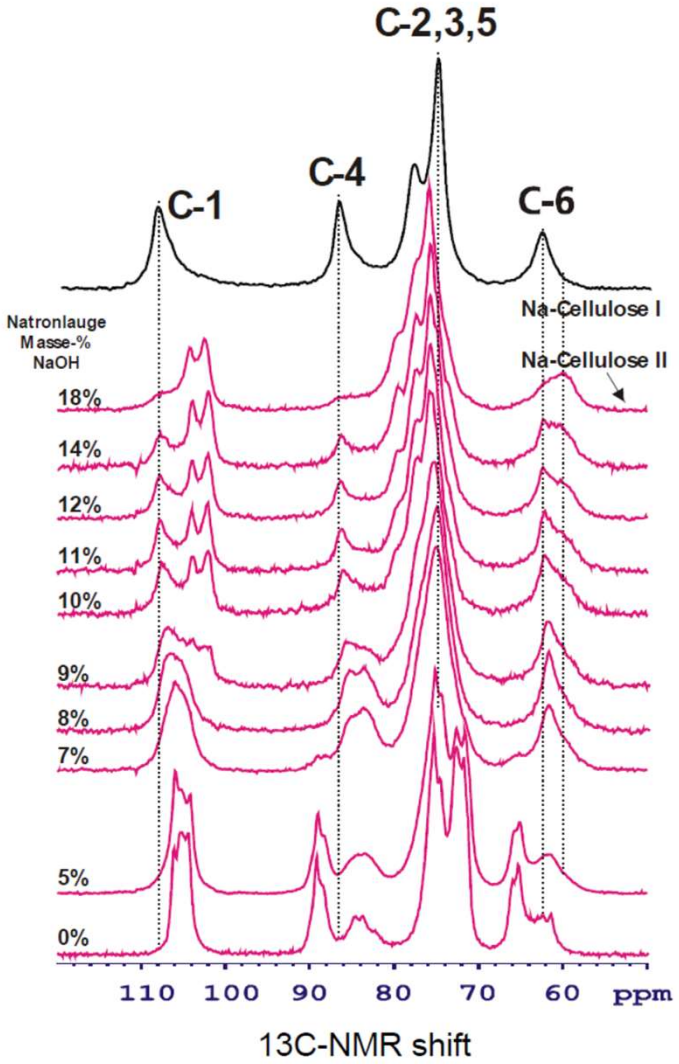

Fink, H-P.; Sixta, H. internal report (2003)

Cellulose I→II Transfer by Alkali Treatment

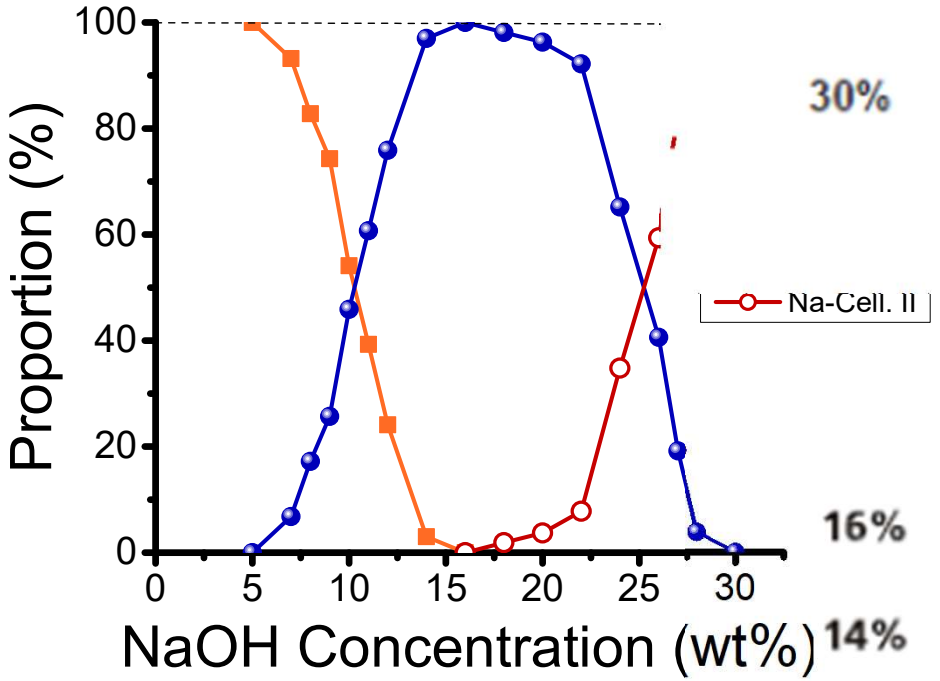

Euca-PHK pulp treated v
NaOH solutions from 9 t
At room temperature

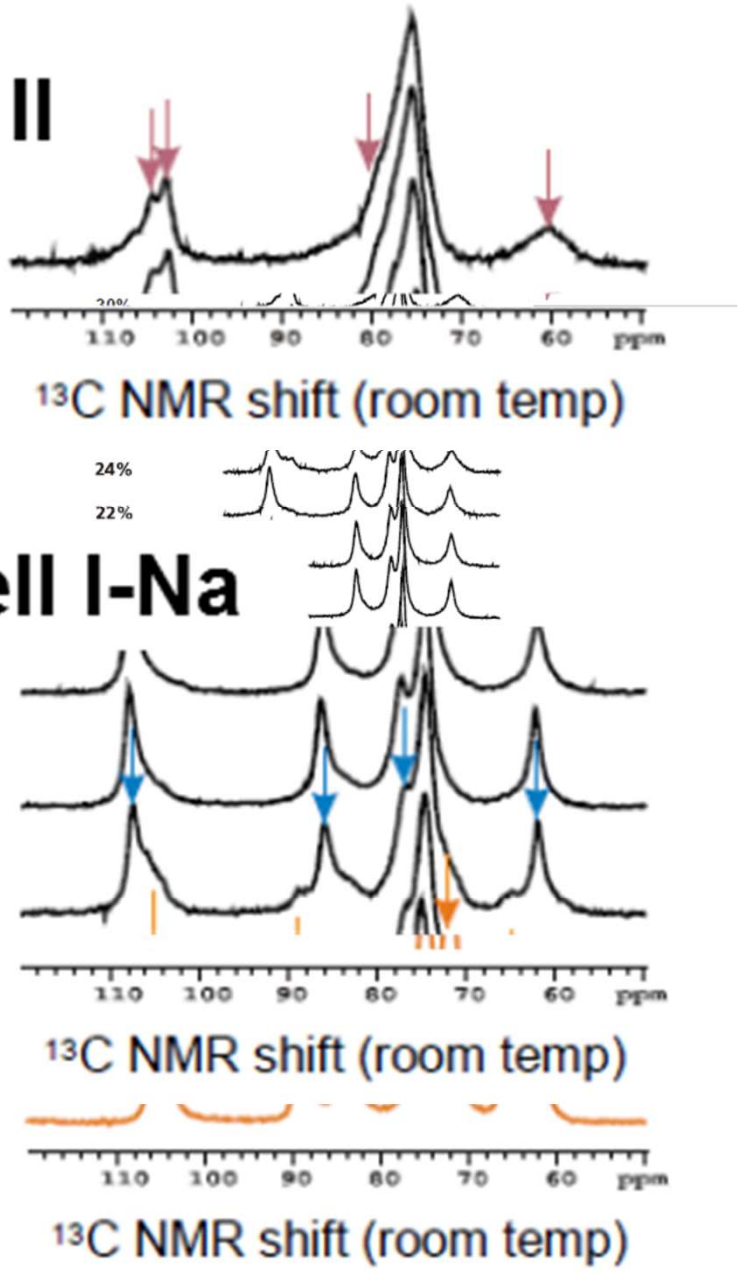

Fink, H-P.; Sixta, H. inter

Cellulose II crystal

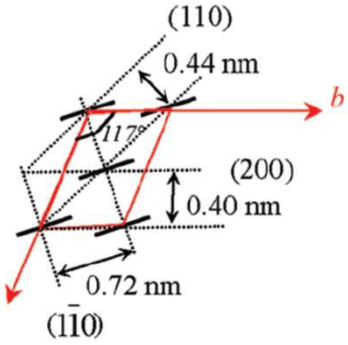

Cellulose II *d*-spacings

Sebe, G., et al., Biomacromol-ecules, 2012. **13**: p. 570-578.

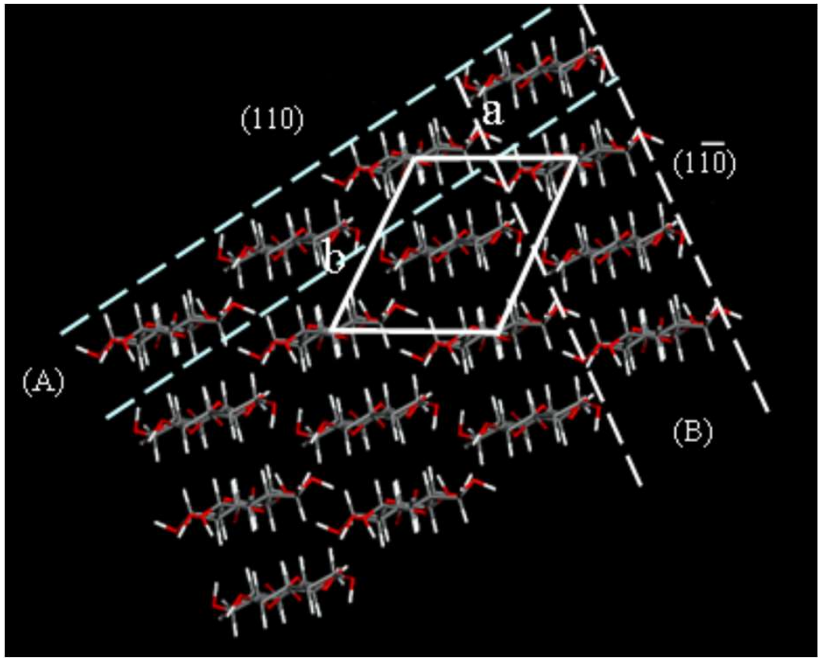

(A), hydrogen-bonded molecular sheet;

(B), van der Waals-associated molecular sheet.

(1-10) Surface hydrophilic: high density of OH groups, parallel to the film surface

(110) Surface hydrophobic

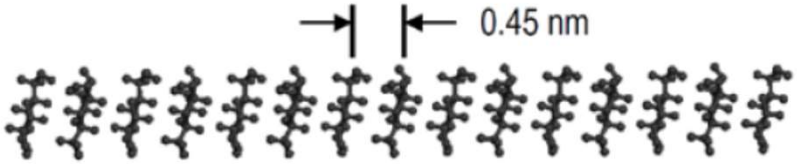

Scattering vector q of (110) reveals the spacing of 0.45 nm between hydrophobically stacked cellulose molecules in the sheet.

Cellulose II hydrate

$$\textit{Ramie fibers} \xrightarrow{5\ N\ NaOH\ ice\ water\ anhyd\ N_2H_2,2\ d,4^{\circ}C,dried} \textit{Cell - II hydrate}$$

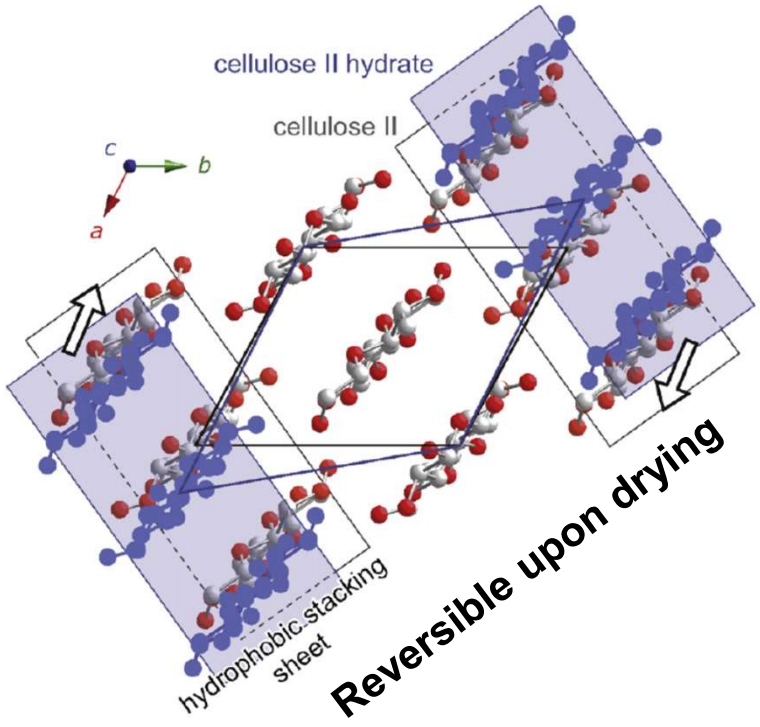

	a [Å]	b [Å]	c [Å]	γ [°]
Cell-II	8.10	9.08	10.36	117.3
Cell-II hydrate	9.68	9.95	10.35	125.8

- Unit cell volume 19% larger than that of cellulose II
- $D_{1\text{-}10}$ spacing decreased from 8.86 Å at 100% RH to 7.36 Å at 0% RH (Cellulose II), while d_{110} and d_{200} remained almost constant.
- Cellulose II hydrate released water located between the hydrophobic stacking sheets; sheets became closer to each other (a-axis).

Kobayashi, K., et al., *Carbohydr. Polym.*, 2011. **86:** p. 975-981.

Supramolecular Cellulose Structure

Micellar Structure

Nägeli, C (1928) (reprint) Oswalds Klassiker No 227

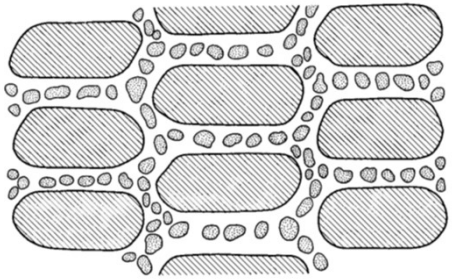

Submicroscopic crystalline particles (=micelles) embedded in undefined intermicellar substances

Extended Micellar structure

Hengstenberg, J and Mark, H.F. (1928) Z.Krist 69, 271

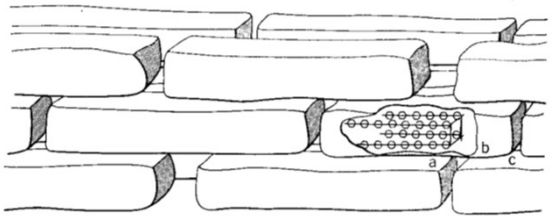

Micelle dimensions in Ramie (rayon) fiber 600 (300) Å in length and 50 (40) Å in width.

Cellulose chains of 60-120 Glucose units (?) Too short, not fiber forming (Staudinger 1932)

Fringe-micellar theory

Mark, H. Nature, 313-314

highly oriented, *elementary cells,* double reflection;

cellulose chains bundled together with a considerable degree of order (micellar structure),

complicated framework of entangled fringes.

Fringed-fibril structure

Hess, Kratky, Frey-Wyssling (1955,..)

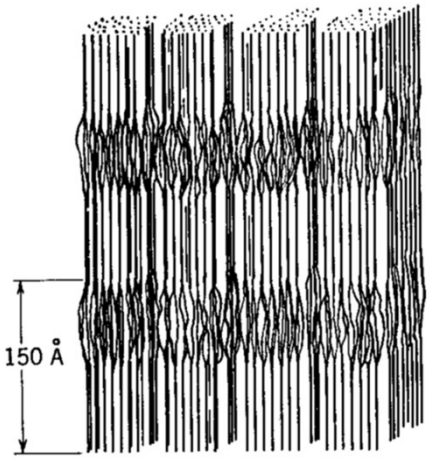

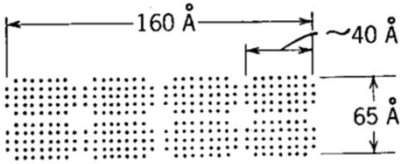

Elemental fibrils linked together in repeating units.

Crystallites held together by long molecules reaching from one crystallite to the next through less ordered regions.

Supramolecular Cellulose Structure

Two models:

- **Elementary fibril one-phase model**
  Concept of single crystal microfibrils with defects
- **Fringed-fibrillar two-phase model**
  Assembly of alternating crystalline and amorphous domains

Periodic Disorder Model - 2 Phase Model

Fringed Fibrillar

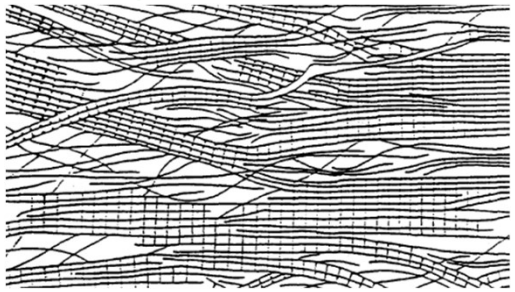

Amorphous region scattered along the microfibril

Frey-Wyssling (1954, 1965); Hearle (1958, 1963)

Fringed Micellar

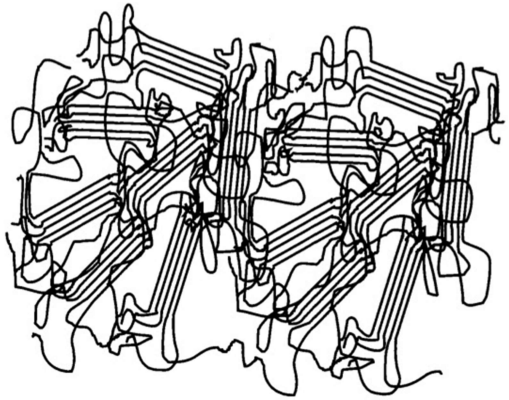

Amorphous regions aggregated in discrete regions

Hess, Kiessig (1944), Hess et al (1957)

The strongest point for the fringed micellar model is its well defined explanation of acid hydrolysis and LODP

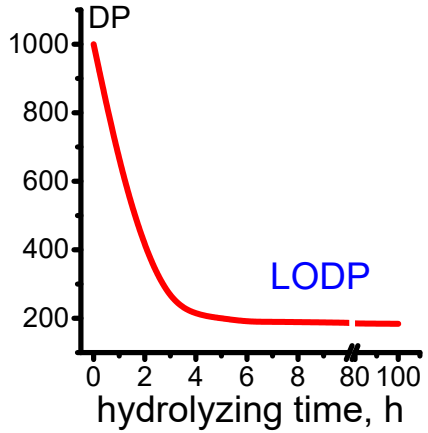

Scallan, A.M. *Textile Res J*. 1971, 41, 647

SANS

Difference diagram
D-ramie-3xH-ramie

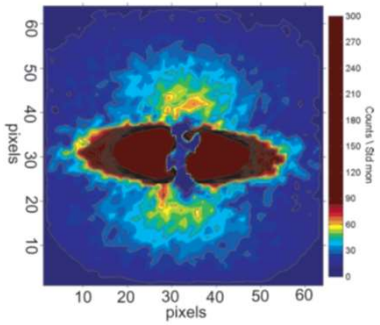

Meridional Bragg reflection of ramie fiber, indicating a periodicity of 150 nm

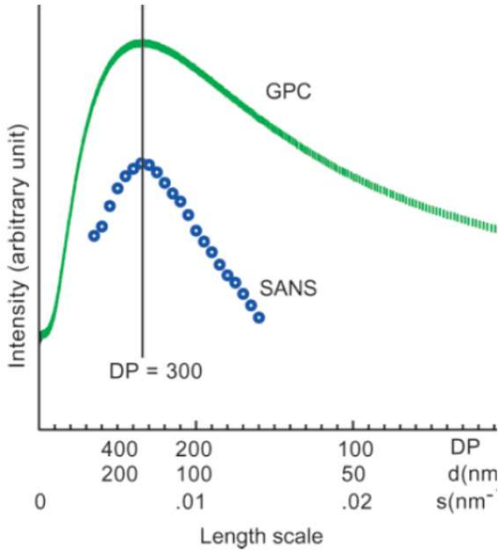

- **GPC of LODP matched exactly the periodicity observed by SANS.**
- **This supports a two-phase model comprising 5 disordered residues every 300 residues (matches with the observed yield loss of 1.5%)**

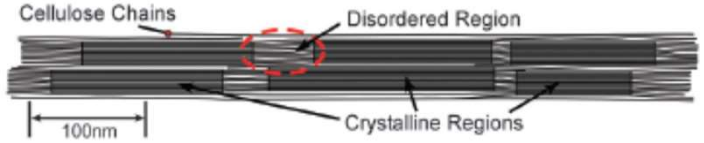

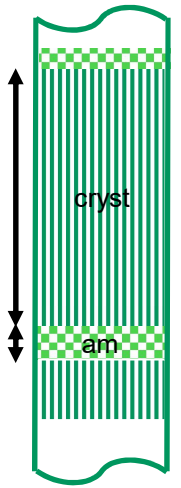

Nishiyama, Y., et al., Biomacromolecules, 2003. **4** p. 1013-7.

Moon, R.J., et al.,. *Chem. Soc. Rev*., 2011. **40:** p. 3941-3994.

Elementary Fibril 1-Phase Model

- Single crystal microfibrils.
- Amorphous contributions are considered to be lattice imperfections.
- Disordered surface structure

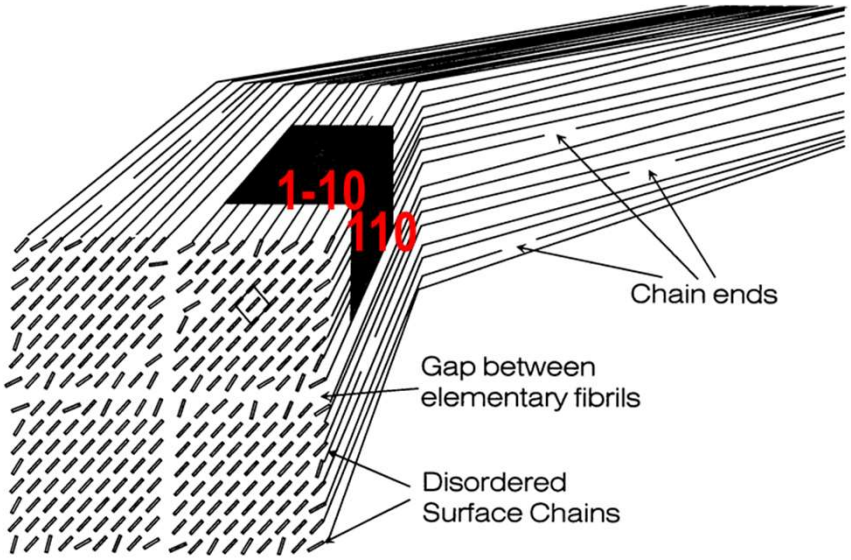

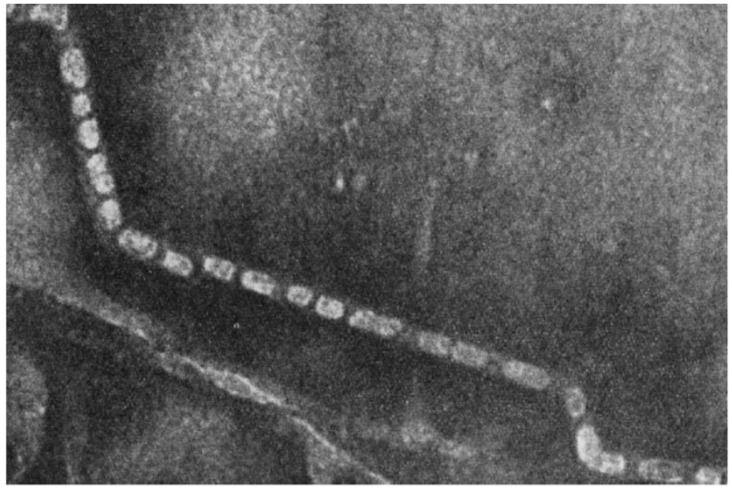

- *Valonia* microfibril has a bent shape
- With the ribbon wound as a helix the molecular chain becomes parallel to the fibril axis

Mühlethaler, 1960; Blackwell, 1976

Manley, R.S., *Nature*, 1964. **204**: p. 1155-1157.

Cellulose crystal with dimensions

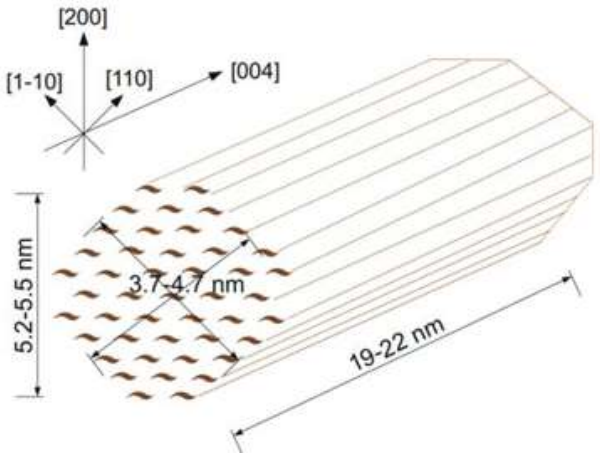

Rämänen, P. et al. *Cellulose* (2012) 19:901–912

Cross-sectional crystallite dimensions corresponding to the (1-10) and (110) lattice planes are typically both between 3.7 and 4.7 nm.

The crystal lengths, using the 004 reflection, are between 19-22 nm.

36-glucan-chain microfibril in primary cell wall (by AFM)

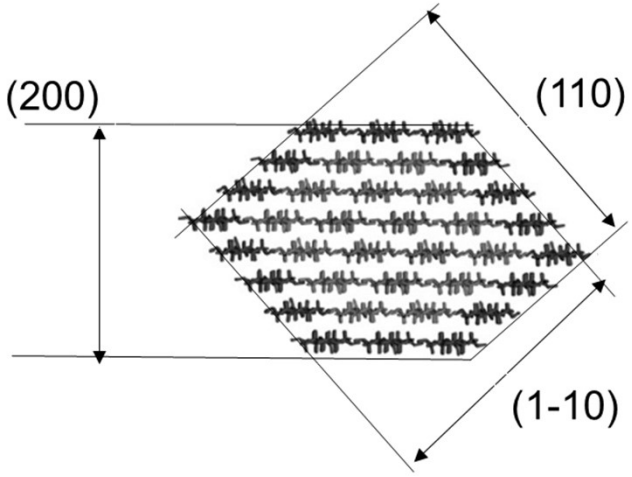

Marriott, P.E., et al., *New Phytol*, 2016. **209:** p. 1366-81.
Ding, S.-Y. and M.E. Himmel,. *J. Agric. Food Chem.*, 2006. **54**: p. 597-606.

Spruce cellulose microfibril shows a rectangular cross-section of 24 chain 3.2x3.1 nm: $(\frac{3.15^2\pi}{4}/0.317) \approx 24)$

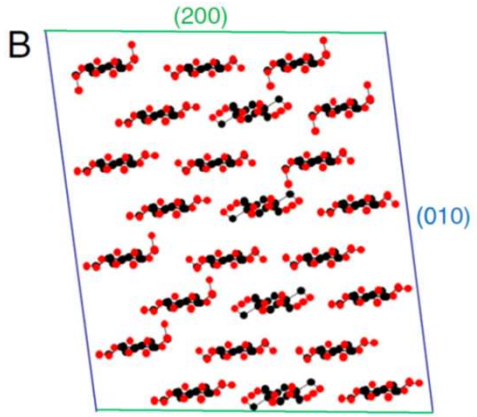

Fernandes, A.N., et al., *Proc. Natl. Acad. Sci. U. S. A.*, 2011. **108** p. 18863.

Structural characterization methods

Structures	Information	XRD	SAXS	SANS	Comment
Crystallinity		X			Peak height; peak deconvolution; amorphous substraction
Microfibrils	Diameter		X	X	Fitting the SAXS / SANS data to form factors of long cylinders; Guinier law: $I(q) \propto Exp(-\frac{{R_g}^2}{3} q^{-2})$
	Crystallite length	X		X	Peak width of 004 reflections in XRD; Bragg equation in SANS
	Crystallite Width	X			Peak width of reflections 110, 1-10, 220 in XRD
	Microfibril angle	X	X		Angular intensity distributions of reflections 200 and 004
	Aggregates				Deconvolution of C-4 of ^{13}C CP MAS NMR
Pores	Porosity		X	X	Scattering invariant; or fitting the data to polydisperse spherical model
	Surface area		X	X	Inner surface, $O_s = \frac{S}{V} \propto \frac{1}{Q}; Q = \int_0^\infty I(q) q^2 dq \ = Invariant$
	Pore size distribution		X	X	Information included in the shape of the SAXS curve. Pore size distributions are derived from model curve fits. Areas under the the curves are normalized to one. E.g. Bimodal Schulz-Zimm distribution
	Surface roughness		X	X	Surface fractal dimensions, $D_{surface} = 6 - x; x = power\ law\ exponent; I(q) = Aq^{\alpha} + B\ (power\ law)\ ; Smooth:\ D_{surface} = 2, rough:\ D_{surface} = 2.5$
	Porod length		X	X	$O_s = \frac{S}{V} = \frac{4\phi(1-\phi)}{l_P}; \phi = volume\ fraction of\ pores\ and\ (1-\phi) of\ pore\ walls$

Cheng, G., et al., Energy Environ. Sci., 2015. **8** p. 436-455.

Dimensions of native cellulose microfibril

Cross section of a native
cellulose microfibril in higher plants

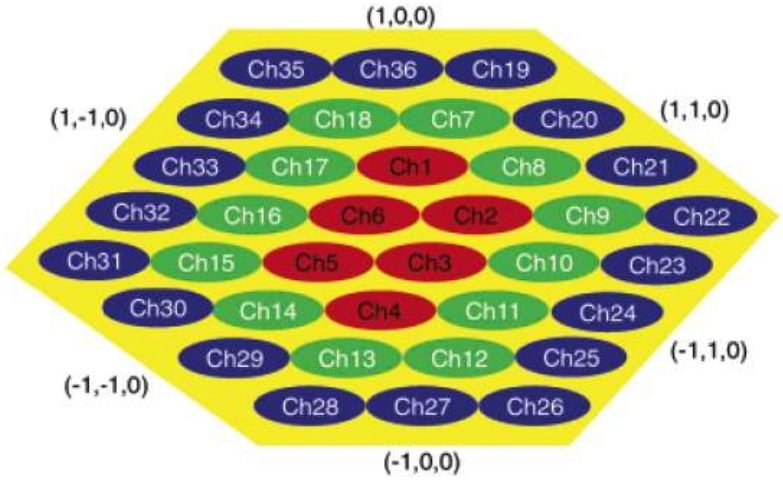

CURRENT VIEW:

WOOD MICROFIBRILS ARE ca. 3.5 nm WIDE AND CONSIST OF 36 INDIVIDUAL CELLULOSE CHAINS.

Ding and Himmel. *J. Agric. Food Chem.* **2006**, *54*, 597.

Crystallite Dimensions
Microfibril Aggregation

Microfibril Dimensions of Cellulose I

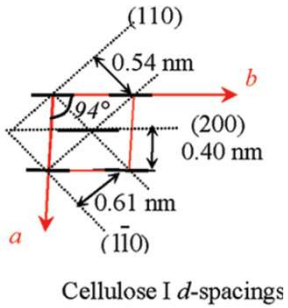

Cellulose I *d*-spacings

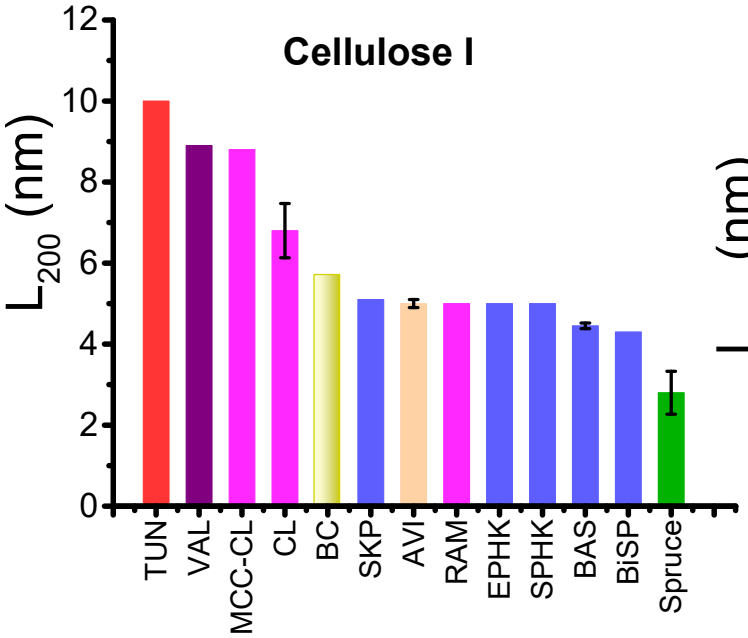

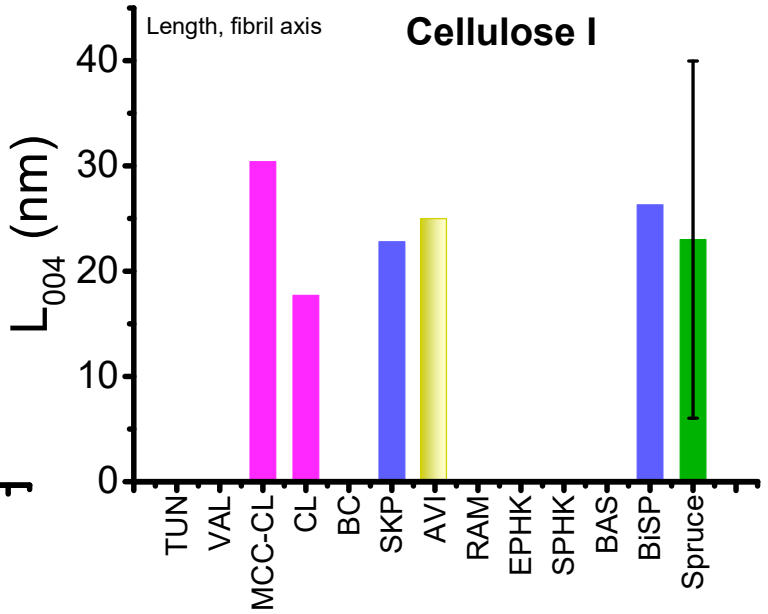

$$L_{hkl} = \frac{K \cdot \lambda}{FWHM \cdot cos\theta}$$

- $FWHM\ of\ a\ specific\ diffraction\ peak\ at\ 2q\ can\ be\ related\ to\ the\ crystallite\ size\ along\ the\ d-spacing\ direction\ of\ that\ peak.$
- $K \ldots\ldots shape\ factor\ \approx 0.89;\ \lambda \ldots\ldots X-ray\ wave\ length$
- Each chain occupies an area of 0.317 nm^2 in cellulose I$_\beta$ (JACS (2002) 124: 9074)

Sebe, G., et al., Biomacromolecules, 2012. **13**: p. 570-578.
Seong H. Kim et al. *Korean J.Chem.Eng*. (2013), 30(12), 2127-2141

TUN	Biomacromolecules (2008), 9:57
VAL	Acta Polymerica (1990), 41: 131
MCC-CL	Cellulose (2009) 16:999
CL	Biomacromolecules (2008), 9:57
CL	Cellulose (2009) 16:999
CL	Acta Polymerica (1990), 41: 131
BC	Acta Polymerica (1990), 41: 131
SKP	Cellulose (2009) 16:999
AVI	Biomacromolecules (2008), 9:57
AVI	Cellulose (2009) 16:999
RAM	Acta Polymerica (1990), 41: 131
EPHK	Cellulose (2004), 11: 85
SPHK	Cellulose (2004), 11: 95
BAS	Cellulose (2004), 11: 85
DWP	Acta Polymerica (1990), 41: 131
BiSP	Cellulose (2009) 16:999
Spruce	Cellulose (2009) 16:999
Spruce	Macromolecules (1995), 26:8782
Spruce	Proc. Natl. Acad. Sci., (2011) 108: 18863

Microfibril Length of Cellulose I

TEM and AFM:

Microfibrils can be considered as a crystalline entity continuous over a **few microns**, having a range of lateral dimension depending on the biological origin and development stage
Periodic defects along the microfibril have been expected from the acid hydrolysis behavior of cotton fibers.

An interesting observation is reported on cellulose microfibrils produced in vitro from membrane fragments, which cannot be fragmented by acid hydrolysis, whereas the in vivo counterpart will be fragmented as any other cellulose from higher plants.
The density of microfibrils in the cell wall would result in a tight lateral aggregation concentrating the internal strain in a limited zone distributed along the chain axis

Nishiyama, Y., J. Wood Sci., 2009. **55**: p. 241-249.

Microfibril cross-sections

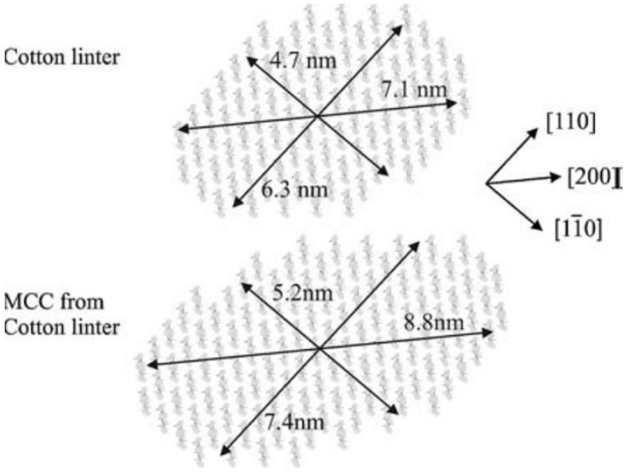

Leppaenen, K., et al., Cellulose 2009. **16** p. 999-1015.

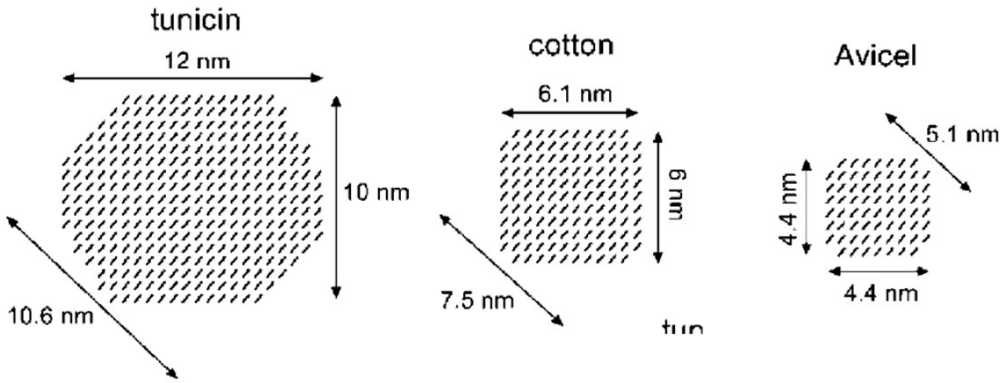

Elazzouzi-Hafraoui, S., et al., Biomacromolecules, 2008. **9** p. 57-65.

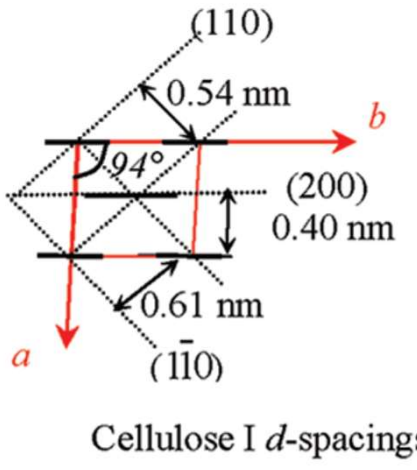

Cellulose I *d*-spacings

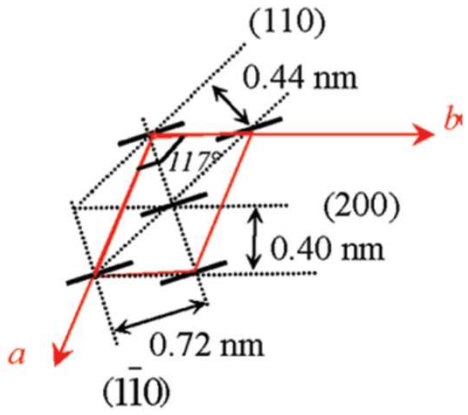

Cellulose II *d*-spacings

Monoclinic unit cell of I_β & (II) with d-spacings

- **0.40 (0.40) nm (220)**
- **0.54 (0.44) nm (110)**
- **0.61 (0.72) nm (1-10)**

Sebe, G., et al., Biomacromolecules, 2012. **13**: p. 570-578.

Sugiyama, J. et al., Macromolecules, 1991. **24:** p. 4168-75.

Microfibril Dimensions of Cellulose II

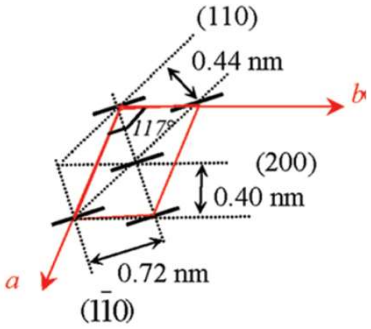

Cellulose II *d*-spacings

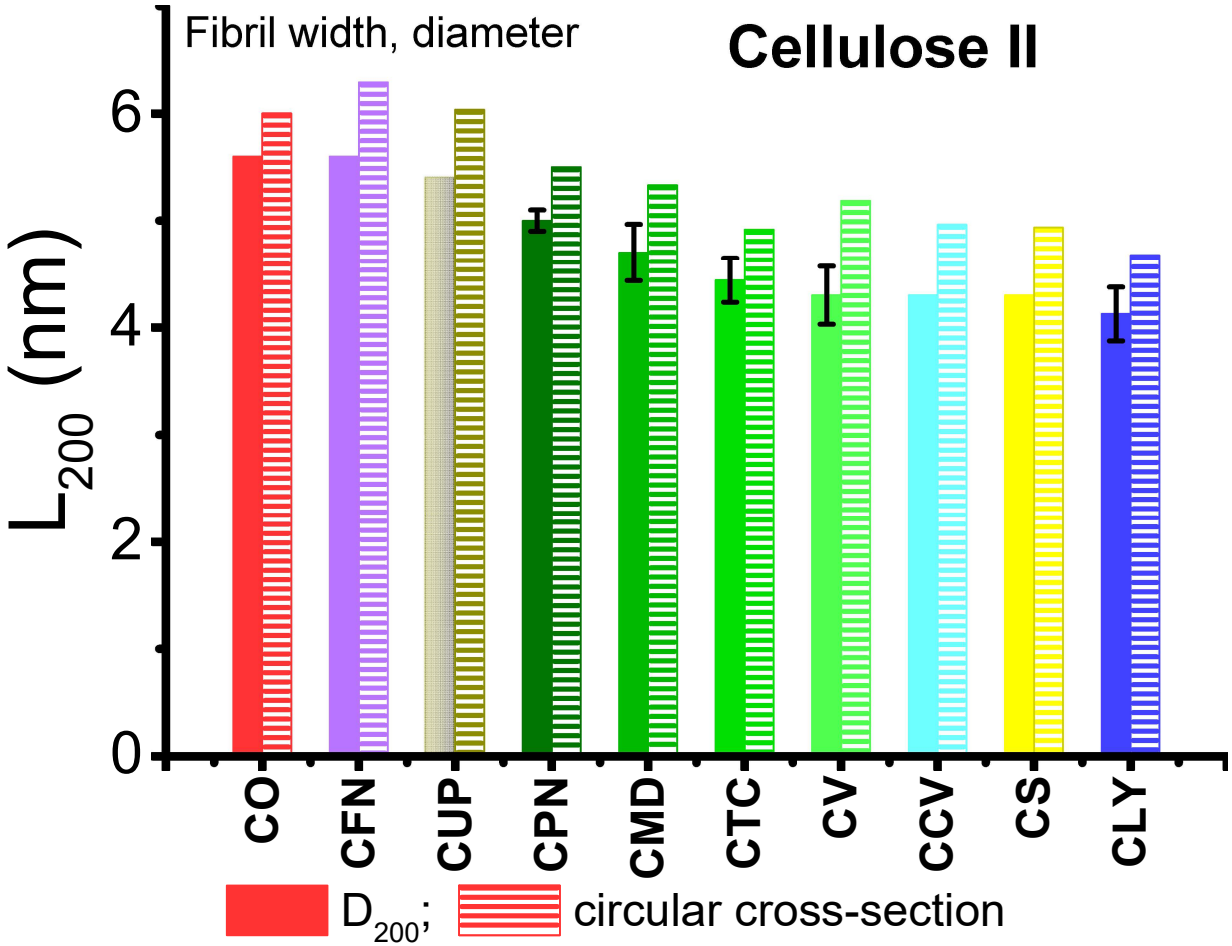

$$A = D_{200} \cdot 0.5(D_{1-10} + D_{110})$$

$$D_{circ\ cross-sectio} = 2\sqrt{A/\pi}$$

CO	Cotton	Sixta, H. Lenzing AG (2004)
CFN	Fortisan	Sixta, H. Lenzing AG (2004)
CUP	Cupro	Sixta, H. Lenzing AG (2004)
CPN	Polynosic	Sixta, H. Lenzing AG (2004)
CMD	Modal	Sixta, H. Lenzing AG (2004)
CTC	Tyre Cord	Sixta, H. Lenzing AG (2004)
CV	Rayon	Sixta, H. Lenzing AG (2004)
CCV	Carbamate	Sixta, H. Lenzing AG (2004)
CS	Biocelsol	Sixta, H. Lenzing AG (2004)
CLY	LYOCELL	Sixta, H. Lenzing AG (2004)
CLY, CV		Cellulose (2004), 11: 85 Cellulose (1995), 2: 54

Patil et al. *Text. Res. J.* 32:460 Sugiyama, J. et al., *Macromolecules*, 1991. **24:** p. 4168-75.

Crystal dimensions vs Orientation

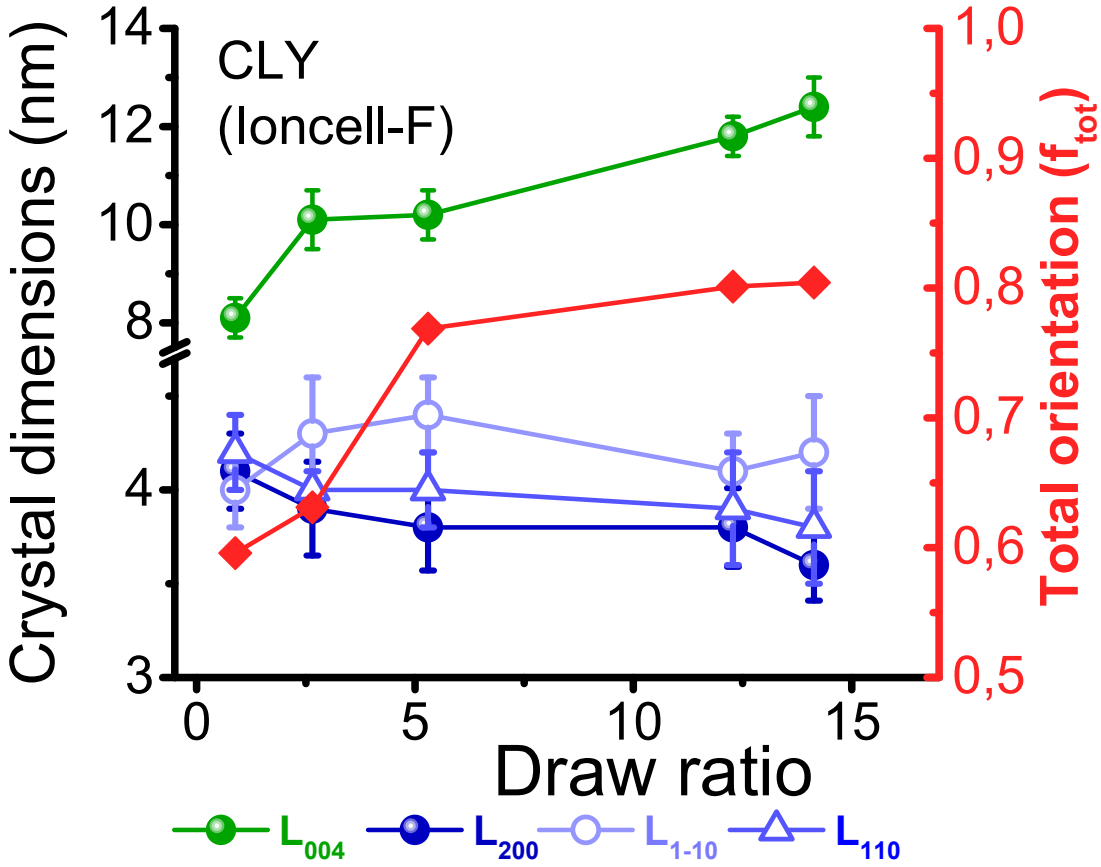

CLY-Fiber
(Ioncell-F process):

- **Crystal length clearly increases with increasing fiber orientation**
- **D_{200} cross-section slightly decreases with increasing orientation**

Sixta, H et al. Unpublished results (2016)
Sixta, H., et al., *Nord. Pulp Pap. Res. J.,* 2015. **30**: p. 43-57.

Overview on Crystallinities

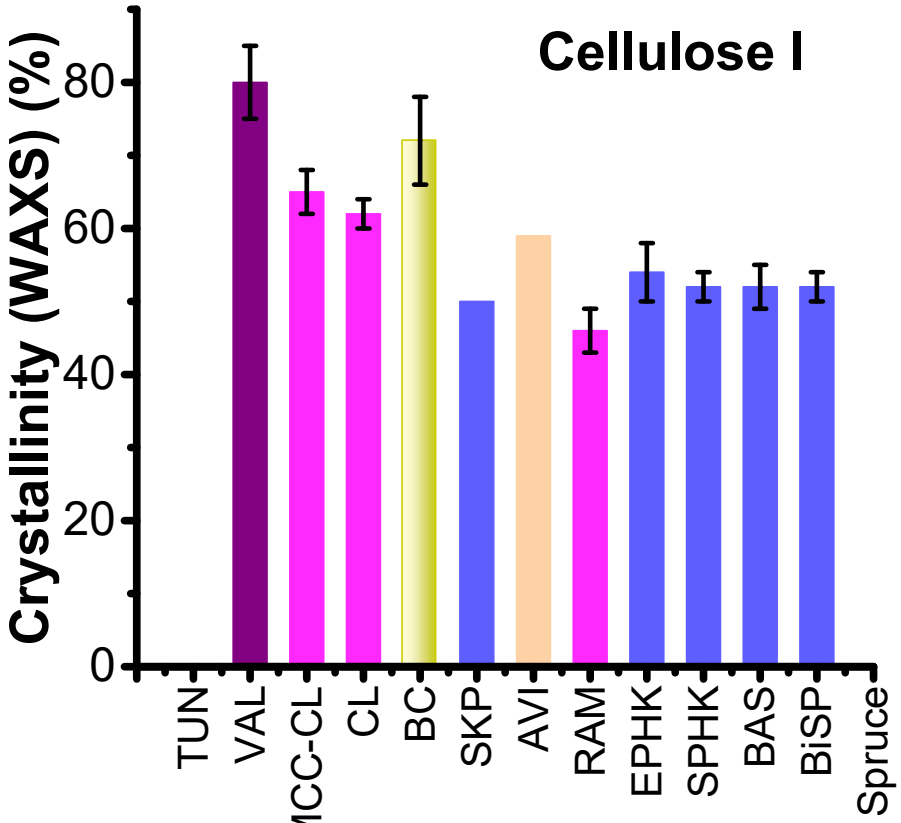

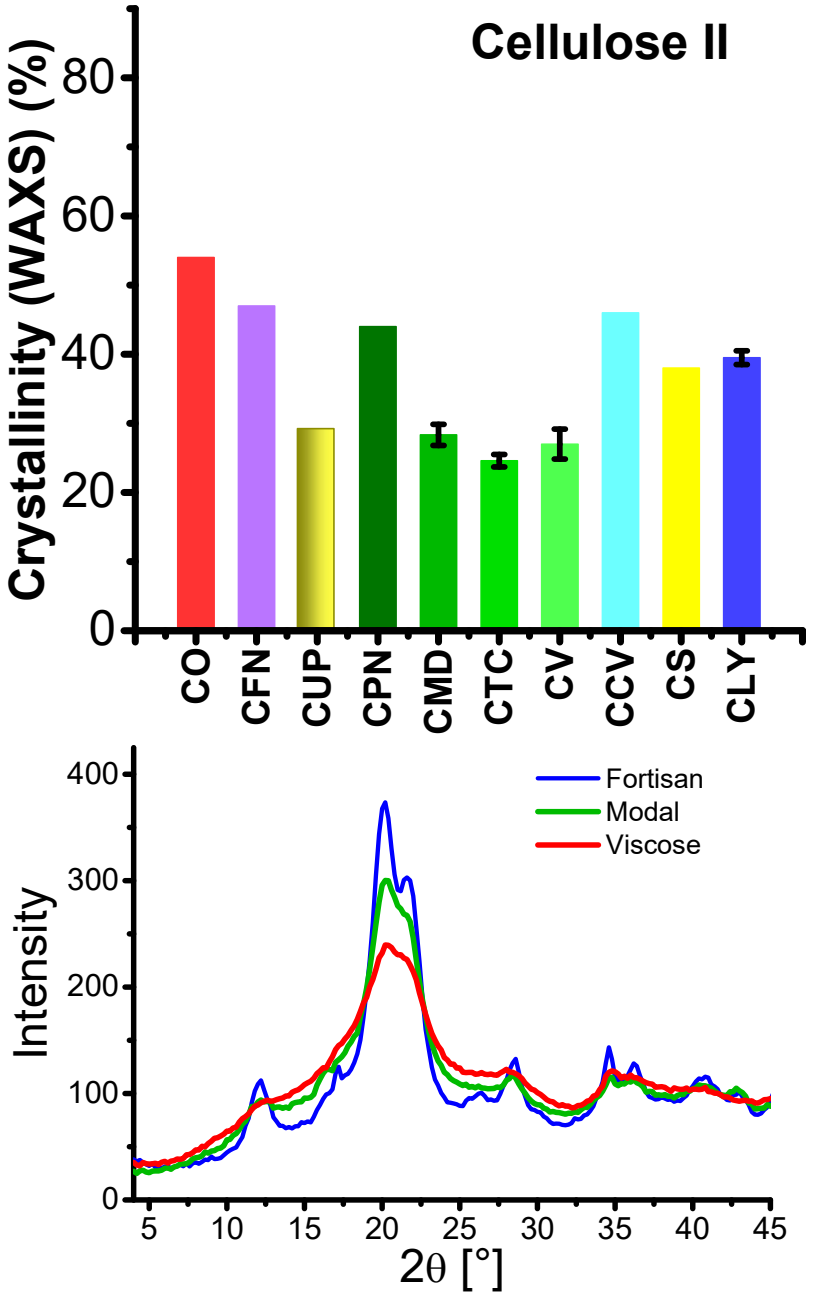

Sixta, H. H-P. Fink, T. Röder, (2004)

Fibril Aggregates

Microfibrils are arranged into bundles with outer lateral dimensions of ~ 20 nm

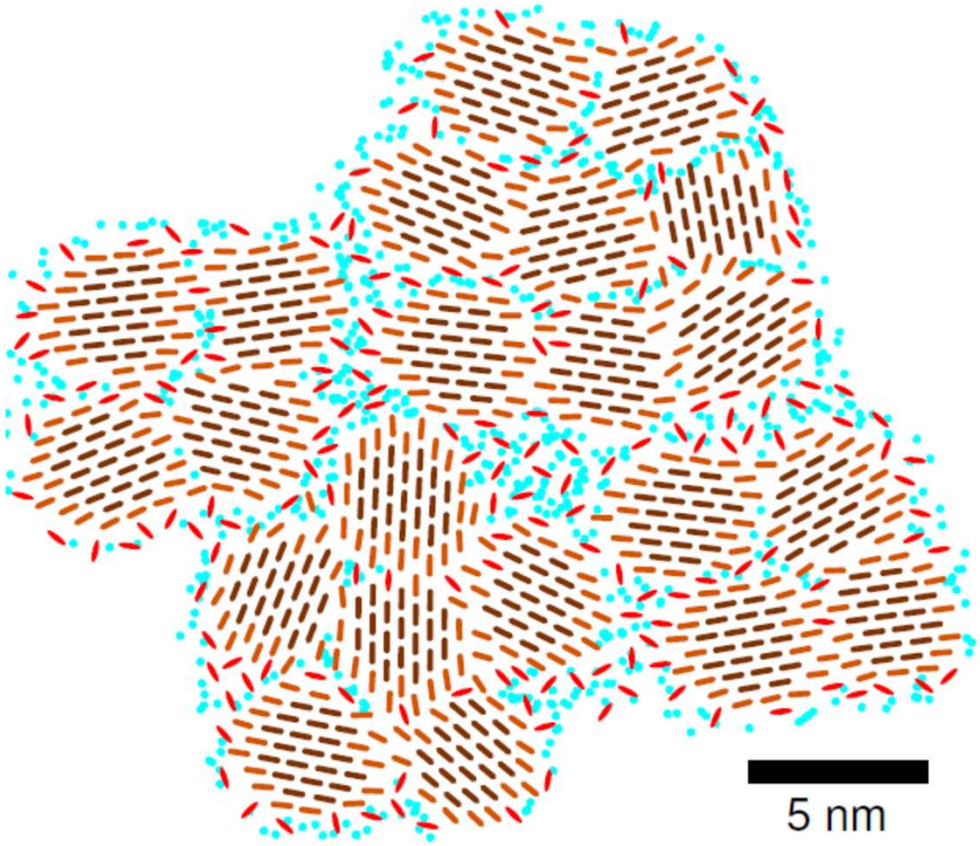

Penttilä, P.; PhD thesis (2013), University of Helsinki

Crystallite & Aggregate Dimensions

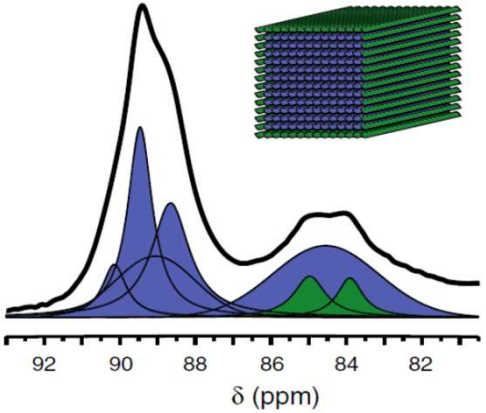

$$q_{fibril} = \frac{I(AS) + I(IAS)}{total\ C4\ area}$$

$$q_{aggregate} = \frac{I(AS)}{total\ C4\ area}$$

Fraction of fibril surface:

$$q = \frac{4 \cdot (n-1)}{n^2}$$

$$n = \frac{2\left(1 + \sqrt{1-q}\right)}{q}$$

$$L = 0.57n$$

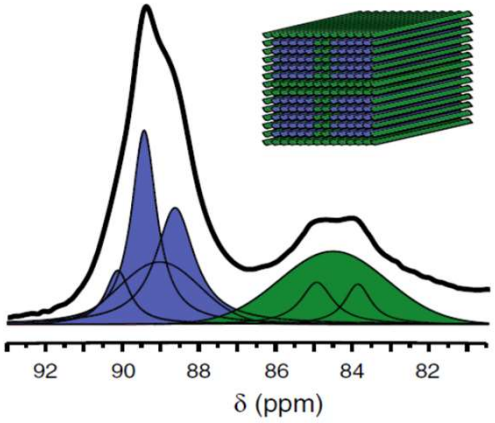

^{13}C-CPMAS NMR of Euca-PHK pulp

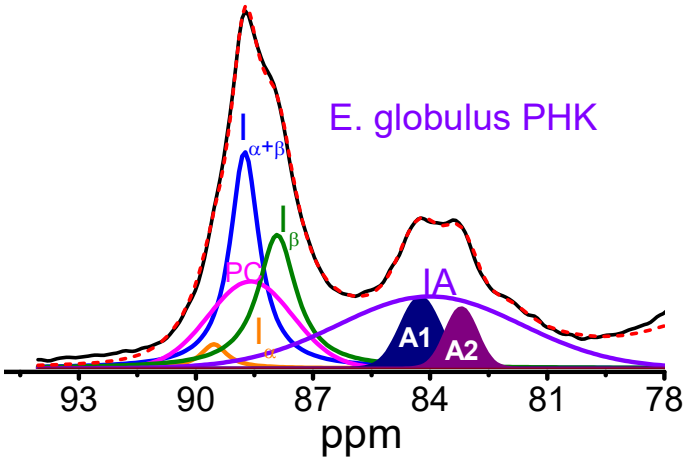

$$CrI = 0.54$$

$$q_{fibril} = 0.46$$

$$q_{aggregate} = 0.11$$

$$FW = 4.3\ nm$$

$(n = 7.54 \rightarrow L = 7.54 \cdot 0.57 = 4.3)$

$$AW = 20.2\ nm$$

$(n = 35.3 \rightarrow L = 35.3 \cdot 0.57 = 20.2)$

Palme, A., et al., *Cellulose* 2014. **21** p. 4681-4691.

R.H. Newman, *Solid State Nuclear Magnetic Resonance* 15(1999), 21-29
P.T. Larsson, K. Wickholm, T. Iversen. *Carbohydrate Research* 302 (1997), 19-25

Structure-Property Relationship

Structure-Property Relationship

1. Pore structure and inner surface
2. Interaction with water
3. Swelling
4. Solution structure
5. Coagulation, Regneration
6. Structure formation during regeneration
7. Oxidized functionalities
8. Degradation of Cellulose
9. Cellulose Reactivity
10. Mechanical properties:
    - E-modulus

Pore Structure and Inner Surface

Pore Structure and Inner Surface

- **Solute exclusion**
- **NMR spectroscopy**
- **Water sorption isotherms**, water retetion value (WRV)
- SAXS
- Thermoporosity (Gibbs-Thompson)
- Cryoporometry (NMR)
- BET: nitrogen absorption
- Mercury-intrusion porosimetry (*Powder Technol* (2005)160:61)
- Others

Pore volume by ISEC

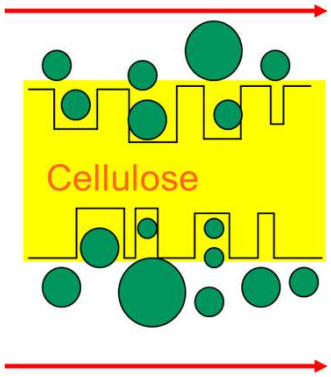

$$V_i = V_p - \frac{O_p}{2} d$$

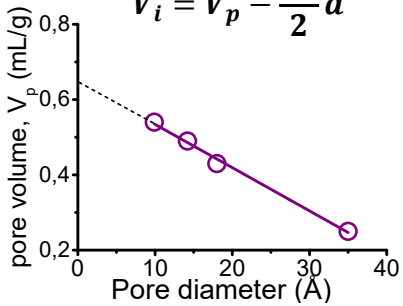

Pulp	V_p	FSP	WRV	D_p	O_p
	mL/g	mL/g	%	nm	m^2/g
HW-S	0.60	0.50	73	5.1	235
HW-PHK	0.65	0.55	71	5.5	240
CL	0.45	0.39	54	4.8	190

Treatment	V_p	WRV	Bright	[η]
HW-AS	mL/g	%	%ISO	mL/g
Never-dried	0.92	91.2	91.2	581
Freeze-dried	0.86			
Air-dried	0.69	91.2	91.2	581
105°C-dried	0.60	90.1	90.1	546
160°C-dried	0.43	79.1	79.1	350

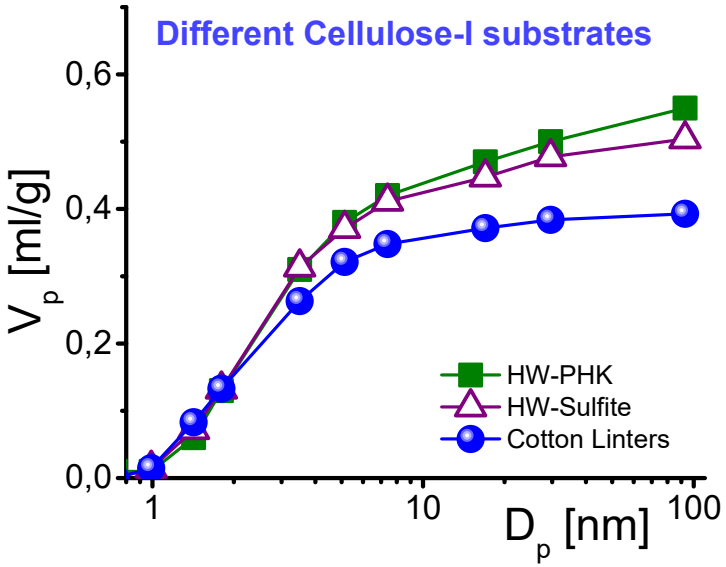

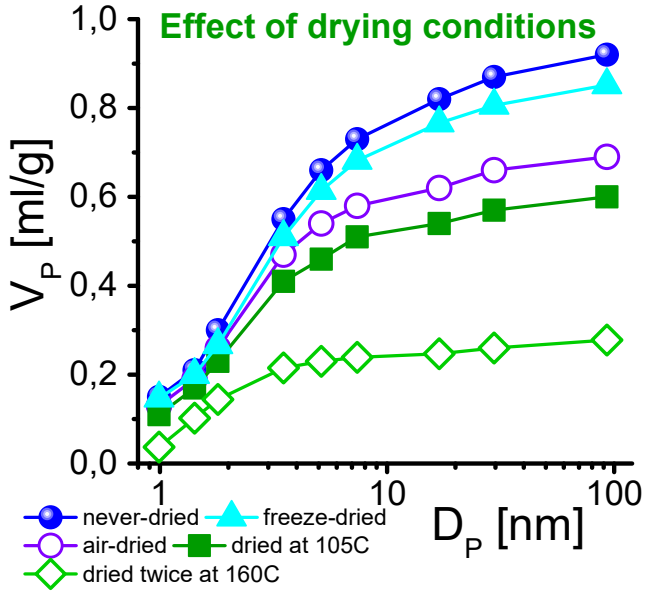

Water sorption isotherm - FSP

Fiber Saturation Point (FSP): When all water has been removed from the gross capillary structure, but no water has been removed from the cell wall.

Pore radius vs relative vapor pressure at which the pore loses its water:
Kelvin equation:

$$ln\frac{p}{p_0} = \frac{-2\gamma M}{r\varrho RT};\ \gamma = 0.0728\frac{J}{m^2}$$

Wet cellulose samples placed upon a porous plate; application of gas pressure, which in equilibrium with the tension forces adjustes a certain water content in the pores: P vs. critical pore radius :

Young- Laplace: $P = \frac{2\gamma}{r}$; $r\ into\ KELVIN \rightarrow gives\ p/p_0$

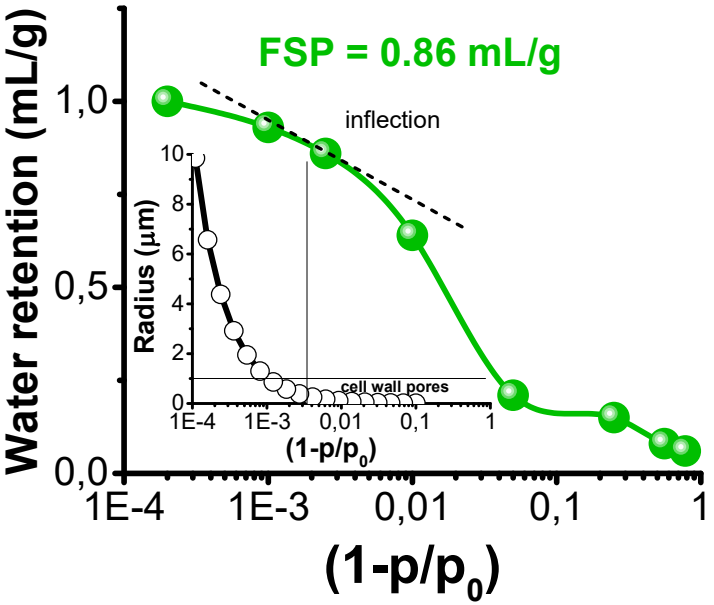

Samples	Yield, %	Lignin, %	FSP, g/g
Spruce	100,0	27,0	0,40
Kraft 20	92,4	27,3	0,67
Kraft 35	89,0	27,6	0,74
Kraft 50	**80,0**	**28,5**	**0,86**
Kraft 80	70,4	25,2	1,06
Kraft 110	53,4	12,3	1,21
Kraft 125	48,7	6,5	1,14

Stone, J.E. and A.M. Scallan,. Tappi, 1967. **50**(10): p. 496-501.

Fibre wall pore sizes in water swollen state

- Based on solid-state NMR for determining the lateral fibril aggregate dimensions ***a***:

$q = (4n - 4)/n^2$;

$\boldsymbol{a = n * 0.57}$

$\boldsymbol{\sigma_{sat} = \frac{4}{a \cdot \varrho_s}}$ $\boldsymbol{\sigma_{sat}}$ ….specific surface area in water-swollen state assuming cylindrical pores, i.e. pore width corresponding to 4V/A

- and FSP (Dextran 2000, R_H=101 nm) measurement

$\boldsymbol{FSP = \sigma_{sat} \varrho_L t}$ t… thickness; 2t = average pore size

$\boldsymbol{2t = \frac{2FSP}{\sigma_{sat} \varrho_L}}$

		Water-swollen state		
Samples	FSP	a (LFAD) NMR	σ_{sat} NMR	Average pore size, 2t
	g/g	nm	m^2/g	nm
Cotton Linters	0,21	32,2	83	5,1
SW-Sulfite DP	0,94	16,9	158	11,9
HW-Sulfite DP	1,05	17,5	152	13,8

Cellulose (2013) 20:623-631

Interaction with Water

Sorption & Desorption Isotherms (DVS)

Cellulose-I und Cellulose-II Substrate

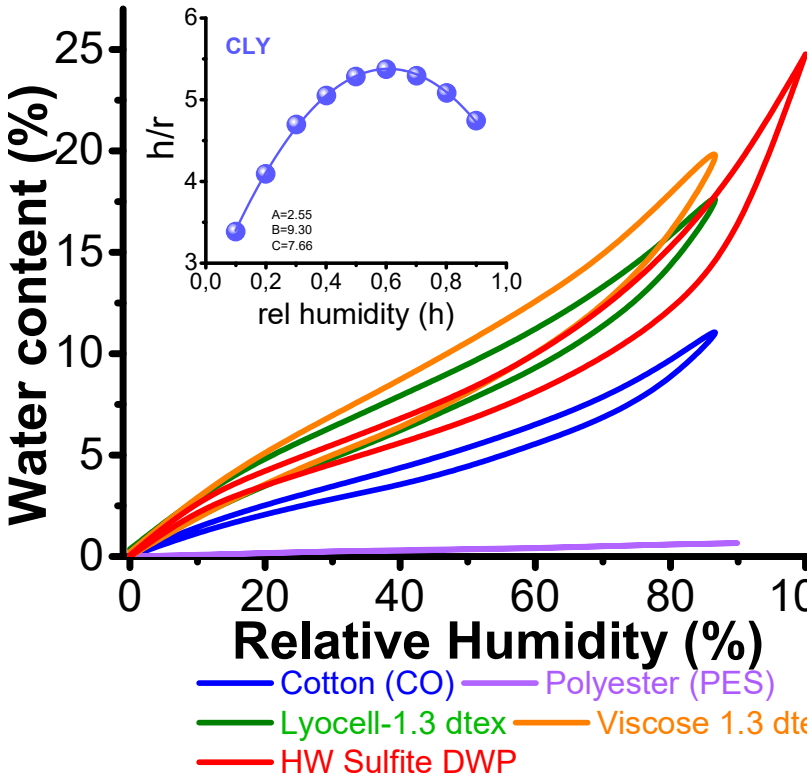

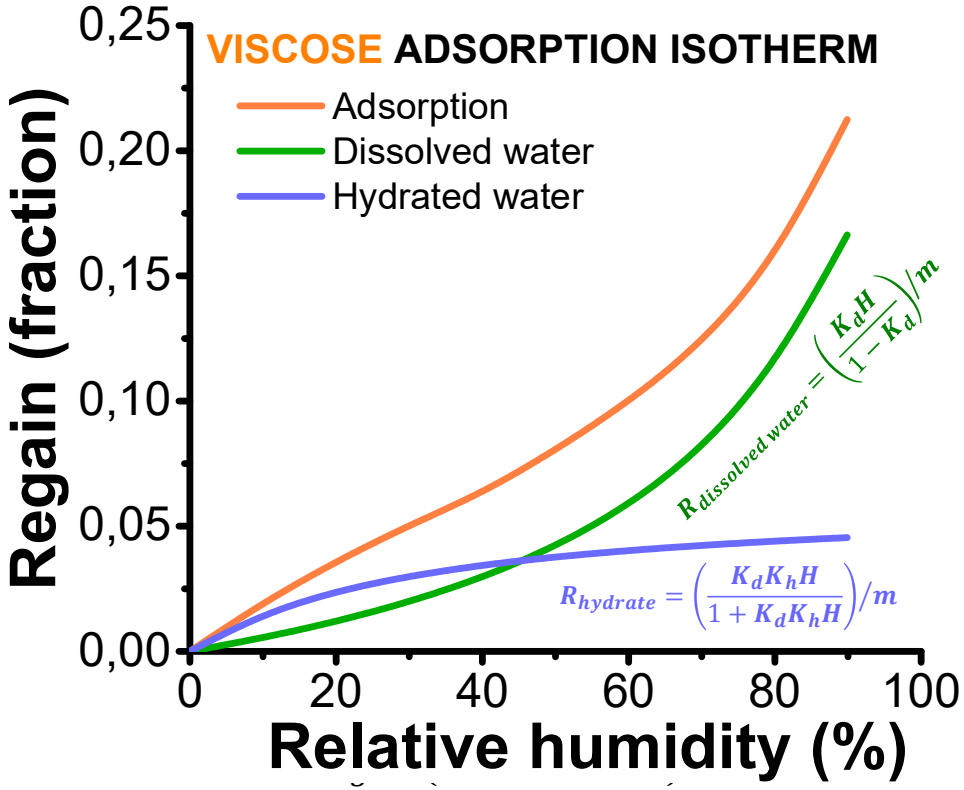

A, B, C *constants derived from fitting*
m_0 *represents the monolayer (ML)coverage*
K_d *is the equilibrium constant of the ML dissolution*
K_h *is the equilibrium constant of the ML hydration*
M *molar mass of water*: $18\ g/mol$
$\Delta G_{h,d}$ *is the standard free energy changes referenced to liquid water in* J/g

Hailwood, A.J. and S. Horrobin, *Trans. Faraday Soc.*, 1946. **42B:** p. 84-92, discussion 94-102

Sorption & Desorption Isotherms (DVS)

Cellulose-I und Cellulose-II Substrate

Sorption-, desorption equilibria based on the model of Hailwood and Horrobin

Sample	Sorption Monolayer water (g/g)	Desorption Monolayer water (g/g)	Hysteresis* %	Surface area m^2/g	Sorption ΔG_h J/g	Sorption ΔG_d J/g	Desorption ΔG_h J/g	Desorption ΔG_d J/g
Cotton lint	0,0323	0,0433	34	97	-217	26	-216	41
Polyester (PES)	0,0041	0,0041	0	12	-165	79	-200	83
Lyocell, 1.3 dtex (CLY)	0,0599	0,0779	30	180	-202	34	-253	51
Viscose, 1.3 dtex (CV)	0,0639	0,0925	45	192	-175	31	-220	54
HW-Sulfite DP	0,0470	0,0575	22	141	-295	32	-287	31

$* H = (ML_d - ML_a / ML_a$

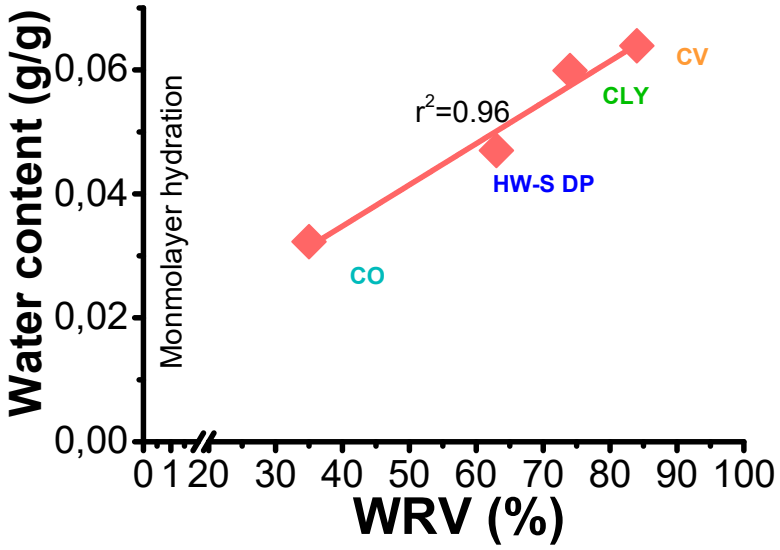

Good correlation between the monolayer hydration and the water retention value (WRV).

WRV of an un-opened cotton ball (never-dried) was 140% (46% of field dried cotton)

Hailwood, A.J. and S. Horrobin, *Trans. Faraday Soc.*, 1946. **42B:** p. 84-92, discussion 94-102

Palme, A., et al., *Cellulose* 2014. **21** (p. 4681-4691.

Hydration vs. Crystallite Width

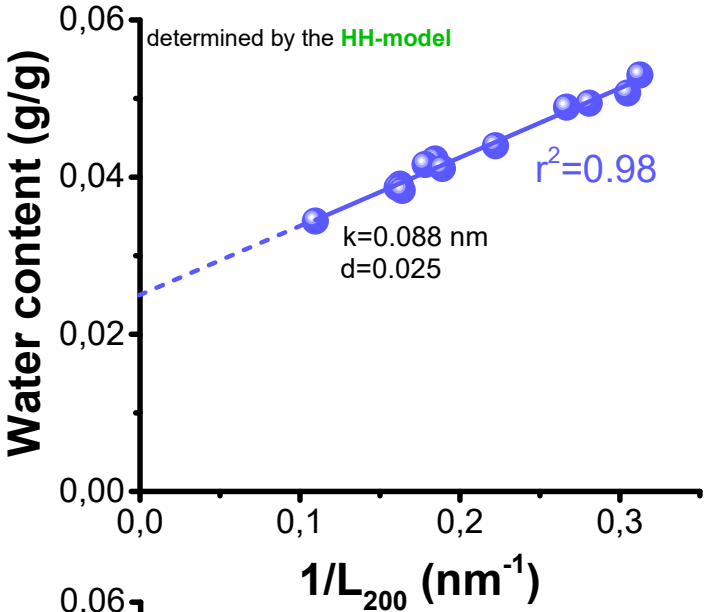

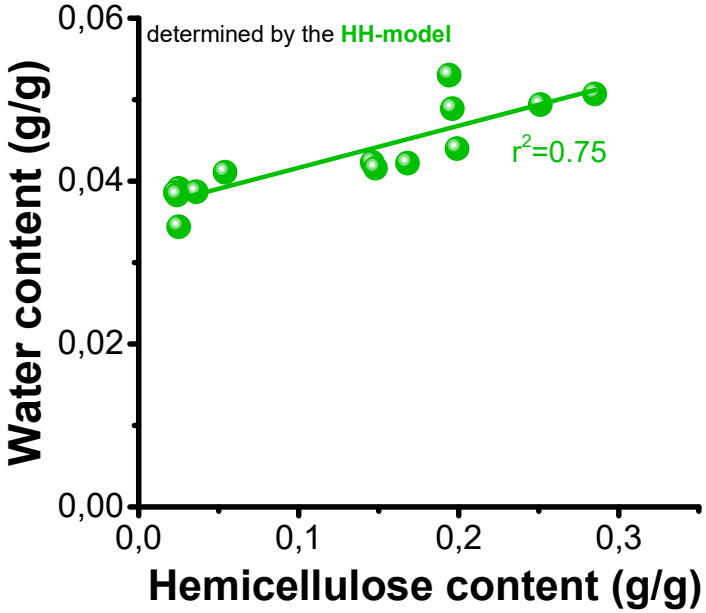

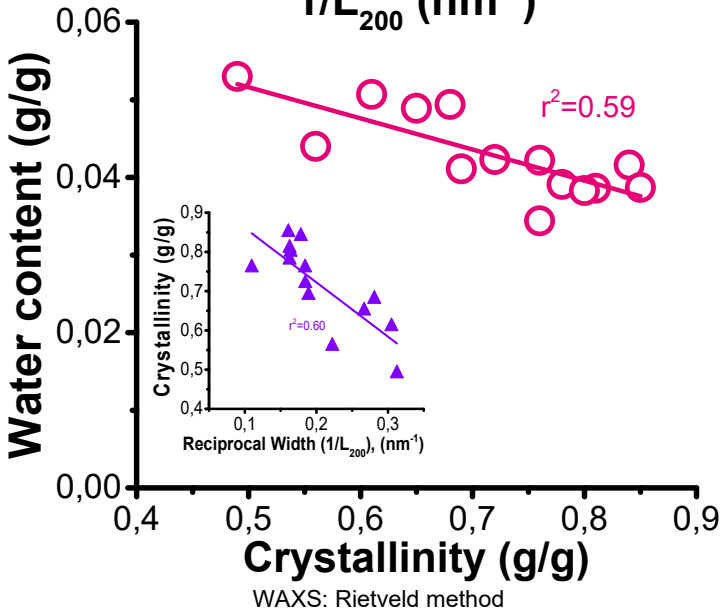

WAXS: Rietveld method

- **Observed linear relation between monolayer hydration and reciprocal crystallite width theoretically explained by geometric model**

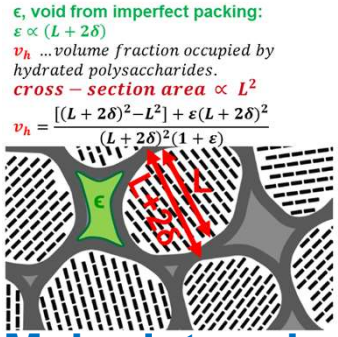

$$v_h \approx \frac{\varepsilon}{\varepsilon + 1} + \frac{4\delta}{(1+\varepsilon)}\left(\frac{1}{L}\right)$$

- **Main determinant of monolayer water sorption is structural (crystallite width) not compositional (hemi)**

Driemeier, C. and J. Bragatto, *J. Phys. Chem. B*, 2013. **117** p. 415-421.

Swelling

Cellulose is an amphiphilic molecule

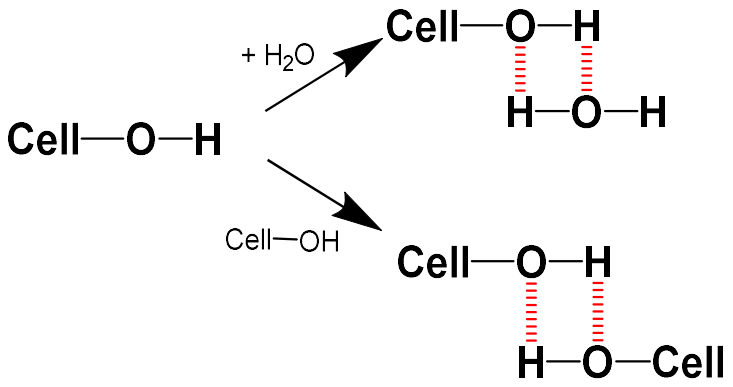

- Polymers are amphiphilic, i.e. contain both polar and nonpolar groups/segments.
- Equatorial direction of a glucopyranose unit is hydrophilic, the axial direction hydrophobic (C-H bonds).
- Significant hydrophobic pairing energy favoring the stacking association of cellulose chains (2.0 kcal/mol/residue).
- Thus, hydrophobic association favors a crystal-like structure over the solution state.

Medronoh, B.; A. Romano; M.G. Miguel; L. Stigsson; B. Lindman. *Cellulose* (**2012**), 19, 581-587
Bergenstråhle,M.; J.Wohlert, ME Himmel, JW Brady. *Carbohydr Res* (**2010**), 14, 2060-2066

Swelling and dissolution

Cellulose in NMMO (CP-MAS)

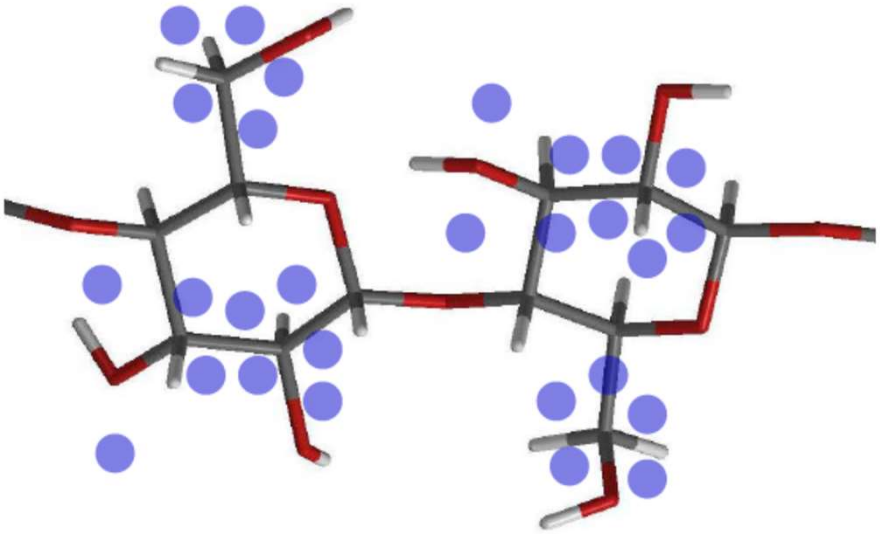

^{13}C perlabeled
Cellulose DP40

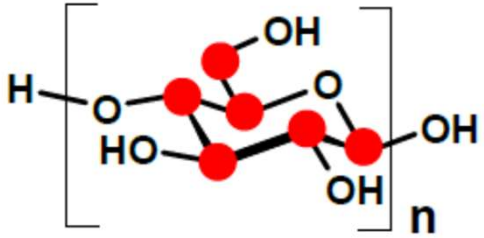

NMMO-d_{11}(-^{15}N)

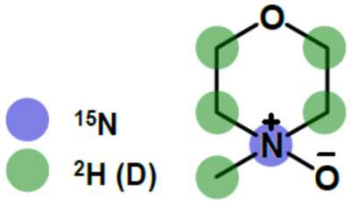

- Measuring average distances between solvent and solute atoms by triangulation
- In the swollen state, the solvent molecules surround C-6 and C-2.
- **Upon dissolution, the solvent approaches C-3.**

Water Vapour Sorption

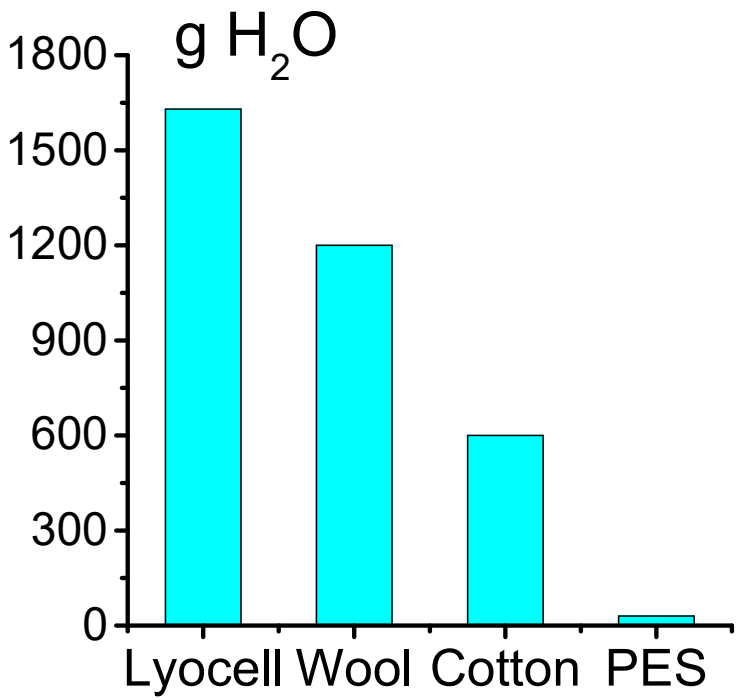

Absorption capacity of equivalent beds at 100 % RH

Lyocell beds help to make a comfortable sleeping climate.

Water absorption takes place in the capillaries between the fibrils only

H. Firgo et al., Dornbirn 2003

Absorbed Water in Cellulose Fibers

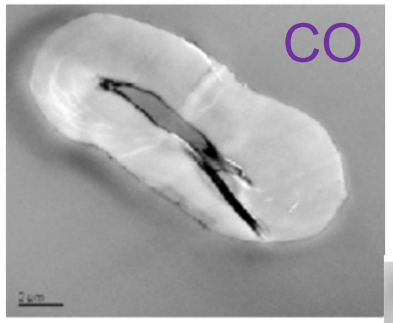

Cotton absorbs only little water

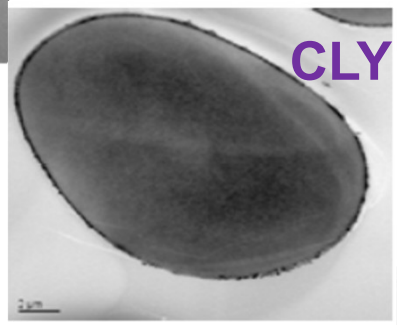

Tencel shows uniform water absorption over the whole fiber cross section

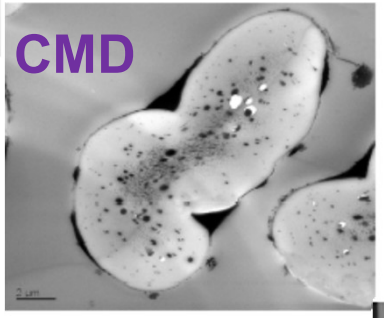

Crystalline skin of **Modal** contains less water than the core

Visualization of water:
Solvent exchange procedure followed by isoprene polymerization and **OsO_4 staining** in aqueous solution:
M. Abu-Rous et al. *Cellulose*, 13, 411-419 (2006)

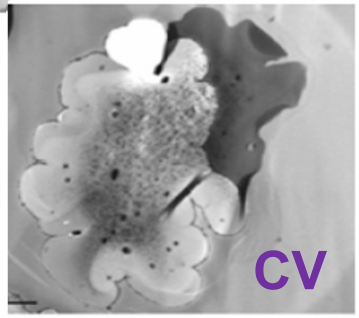

Uneven water distribution in **viscose**

Cellulose Solution Structure

Cellulose dissolution in a vertical kneader

IL / H_2O

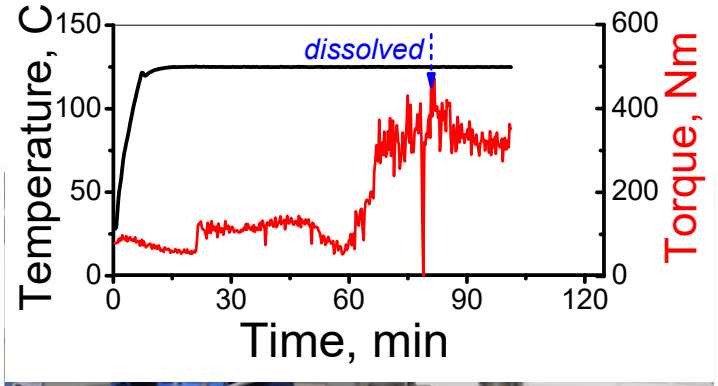

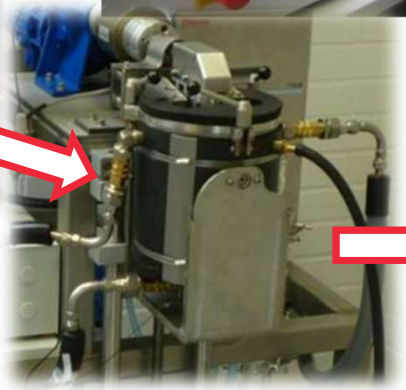

Solubility up to 20 wt%
PHK-Pulp, [η] = 424 mL/g

Final dope has to be filtrated and degassed

Dissolution of Cellulose in ILs

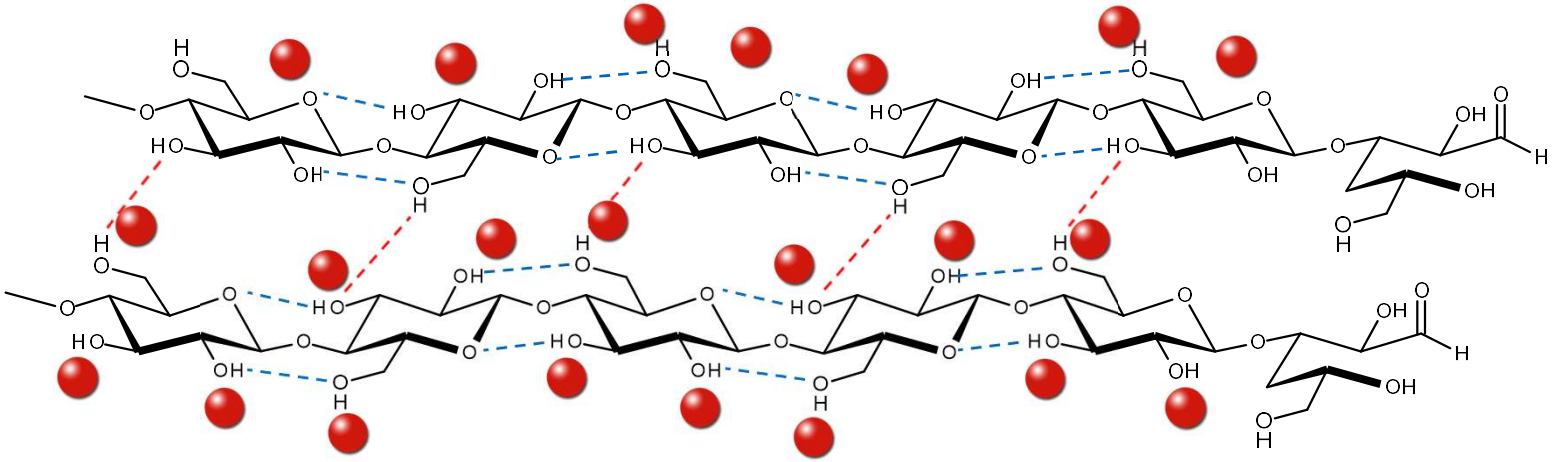

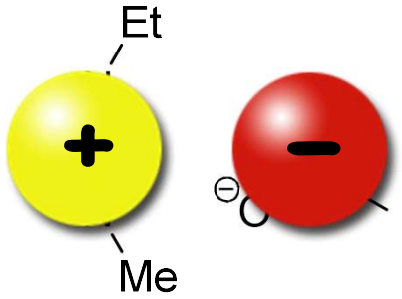

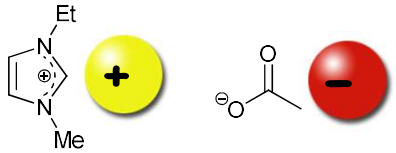

O3-H-O5 intrachain
O2-H-O6 intrachain
O6-H-O3 interchain

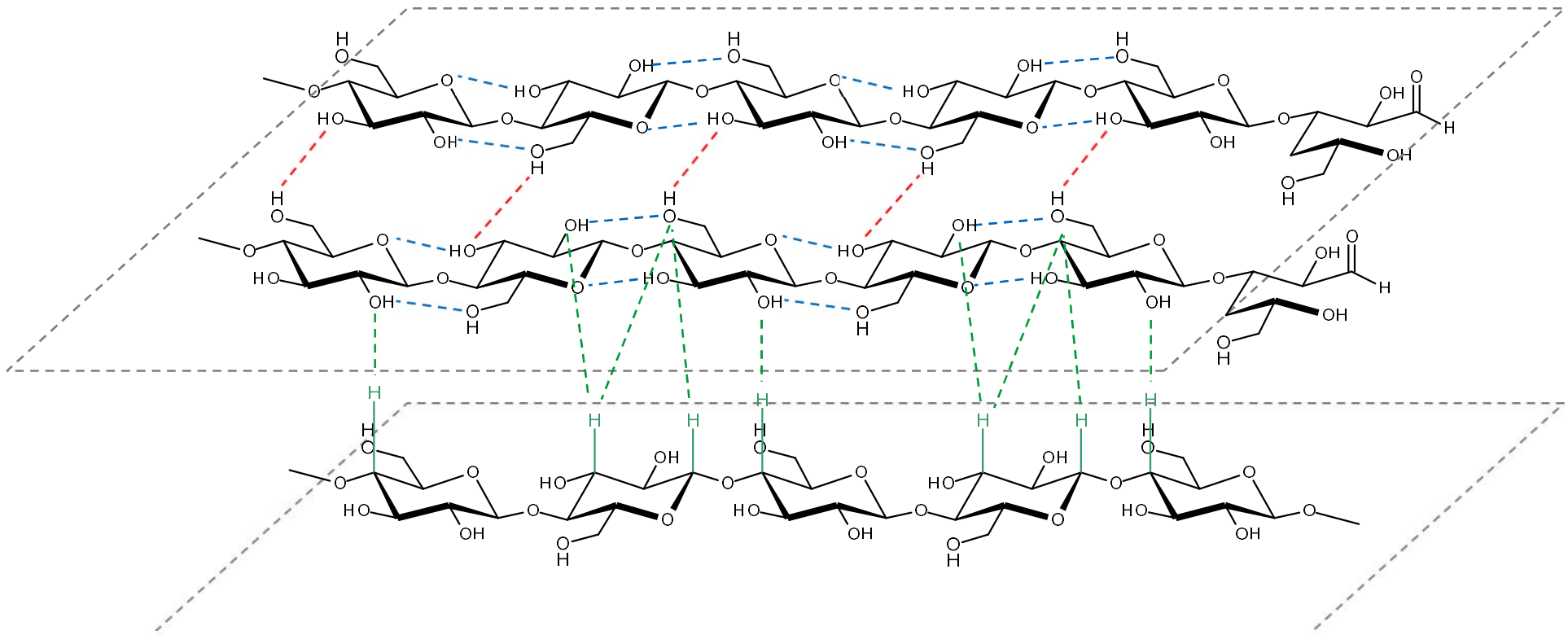

Intersheet bonds

O3-H-O5 intrachain
O2-H-O6 intrachain
O6-H-O3 interchain
intersheet H-bond

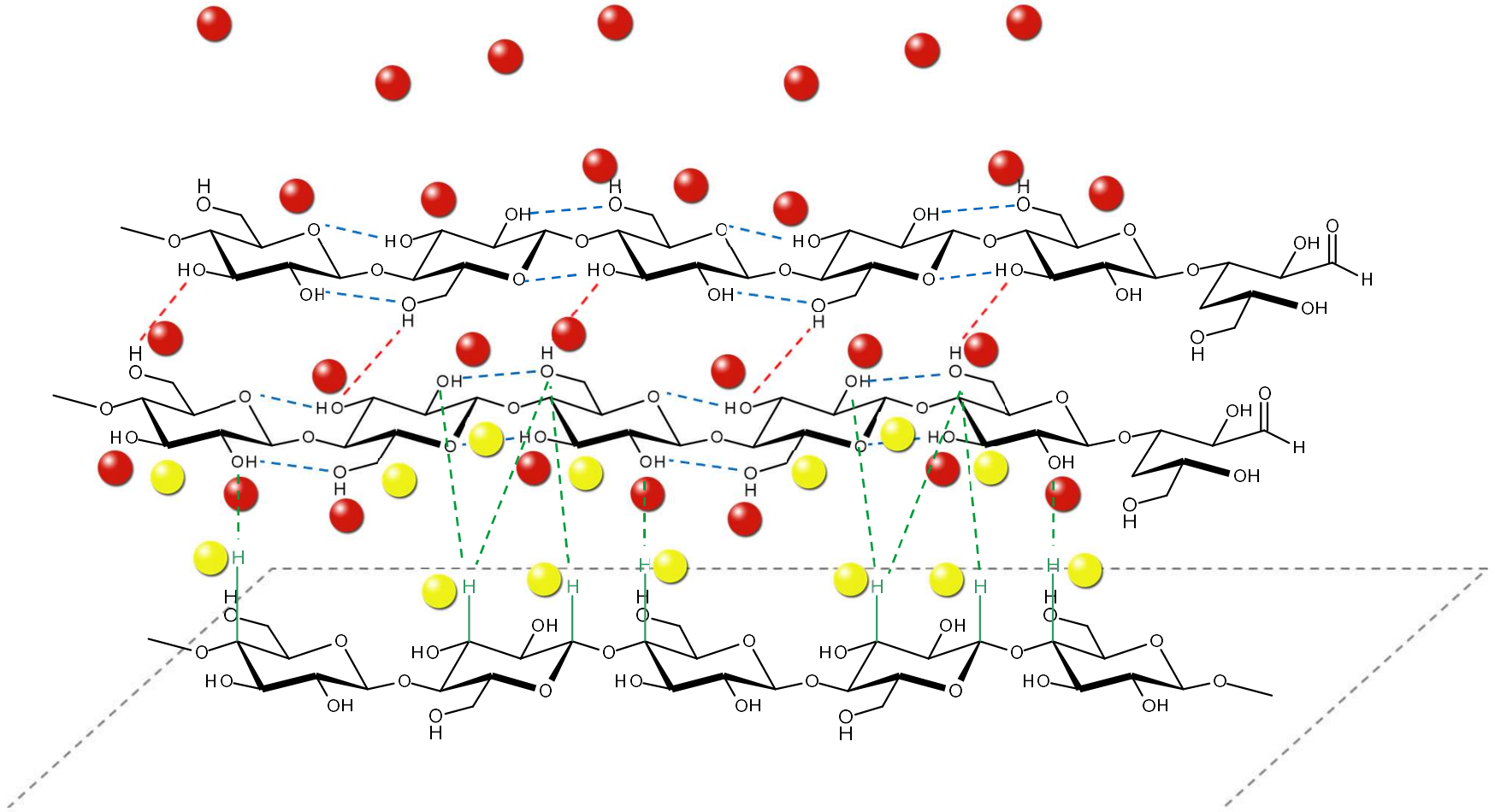

Solvation of nonpolar cellulose surface by the cation

O3-H-O5 intrachain
O2-H-O6 intrachain
O6-H-O3 interchain
intersheet H-bond

Cho, H.M.; Gross, A; Chu J.-W. *J. Am. Chem. Soc.* **2011,** doi 10.1021/ja2046155.

Regeneration of cellulose

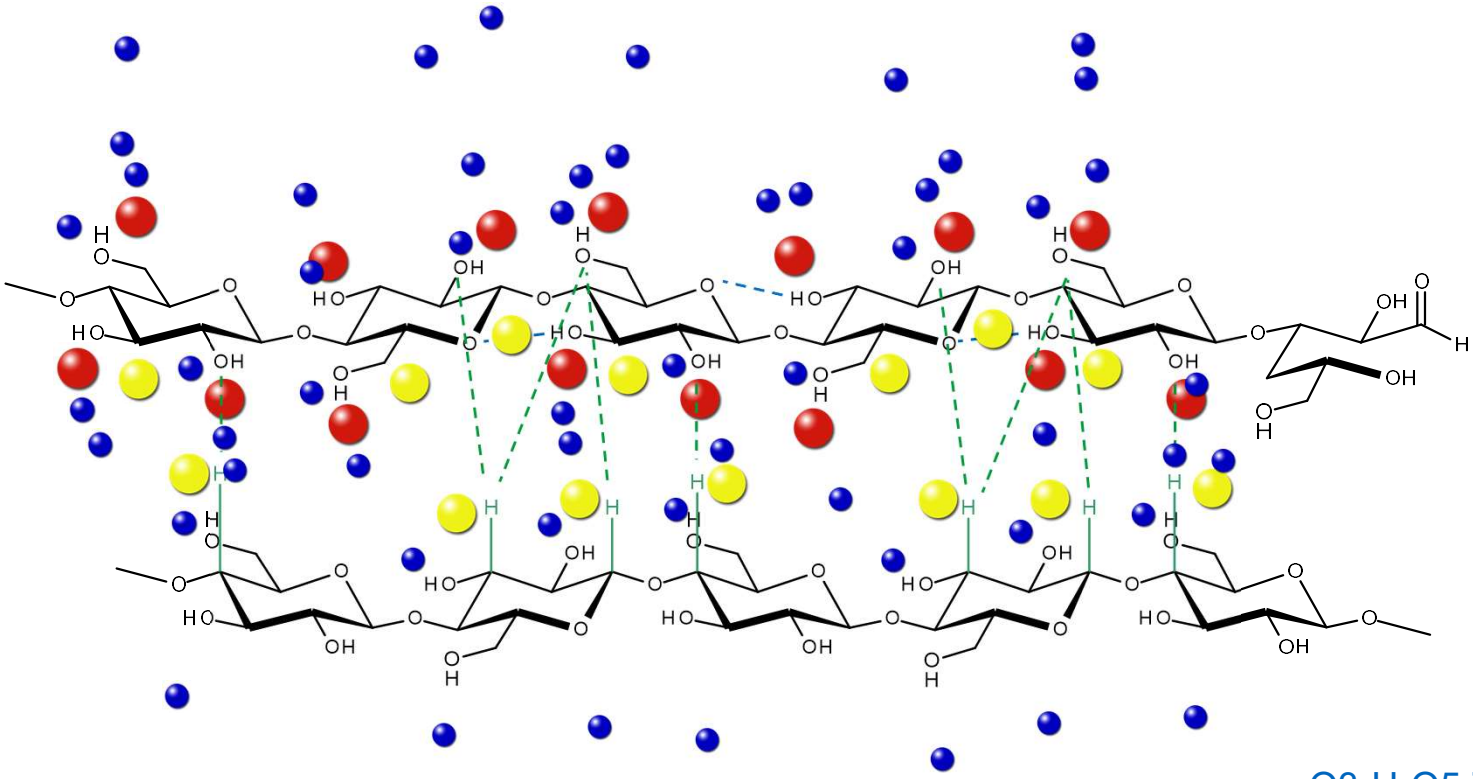

Re-formation of intersheet and intrachain bonds

O3-H-O5 intrachain
O2-H-O6 intrachain
intersheet H-bond

Liu, H.; Sale, K.L.; Simmons, B.A.; Singh, S. *Phys. Chem. B* **2011,** 115, 10251–10258.

Oscillatory rheology of spinning dope

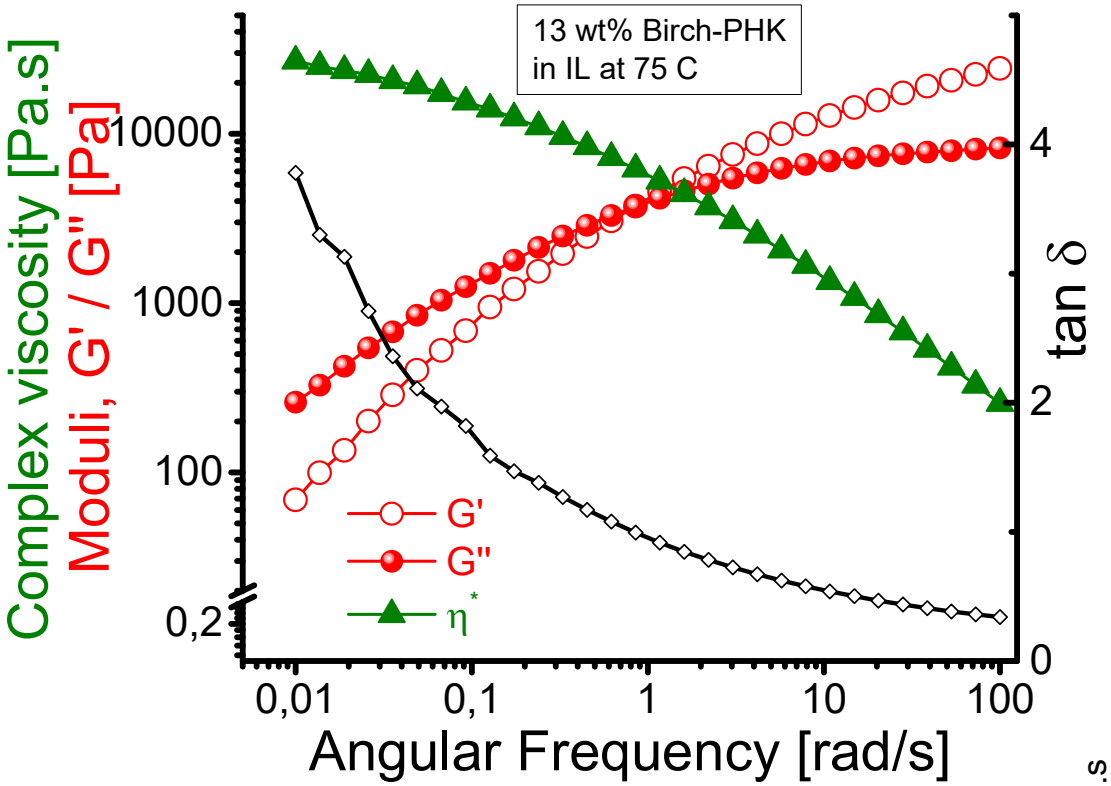

$G' = G'' = 3685\ Pa$

$\omega = 0.83\ s^{-1}$

$\eta_0{}^* = 27.000\ Pa.s$

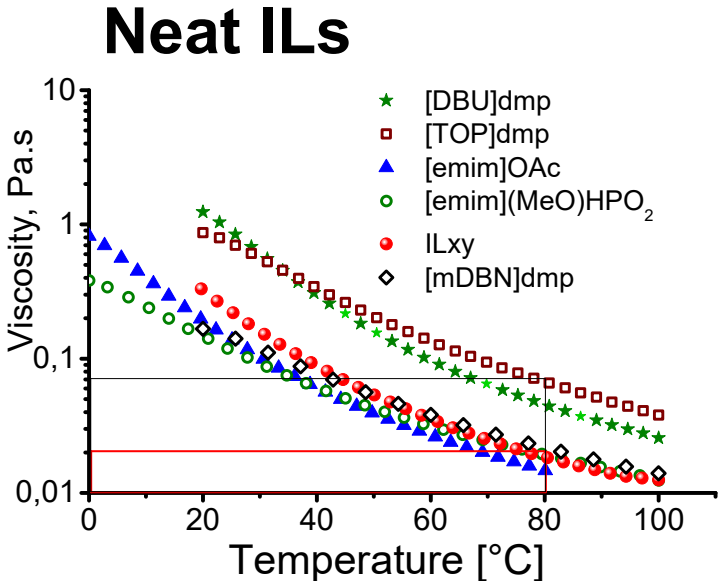

Rheology as a function of T

- SW-Sulfite dissolving pulp: DP_v=1320
- Solvent = [DBNH][OAc]

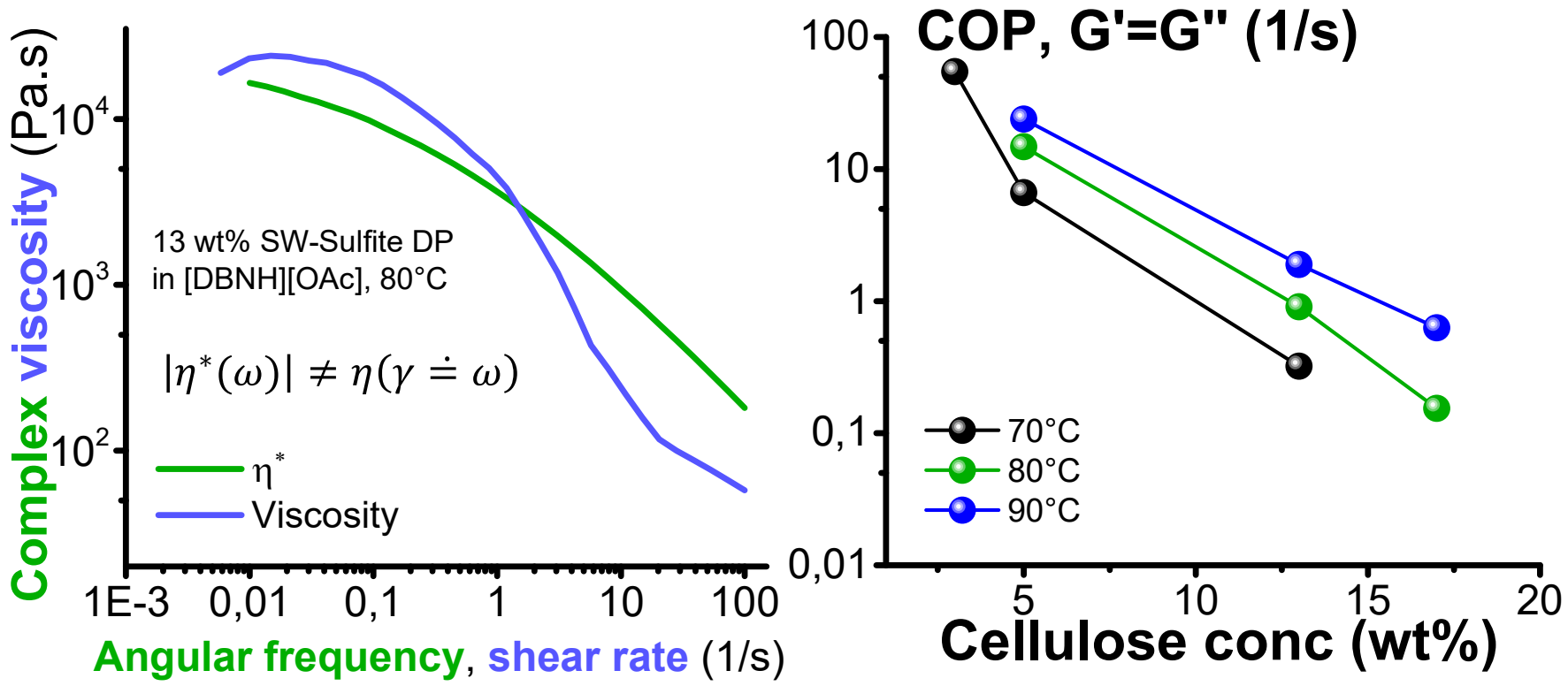

Effect of molar mass on rheology

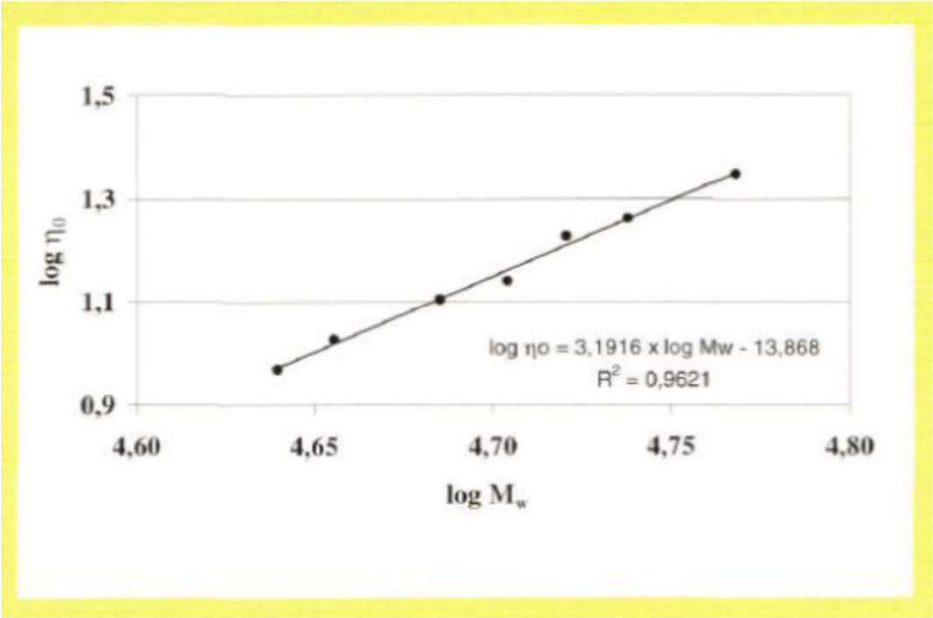

Zero-shear viscosity vs weight-average molecular weight of the cellulose

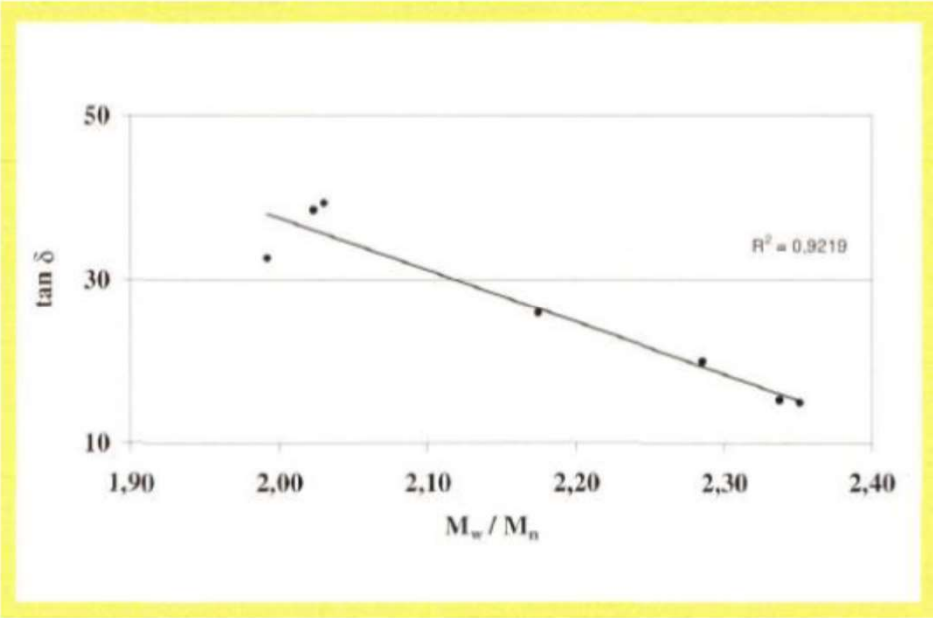

tanδ vs polydispersity index

Schausberger, A.; Möslinger, R. *Das Papier*, 12, 99, 715-721

Solution state

As Xanthate in aqueous NaOH: *diluted* solution: ~1% cellulose

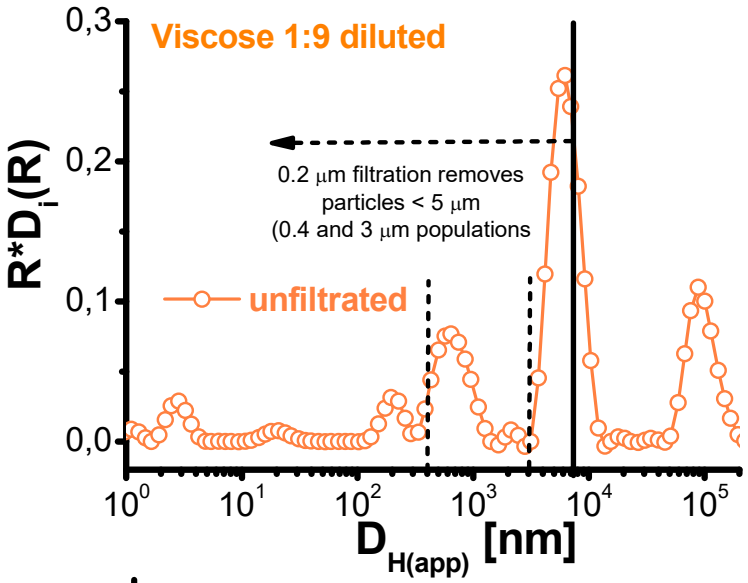

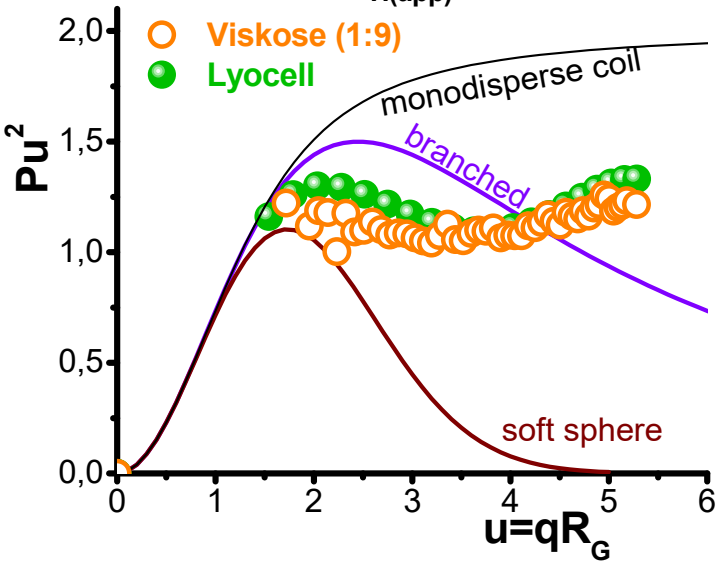

In a direct solvent in NMMO.H_2O: *concentrated* solution: 10wt% cellulose

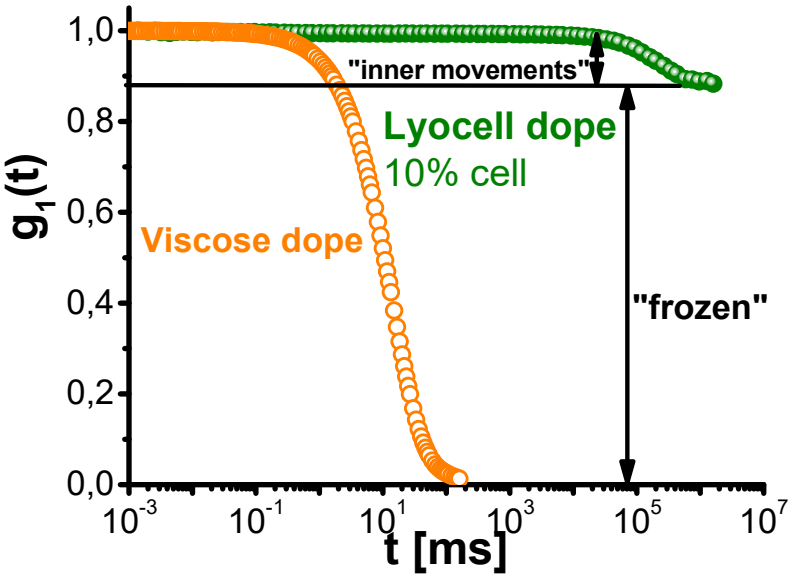

Viscose solution

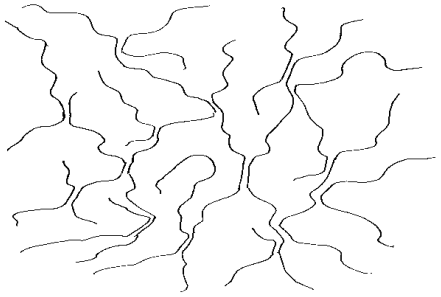

loose network with gel particles
not all OH-groups are available for the formation of H-bonds.

Lyocell solution

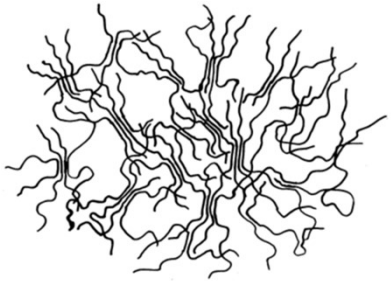

entanglement network with high swollen aggregates

Röder, T et al. *Lenz Ber*, 82, 118 (2003)

Coagulation, Regeneration

Regeneration

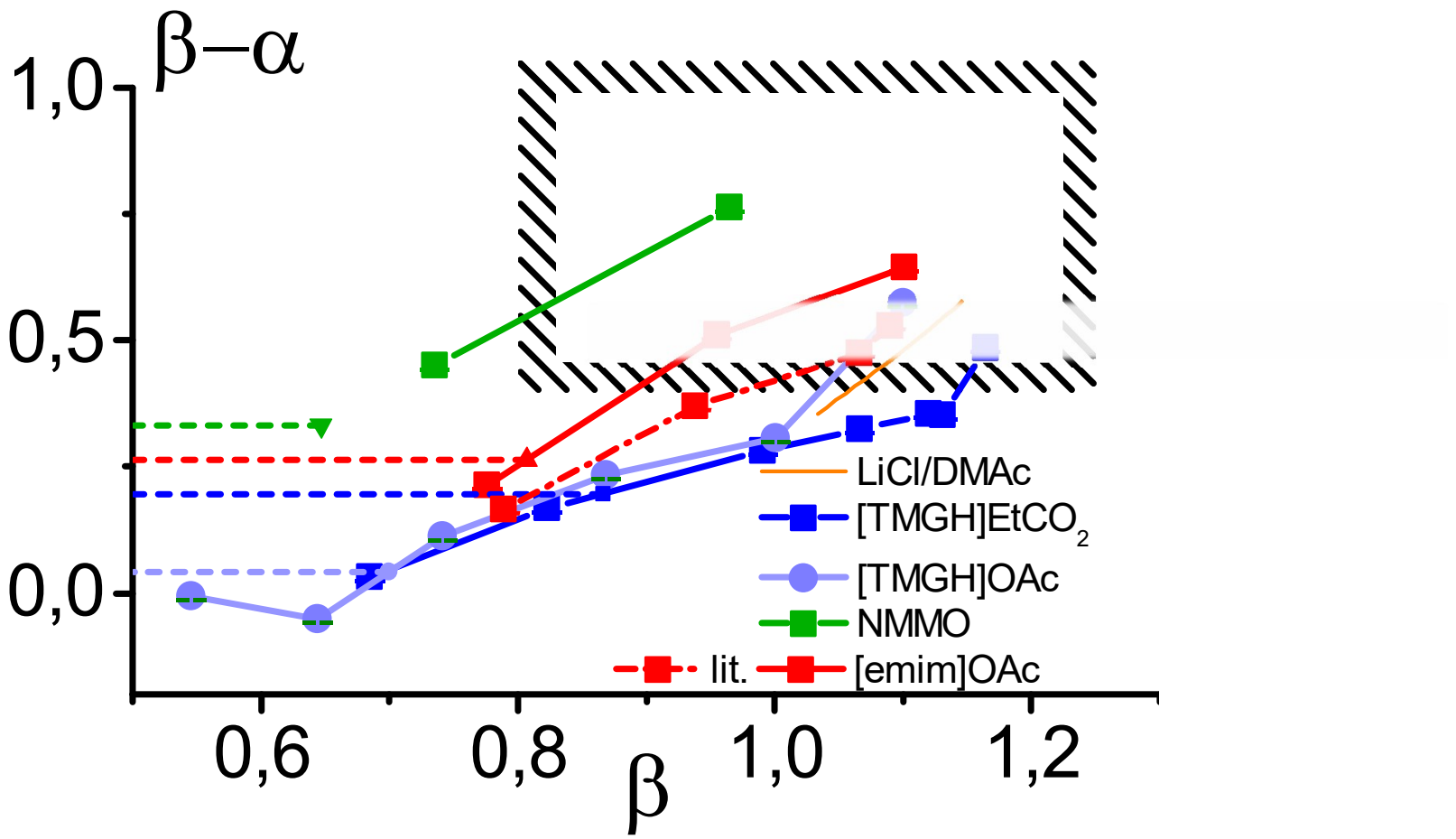

Dissolution vs Regeneration

- β decreases upon water addition.
- [emim][OAc] water-tolerant ~ 16 w/w%
- [TMGH]-ILs water-intolerant 1-4 w/w%
- $[TMGH]^+$ hydrotrope, bulky, hydrophobic

Order of water tolerance:

[TMGH][OAc] < $[TMGH][EtCO_2]$ << [emim]OAc

Hauru, L.K.J.; Hummel, M.; King, A.W.T.; Kilpeläinen, I.; Sixta, H. *Biomacromolecules* **2012**, 13, 2896-2905. DOI:10.1021/bm300912y.

Coagulation – Phase Changes

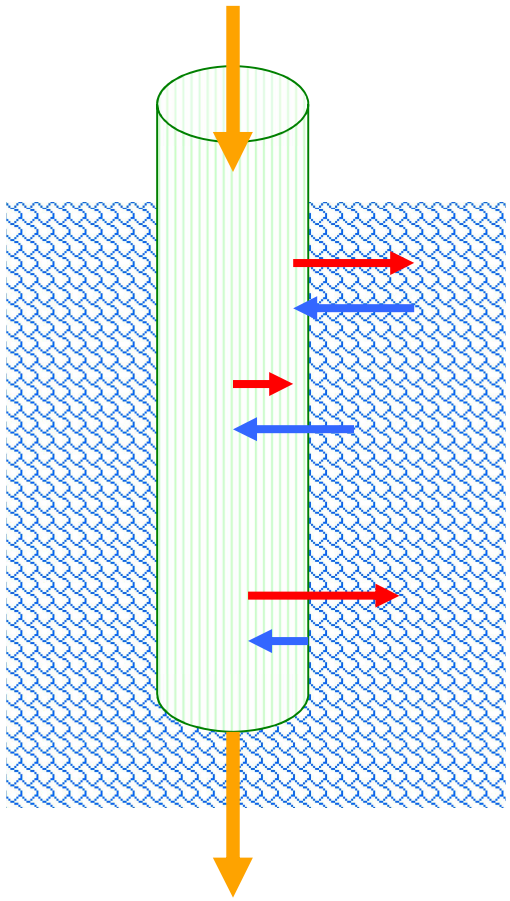

1. Quick exchange of water and NMMO at interface

2. Inside gel, NMMO diffusion impeded

3. Later, rapid desolvation, phase separation inside the biphasic region, where ***spinodal decomposition*** occurs:

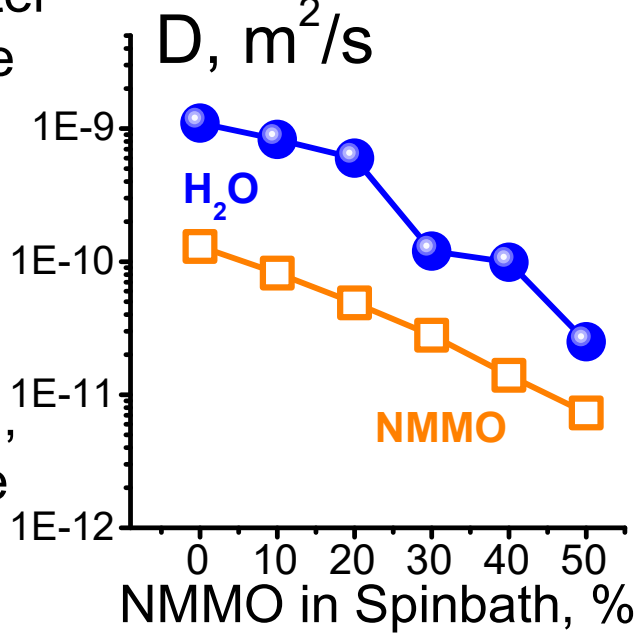

formation of mutually interconnected polymer chains and pores.

P.R. Laity et al. *Polymer* 43, 5827-5837 (2002)
O. Biganska, P. Navard. *Biomacromolecules*, 6, 1948-1953 (2005)

Diffusion of water into the filament

Diffusion front of inside a pellet water monitored via microscope

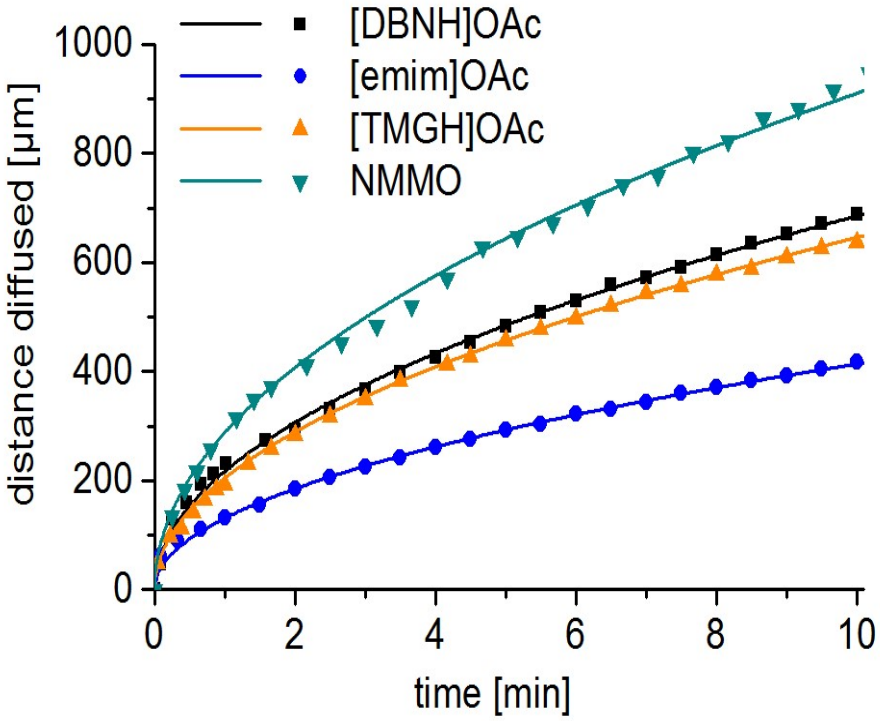

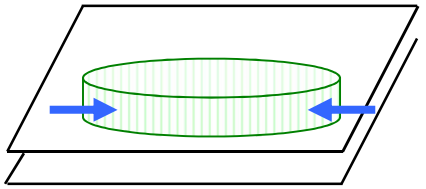

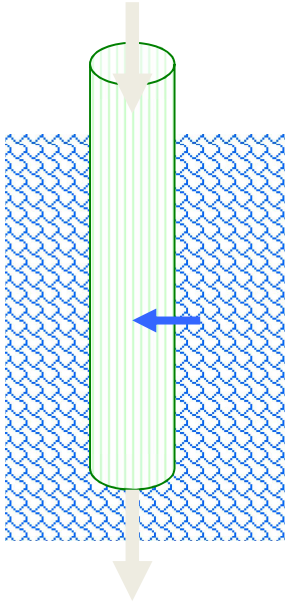

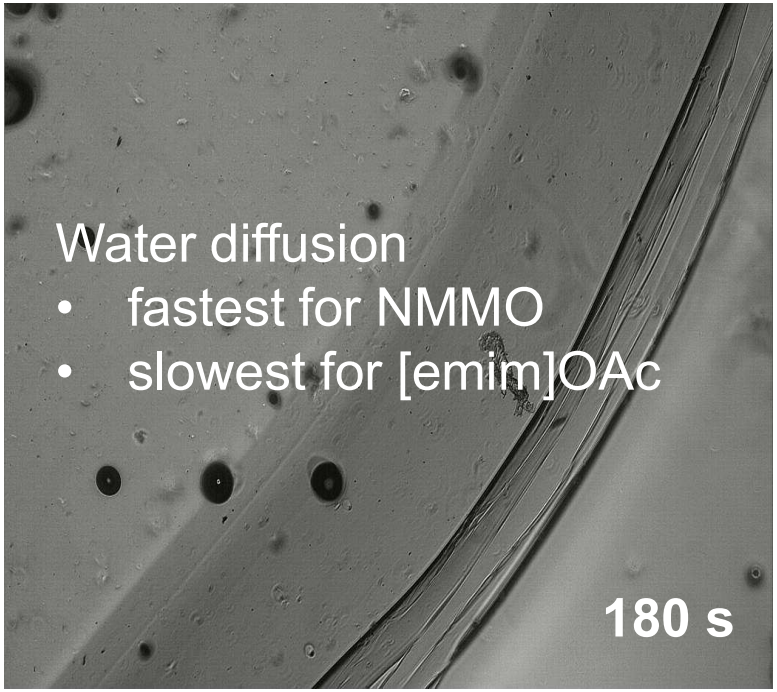

L. K. J. Hauru, M. Hummel, K. Nieminen, A. Michud and H. Sixta. ***Soft Matter***, **2016**, 12, 1487--1495

Regeneration time and depth

The incipient diameter of a filament, $d_x = 2\sqrt{\frac{{r_0}^2}{DR}}$

Diffusion equation for water, $\frac{M_t}{M_\infty} = \frac{4}{\sqrt{\pi}}\sqrt{\frac{D_w t}{{L_x}^2}}$ is solved for the time where the diffusion front has reached the filament radius, or d = 1 = r, and ${r_x}^2 = {r_0}^2/DR$, to yield the regeneration time, $\boldsymbol{t_{reg}}$:

$$1 = \frac{4}{\sqrt{\pi}}\sqrt{\frac{D_w t}{{r_x}^2}} \qquad \Rightarrow \boldsymbol{t_{reg} = \frac{{r_0}^2 \pi}{16 D_w}\frac{1}{DR}}$$

Regeneration depth, $\Delta X_{reg} = v_x t_{reg}$ with $DR = v_x/v_0$

$$\boldsymbol{\Delta X_{reg} = \frac{v_0 \cdot \pi \cdot {r_0}^2}{16 \cdot D_w}}$$

$v_0 = extrusion\ velocity$
$v_x = take-up\ veölocity$
$r_0 = spinneret\ diameter, 100\ \mu m$
$D_w = 1.55 \cdot 10^{-10}\ m^2/s$

Lauri Hauru, et al. *Soft Matter,* 2016, 12, 1487--1495

Regeneration time and depth

D_w 2,70E-10 m^2/s

$$t_{reg} = \frac{{r_0}^2 \pi}{16 D_w} \frac{1}{DR}$$

$$\Delta X_{reg} = \frac{v_0 \cdot \pi \cdot {r_0}^2}{16 \cdot D_w}$$

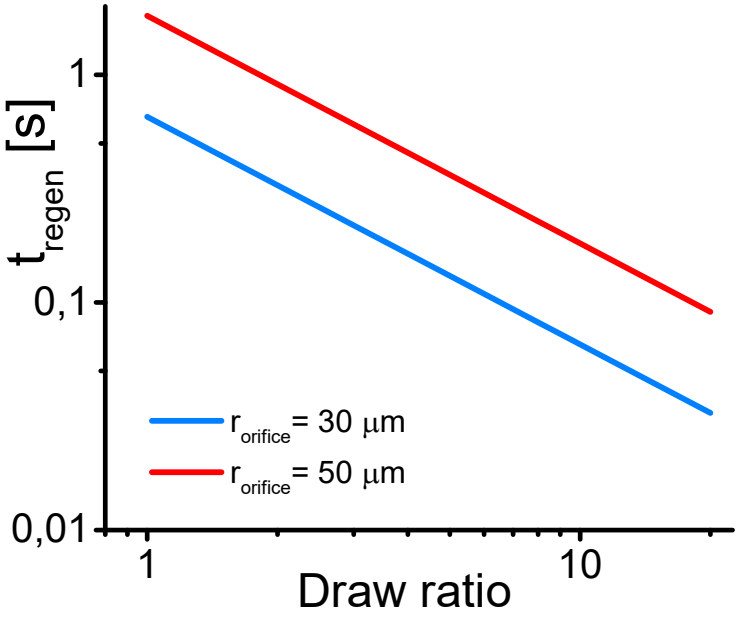

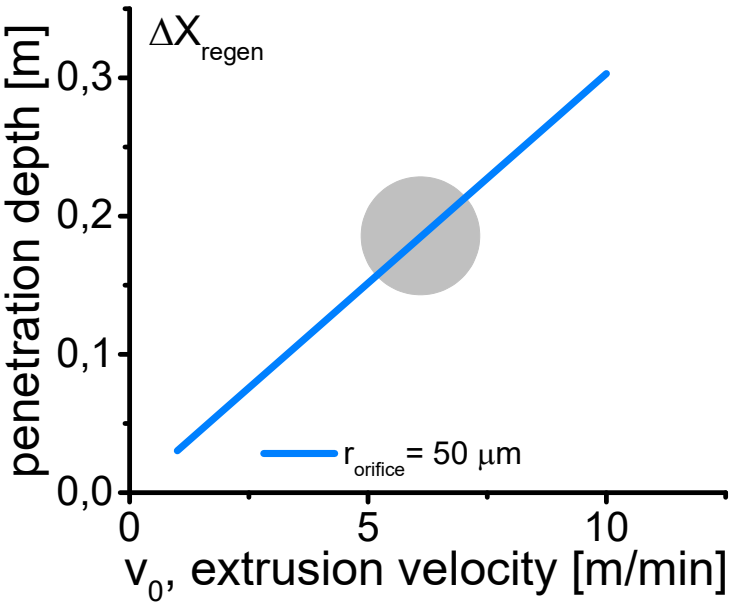

Lauri Hauru, et al. *Soft Matter,* 2016, 12, 1487--1495

Structure formation during regeneration

Solvent Effect on Spinnability

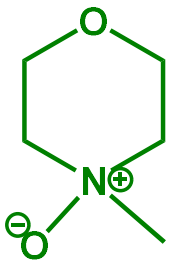

H_2O

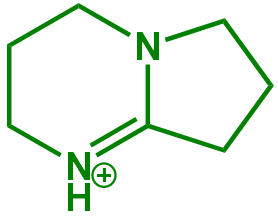

OAc^-

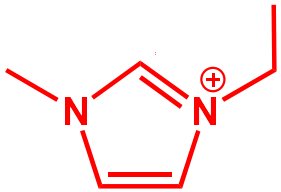

OAc^-

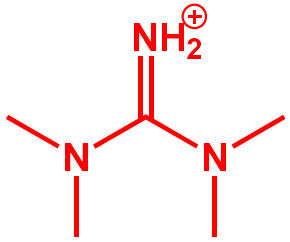

OAc^-

$NMMO.H_2O$
N-methylmorpholine-N-oxide

[DBNH][OAc]
1,5-diazabicyclo[4.3.0] nonenium acetate

[emim][OAc]
1-ethyl-3-methyl imidazolium acetate

[TMGH][OAc]
N,N,N,N-tetramethyl guanidinium acetate

Pulp: Eucalyptus Prehydrolysis Kraft: Mw = 269 kg mol^{-1}, Mn= 79 kg mol^{-1}

Polymer concentration 13 wt%

$NMMO.H_2O$ stabilized by propyl gallate and spun with a 18 x 100 mm spinneret; 1 cm air-gap, 100 μm spinneret, 15° C air bath temperature, 0.04 mL min^{-1} extrusion velocity.

L. K. J. Hauru, M. Hummel, K. Nieminen, A. Michud and H. Sixta. ***Soft Matter,*** **2016**, 12, 1487--1495

Spinning result

Spinning solvent	d_0	T_{extr}	T_{bath}	DR_{max}	Titer	Tenacity
	[μm]	[°C]	[°C]		[dtex]	[cN tex^{-1}]
[DBNH][OAc]	100	70	15	**7,5**	3.0±0.9	**38.5±8.4**
$NMMO.H_2O$	100	95	15	**6,2**	3.7±0.7	**31.2±6.6**
[TMGH][OAc]	100	80	15	**2,0**	15.5±0.9	**10.9±1.1**
[emim][OAc]	250	90	45	**2,9**	44.4±1.7	**13,9±1.6**

$NMMO.H_2O$ and **[DBNH][OAc]** give spinnable dopes, while the dopes made from **[TMGH][OAc]** and **[emim][OAc]** were not spinnable.

Solvent diffusion constants vs water content

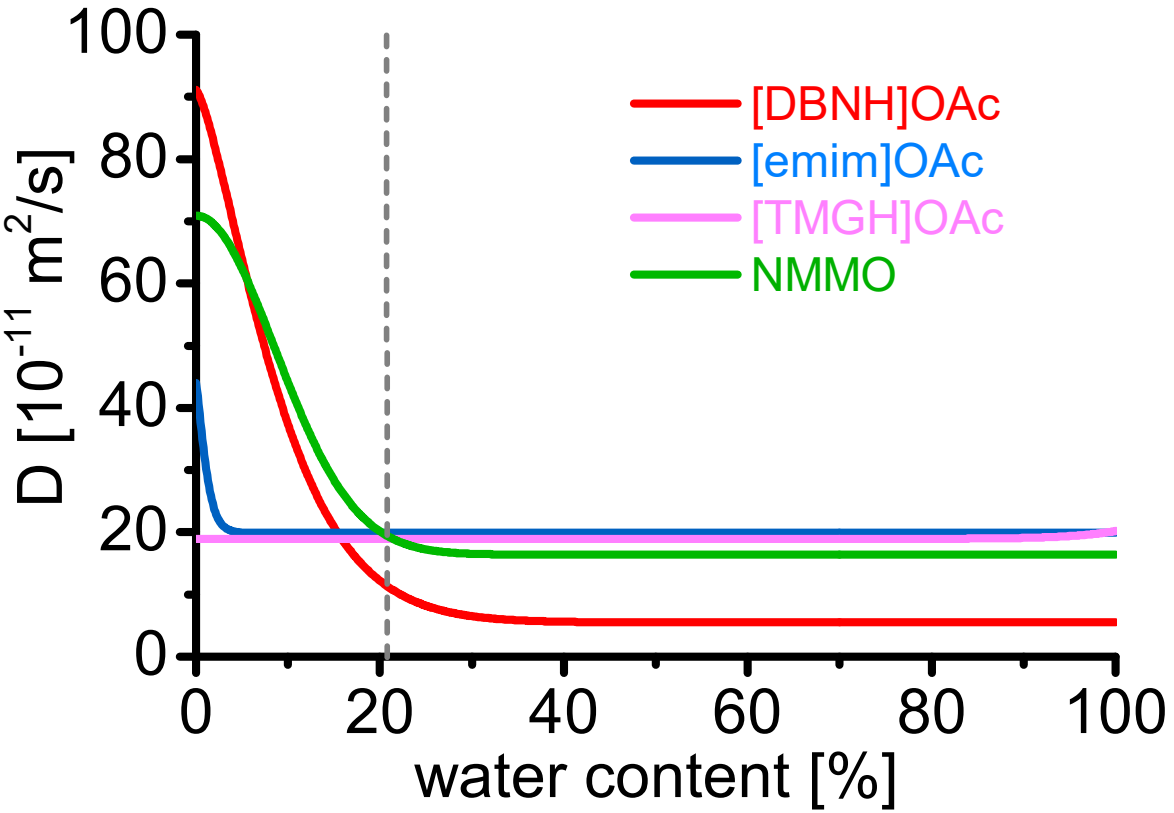

Poorly orientable network indicative for poorly spinnable dopes as prepared from [TMGH][OAc] and [emim][OAc].

Gelatinous regenerated polymer network forms → main resistance to further diffusion

L. K. J. Hauru, M. Hummel, K. Nieminen, A. Michud and H. Sixta. ***Soft Matter,* 2016**, 12, 1487--1495

Incipient [emim][OAc] filament

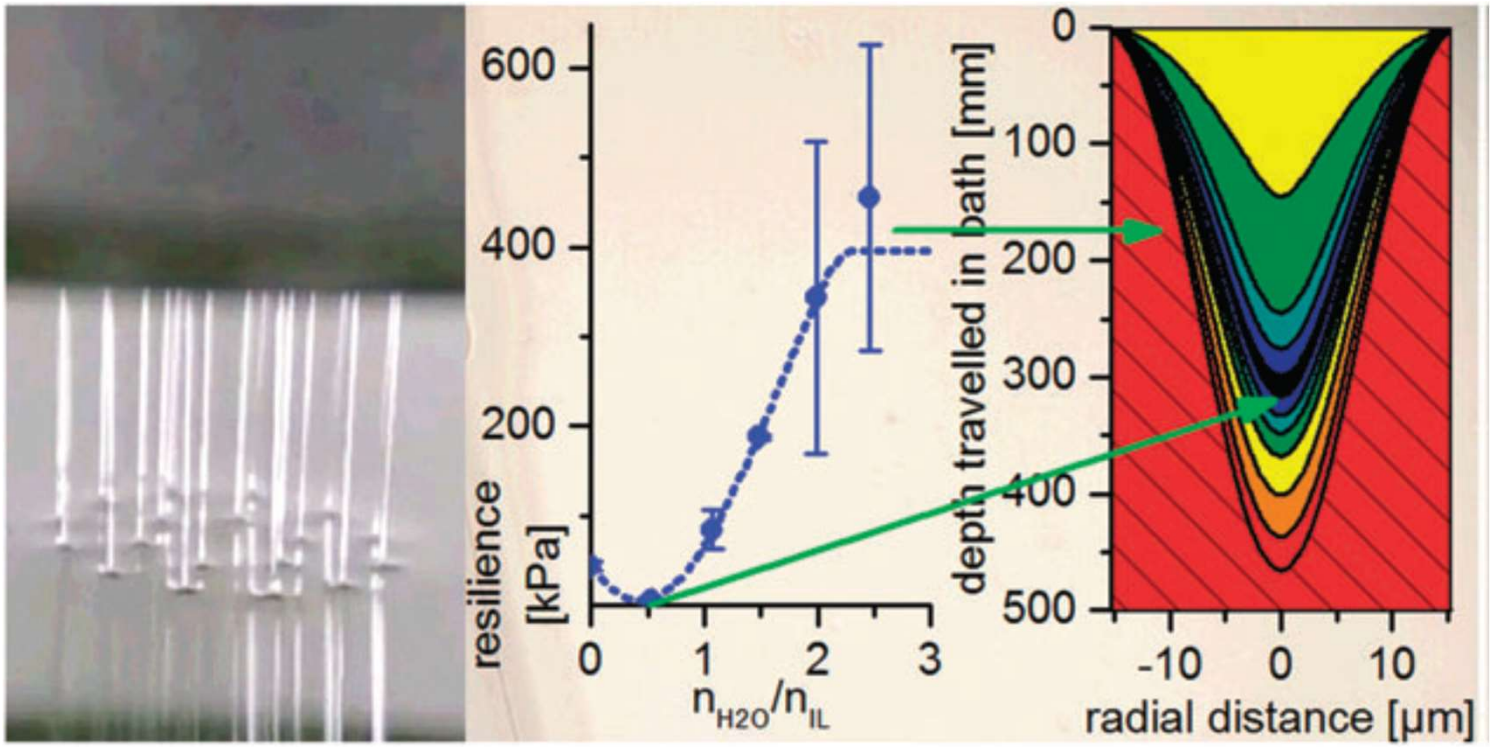

Telescopic-type breach because of very low resilience in the core during the onset of regeneration.

Both, yield strain and stress decrease at 0.5 n_{H2O}/n_{IL} obviously due to a low water diffusion.

L. K. J. Hauru, M. Hummel, K. Nieminen, A. Michud and H. Sixta. ***Soft Matter*, 2016**, 12, 1487--1495

Final fiber orientation vs. DR

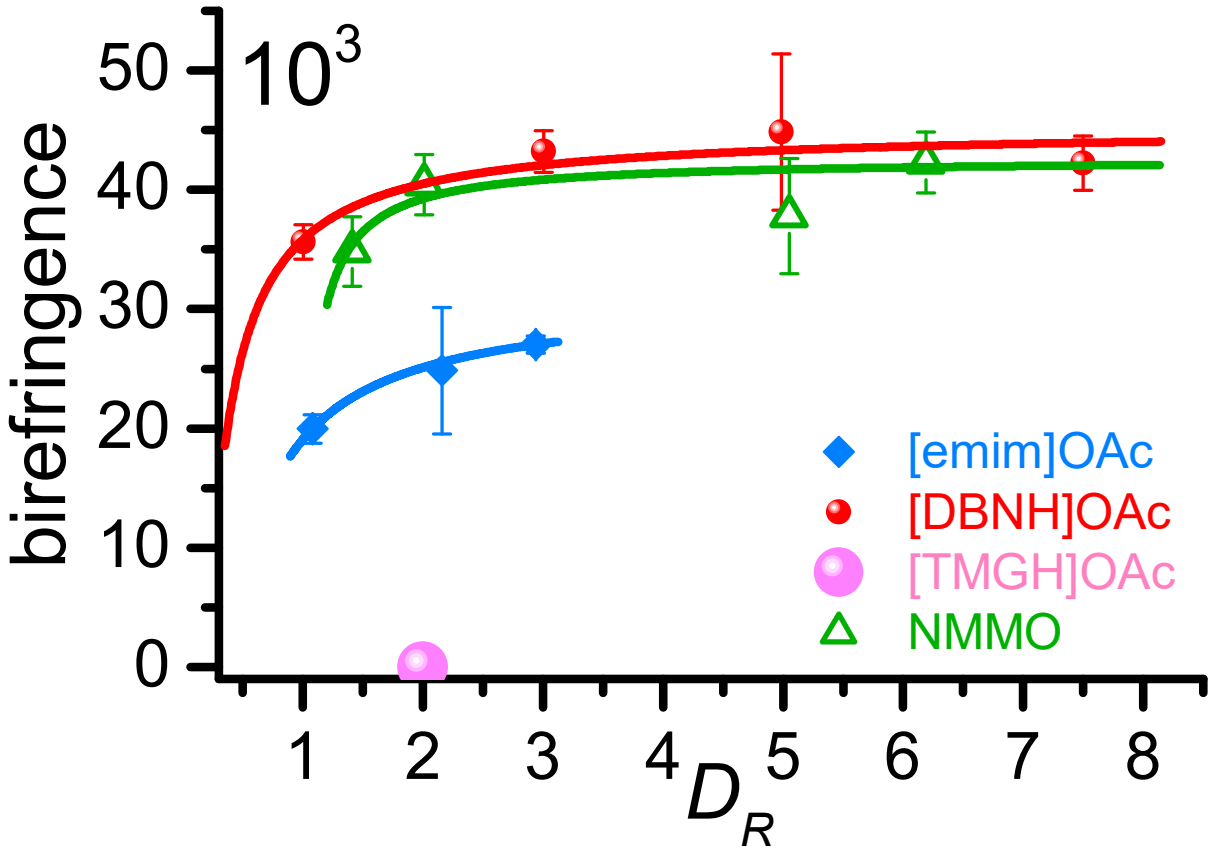

[emim][OAc] fibers: orientation develops poorly due to low resilience in the core.

[TMGH][OAc] fibers: solidified gel->solution behaves as a permanent network.

L. K. J. Hauru, M. Hummel, K. Nieminen, A. Michud and H. Sixta. ***Soft Matter,*** **2016**, 12, 1487--1495

Degradation of Cellulose

Fringed Fibrillar Model

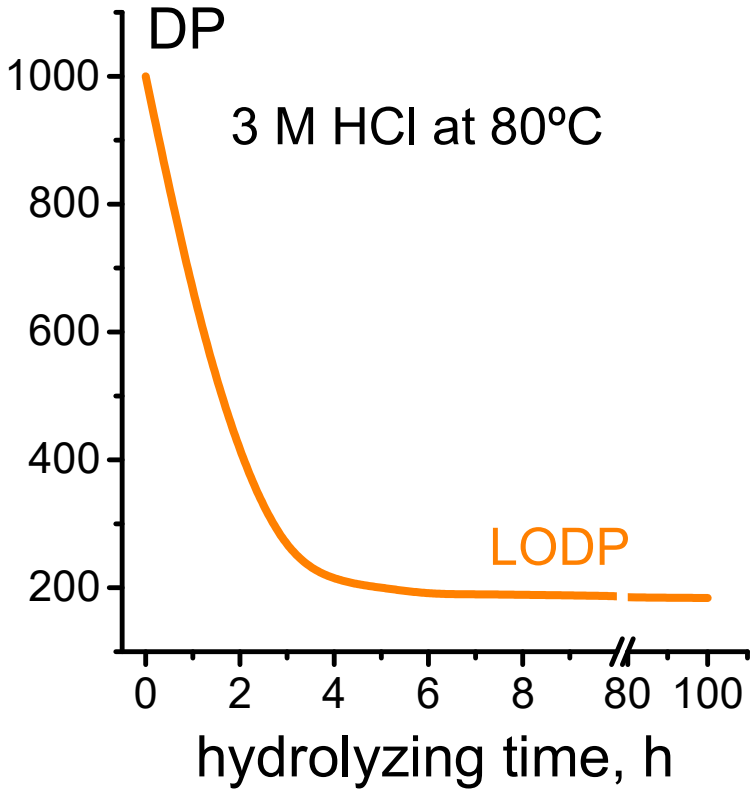

What is known?

- Level-off degree of polymerization (LODP) upon acid hydrolysis,
- cellulose depolymerizes rapidly down to a certain level after which the degradation is minimal.
- **Proposition:** amorphous domains are hydrolyzed leaving the crystalline domains intact.
- **Crystallite length by SAXS agrees with the level-off degree of polymerization (LODP).**

Nishiyama et al. *Biomacromolecules* **2003**, *4*, 1013
Battista *Ind. Eng. Chem.* **1950**, *42*, 502.

Acid-catalysed Degradation

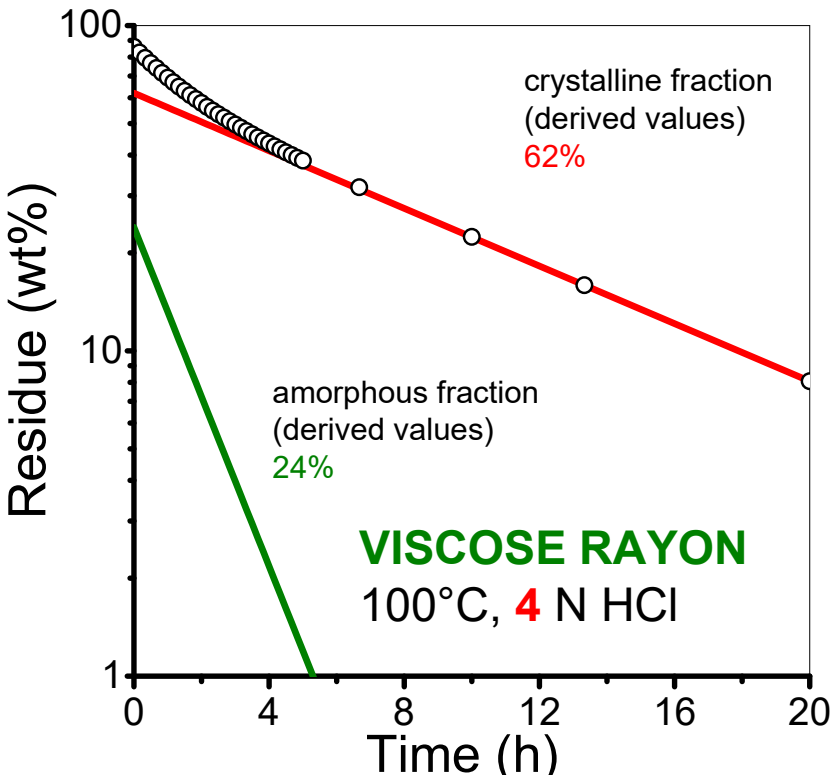

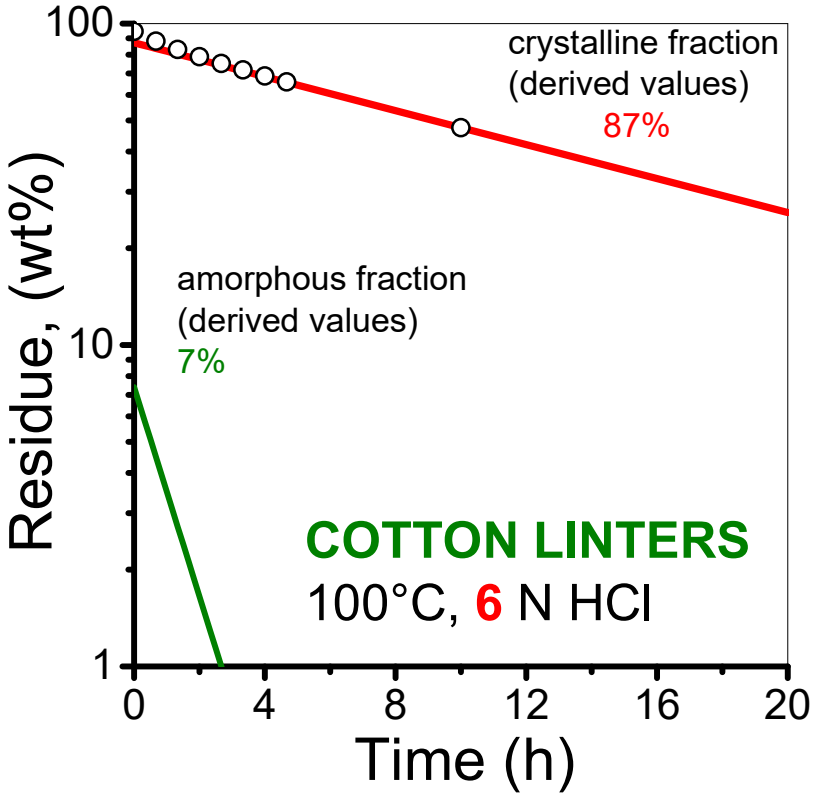

Gives an indication of the weight loss kinetics of the crystalline and amorphous fractions.

Amorphous fraction calculated from the **experimental curve** and the **linearly extrapolated crystalline fraction**.

M. Nelson. *J. Polymer Science*, Vol XLIII, 351-371, 1960

Leveling-off DP (LODP) vs Substrate

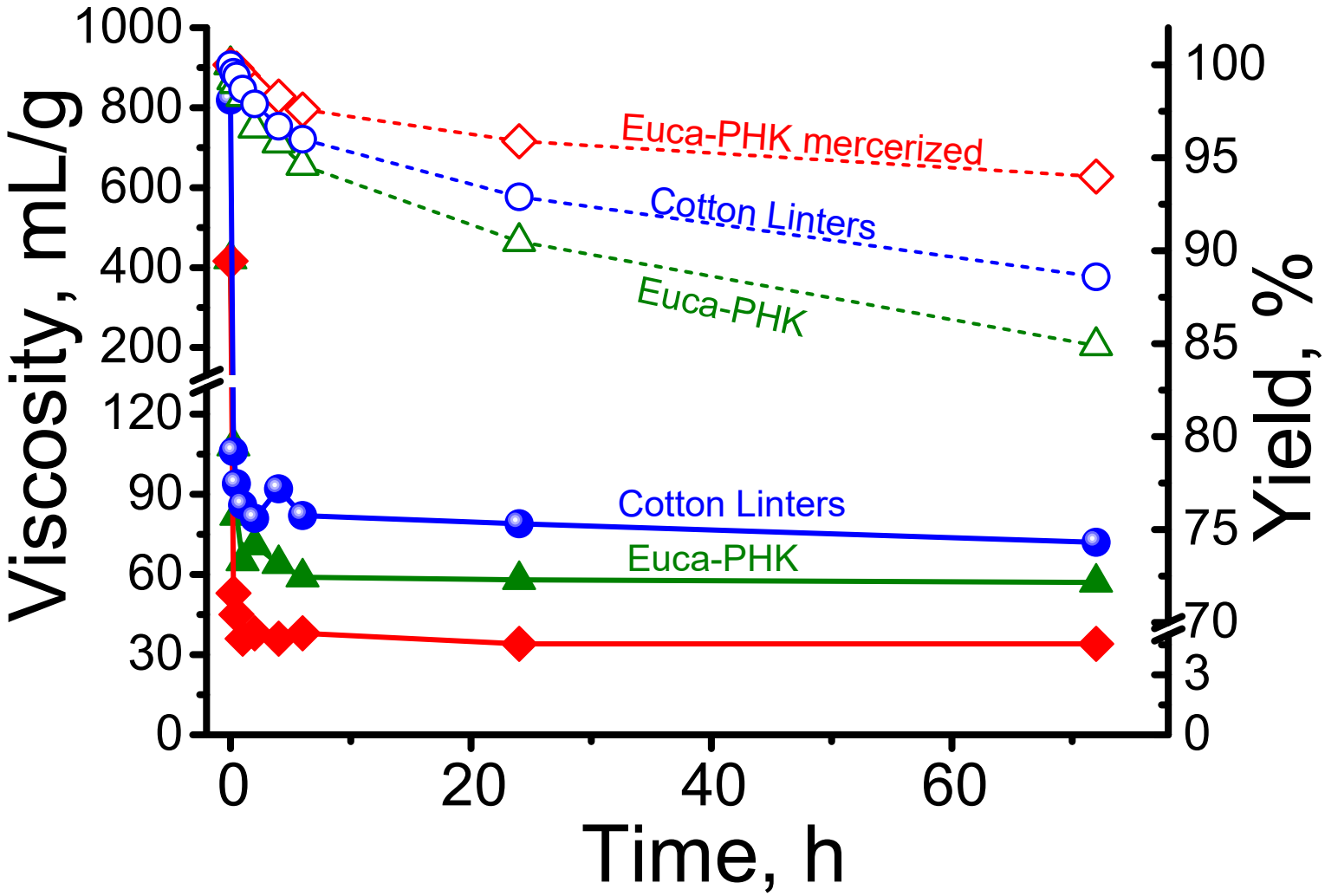

Laine, R.; Tolonen, L.: Aalto, 2012 Sixta, H, 1999

Acid hydrolysis of crystalline cellulose

According to **Sharples**, crystallites are attacked from its ends: **end-attack model**

For Cellulose II, $\frac{1}{k} \propto DP_w$

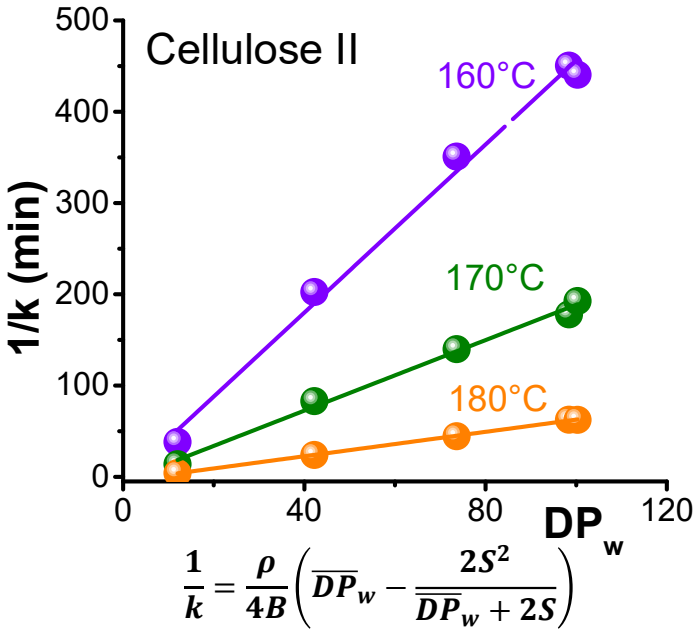

For **Cellulose I** the DP_w is **not the only factor** affecting the hydrolysis rate:

The presence of two different H-bonding patterns in Cellulose I might be the reason for this behavior:

They do not hydrolyse at the same rate

Lin, Ch-H., A.H. Conner, Ch.G. Hill, Jr, *J. Appl. Polym Sci.*, 417 (**1991**).
Lin, Ch-H., A.H. Conner, Ch.G. Hill, Jr., *J. Appl Polym Sci.*, 45(10), 1811-1822 (**1992**).

A. Sharples, *Trans. Faraday Soc.*, **53**, 100313 (1957); **54**, 913-17 (1958).

Alkaline degradation of cellulose

Parameter Values at 160° C

h^{-1}	k_p	k_s	k_h	REG_0 µmol/g	$SREG_0$ µmol/g
CL	554	11	2.0 E-4	4.6 ± 1.1	4.7 ± 1.2
OX	2901	36	1.5 E-4	13.6 ± 2.6	0.1 ± 2.9

The REG values determined experimentally

CL untreated

OX treated with oxalic acid – no stabilization

REG reducing end groups,

SREG stabilized reducing end groups

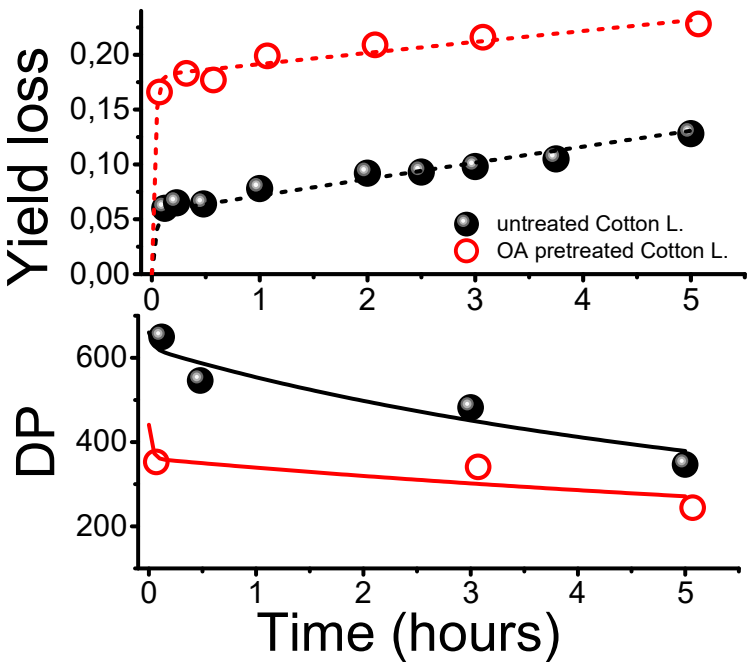

Yield-Loss Model

$$\begin{cases} \frac{dR}{dt} = -k_S R + k_H(\Gamma_0 - P - H) \\ \frac{dP}{dt} = k_P R \\ \frac{dH}{dt} = k_H(\Gamma - P - H) \end{cases}$$

Depolymerization Model

$$DP = \frac{DP_0 - P - H}{1 + H}$$

$$DP_0 = \frac{1}{\xi_0 + \eta_0}$$

k_S - stopping

k_P - peeling

k_H – alkaline hydrolysis

Γ_0 – Total initial material

R – amount of reducing endgroups

P – amount of peeled off material

H – amount of material removed by alkaline hydrolysis

ξ_0 initial REGs

η_0 initial SREGs

PhD theses of Kaarlo Nieminen (2016), Lidia Testova (2015)

Oxidative alkaline treatment

AC: 34% cell; 16% NaOH, air oxygen

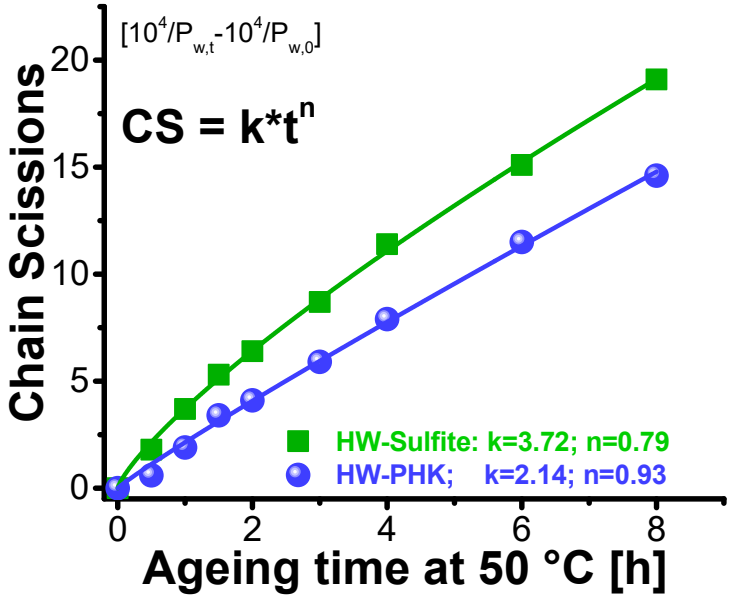

Acid hydrolysis

1.2 M [H⁺], 78° C

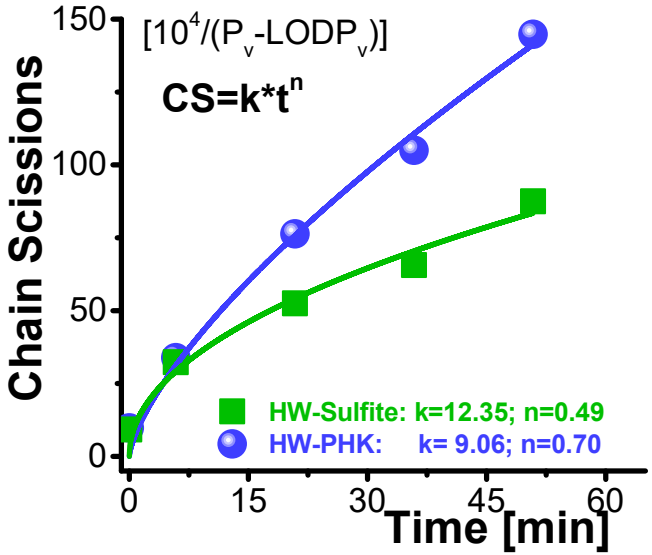

Electron Beam Irradiation

Accelerator: 10 MeV (bis 200 kW, 20 mA)

Pulp	x_C	Crystallite Width D_{102}	Crystallite Width D_{200}	$LODP_v$	WRV
	%	nm	nm		%
HW-Sulfite	54	5,5	4,5	265	73
HW-PHK	56	6,7	5,0	190	71
Cotton Linters	63	9,3	7,4	160	54

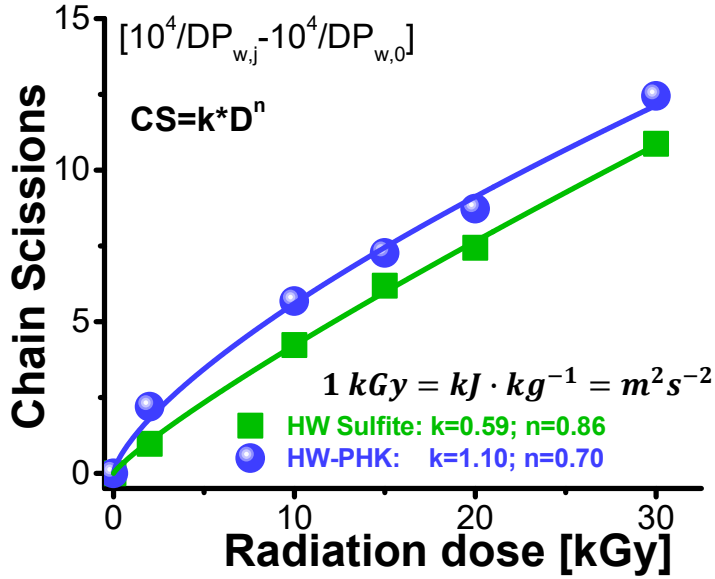

Sixta, H. and A. Borgards, Das Papier, 1999. **53**: p. 220-234.

Laundering of cotton textile – DP Loss

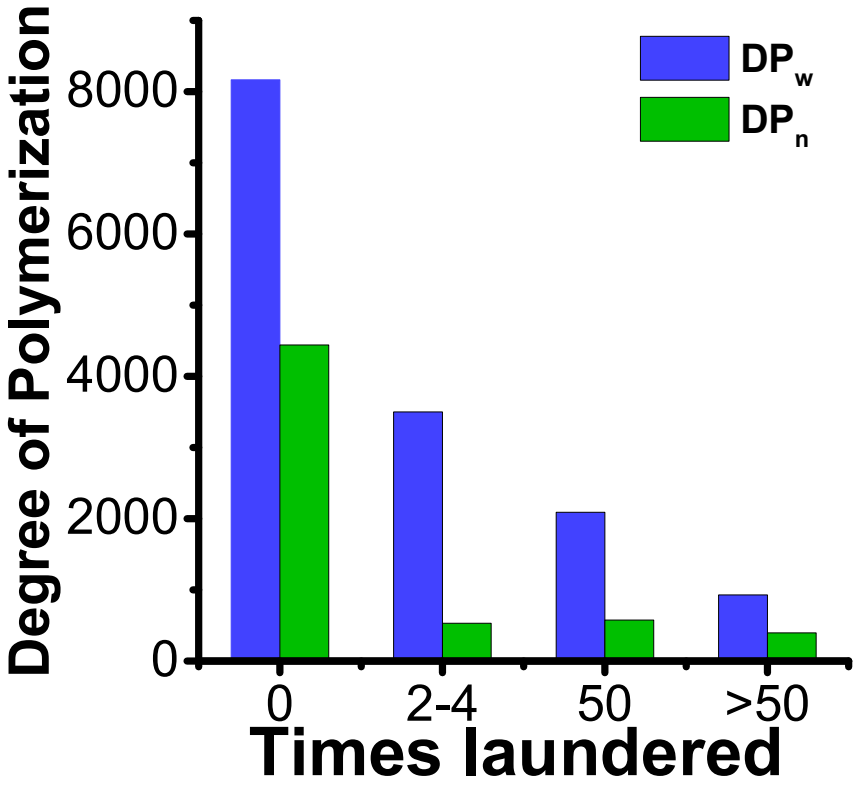

Industrial laundering of cotton sheets (Pakistan):

- Conditions:
  - Temperature (max) = 84°C, Washing agent Clax Hellux free 3EP, alkaline detergent, pH=12-12.5

Times laundered	Crystallinity	Microfibril width	Fibril aggre-gate width
	%	nm	nm
0	62,4	6.4±0.2	21.9±2
2-4	63,6	7.0±0.2	25.6±2
50	64,1	7.2±0.2	24.2±2
>50	63,7	7.2±0.2	24.1±2

Palme, A., et al.,. Cellulose 2014. **21:** p. 4681-4691.

Endoglucanase treatment

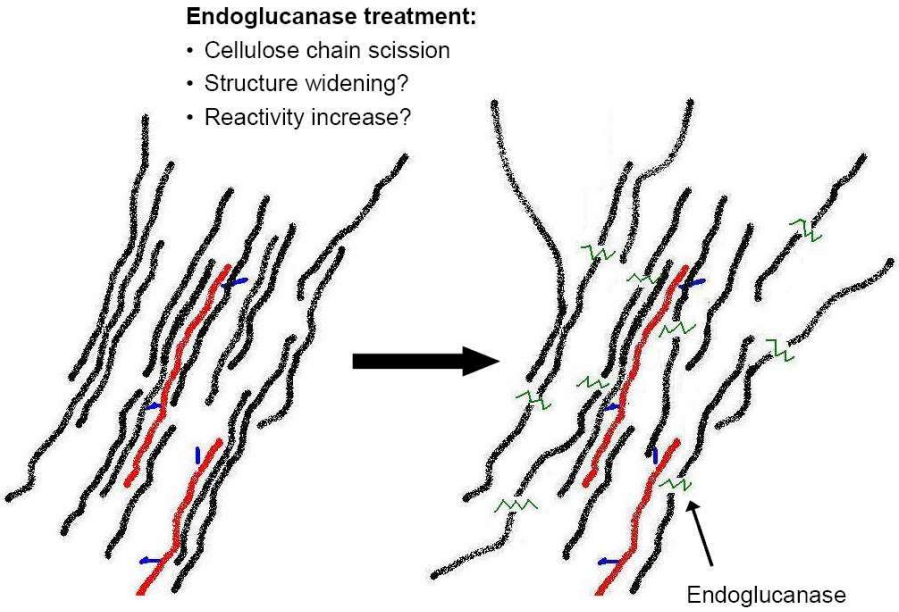

Monocomponent endoglucanase Novozym® 476 produced by submerged fermentation of a genetically modified ***Aspergillus oryzae*** microorganism.

- 3 % pulp consistency in a
- phosphate buffer pH 7 (11 mM NaH_2PO4, 9 mM Na_2HPO_4; deionised water)
- at 50 ° C for
- 60 min

Endoglucanase treatment

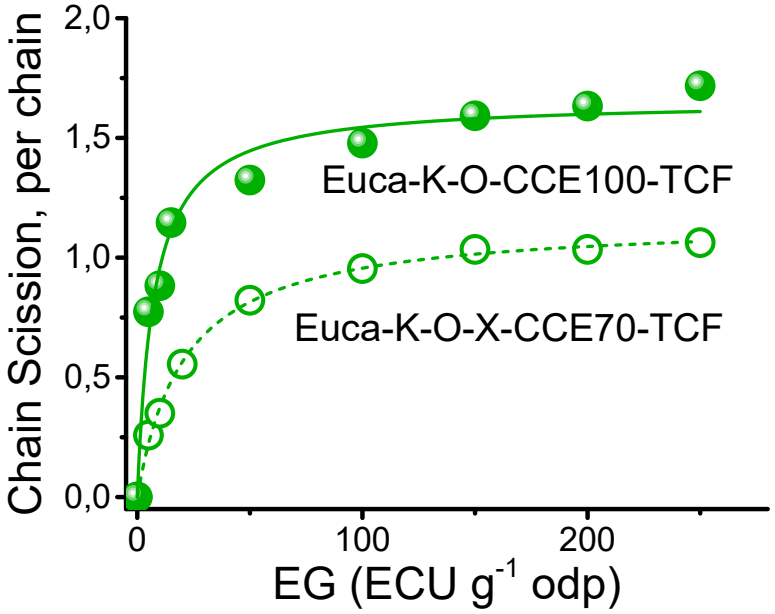

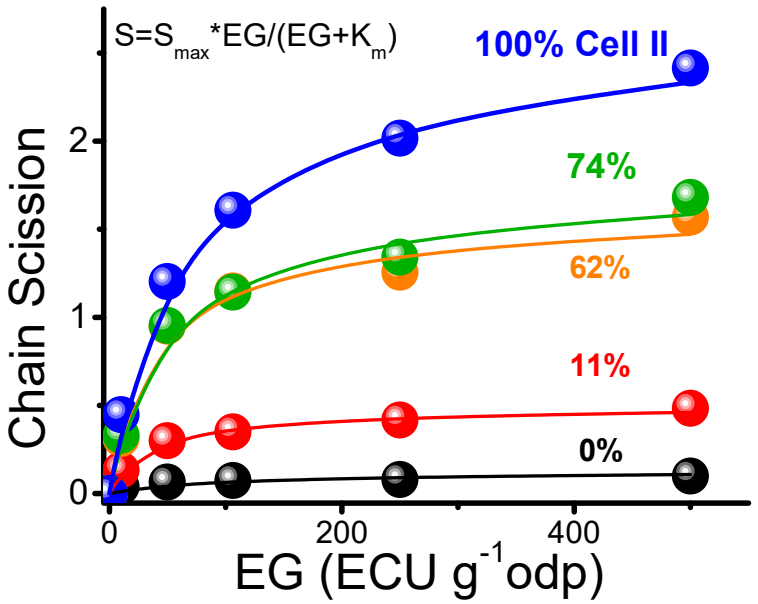

What affects depolymerization by EG treatment:

- Morphology, lignocellulose origin influence the accessibility of EG
- Cellulose II structure more accessible; increased unit cell dimensions, & WRV
- EG accessibility is facilitated in the absence of hemicellulose and
- In the absence of lignin.

Verena Gehmayr: PhD Thesis (2012), TUG

Mechanical Properties
E-Modulus

Elastic properties

Series model

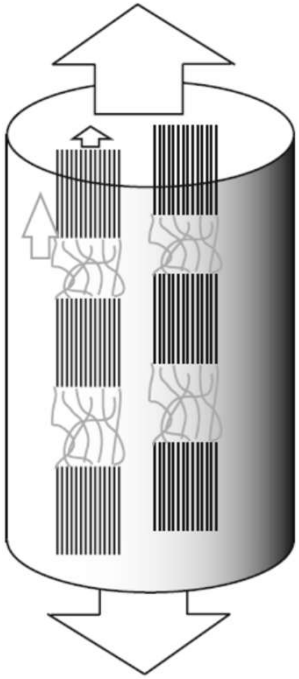

stress transmitted through crystalline regions

Microfibril model

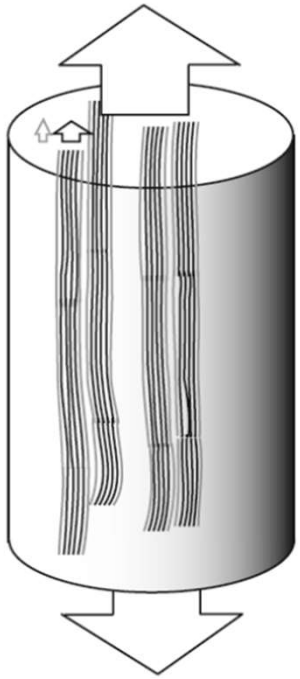

crystalline core and surface chains share the stress

E-Modulus:

- **Axial:** **115–140 GPa**
  220 GPa*
- **Perpendicular:** **14.8±0.8 GPa**
  (H-bonded plane)

Nishiyama, Y., J. Wood Sci., 2009. **55:** p. 241-249.

* Inelastic X-ray scattering technique: Macromolecules, 2008. **24:** p. 9755

Modulus and tensile properties of Ramie fibres as Cellulose I, II, III_I and IV_I

Allomorph	Crystallinity	Cryst width	Cryst length	E_f	σ_b	ε_b
	%	nm	nm	Gpa	Mpa	%
Cellulose I	64	4,8	18,7	27	755	3,2
Cellulose II	53	5,1	15,4	21	798	5,0
Cellulose III_I	38	5,1	15,0	15	693	5,8
Cellulose IV_I	57	3,8	16,1	13	345	5,0

E_f: Young's modulus of a single fibre

σ_b: strength

ε_b: Strain

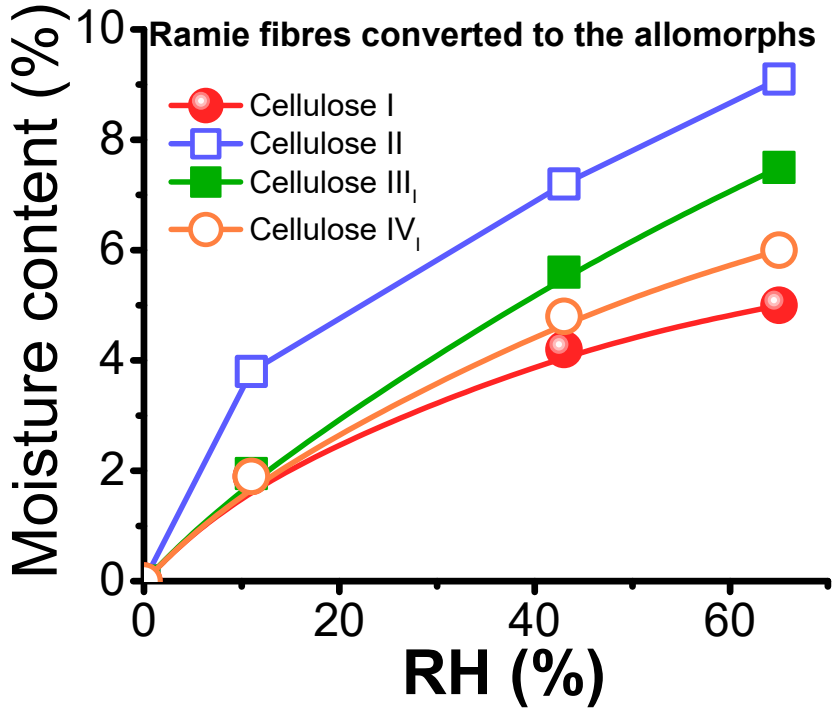

Ishikawa, A., T. Okano, and J. Sugiyama, Polymer, 1997. **38**: p. 463-468.

Lyocell vs Viscose

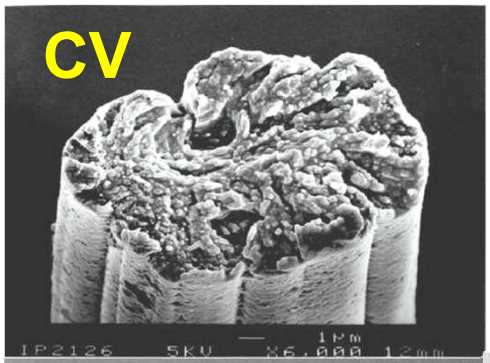

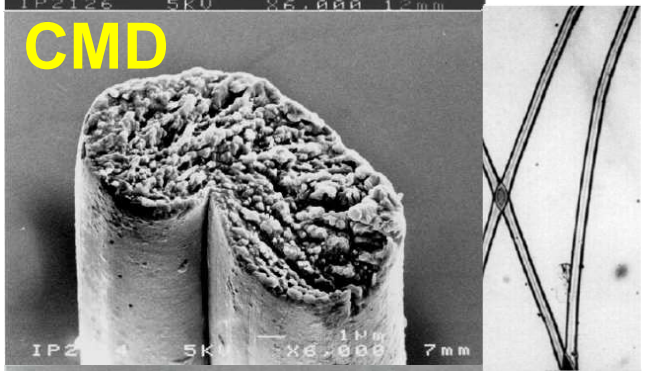

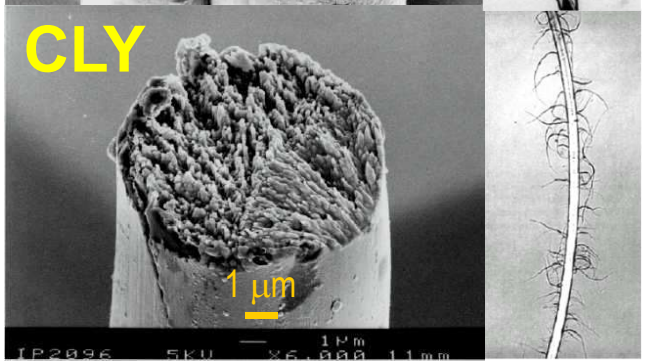

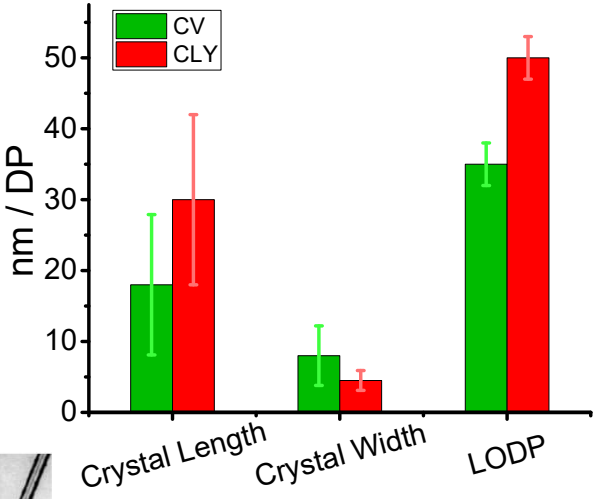

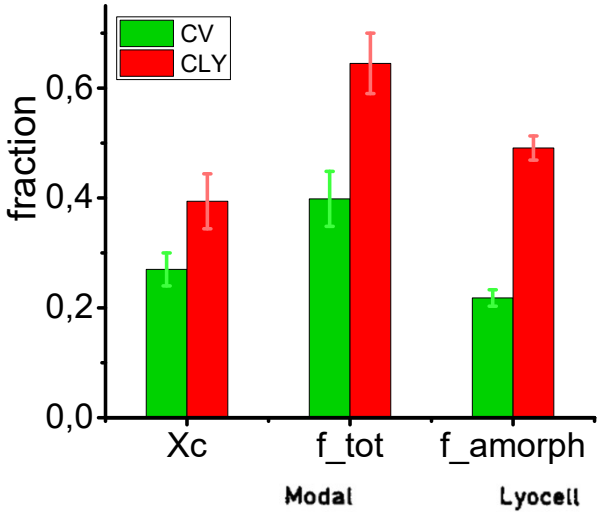

CLY vs CV

- Longer, thinner crystallites
- Less clustering of crystallites
- Anisotropic, elongated voids

Parameter		CLY	CV
Degree of fibrillation		4-6	1
Tenacity (cond)	[cN/tex]	40,2	24,0
Elongation (cond)	[%]	13,0	20,0
Tenacity (wet)	[cN/tex]	34,0	12,5
Elongation (wet)	[%]	18,4	22,0
Ten cond:wet	[-]	0,85	0,52
WRV	[%]	65	95

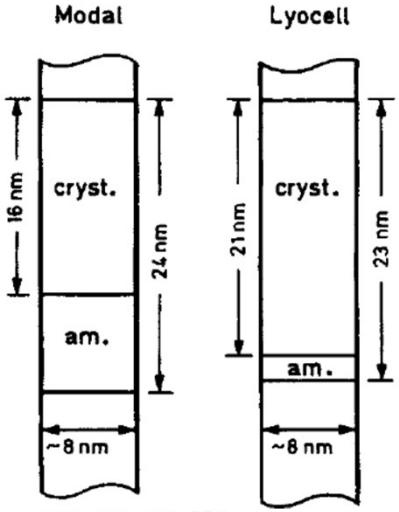

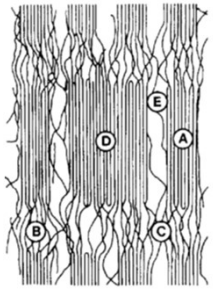

H.-P. Fink et al. *Prog Polym Sci* 26 (2001) 1473-1524
Schurz, J. *Lenz Ber.* 74 (1994), 37-40.
Gindl, W. *Polymer* (2008)
Mortimer, *Cell Chem Technol* (1996)

Mechanical vs. structural properties

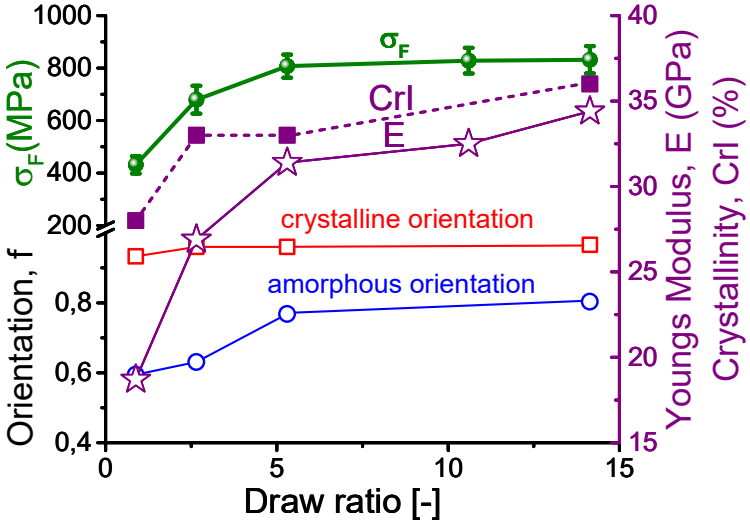

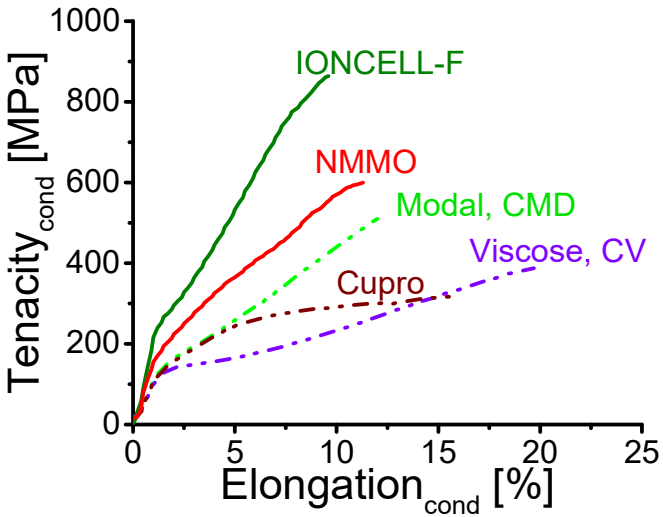

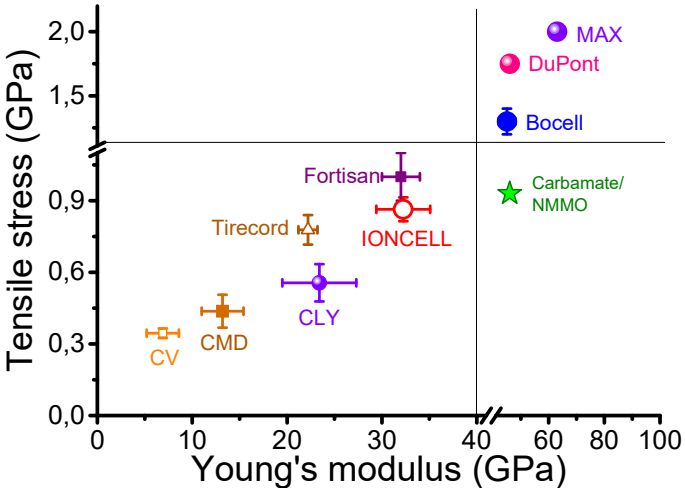

Spinning of **anisotropic solutions** to exploit the full strength potential of **cellulose II**:

E_{max}: ~ 60 GPa (IC-F: 35)

σ_{max}: ~ 2.1 GPa (IC-F: 0.9)

Northolt, M.G. Lenzinger Berichte, (**1985**), 59, 71-79.
De Vries. Appl. Sci. Res. A3, 111 (**1952**).
Sixta, H. et al. *NPPRJ*, 30(1), **2015**, 43-57

Single-Phase Structure

Continuous chain modulus: serial arrangement of crystallites (SAXS patterns do not show meridional reflexes) for well-oriented cellulose fibres

$$\frac{1}{E} = \frac{1}{e_c} + \frac{\langle sin^2\phi \rangle_E}{2g} \qquad \Delta n = \Delta n_{max}\left(1 + \frac{3g}{e_c}\right) - \frac{3g\Delta n_{max}}{E} \qquad \frac{slope}{intercept} = \frac{3g}{1 + \frac{3g}{e_c}}$$

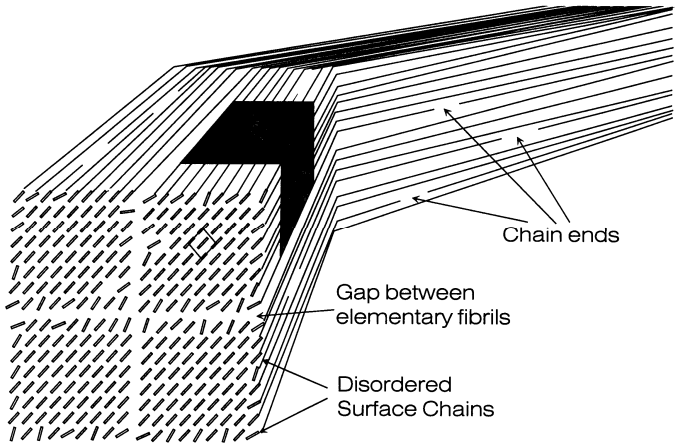

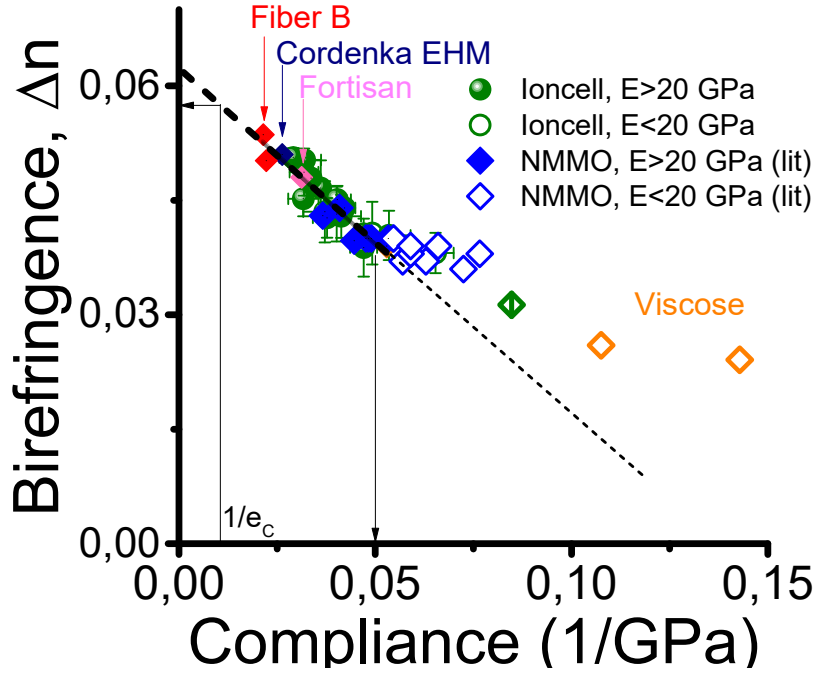

Northolt, M.G. Lenzinger Berichte, (**1985**), 59, 71-79. De Vries. Appl. Sci. Res. A3, 111 (**1952**). . Sixta, H. et al. *NPPRJ*, 30(1), **2015**, 43-57

Two-Phase Aggregate Model

Fringed-micellar model

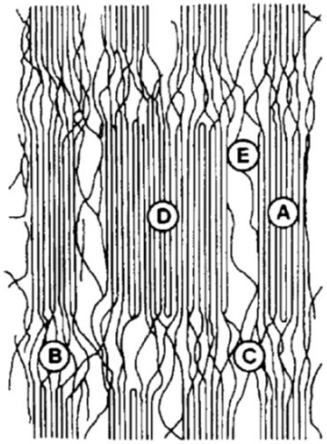

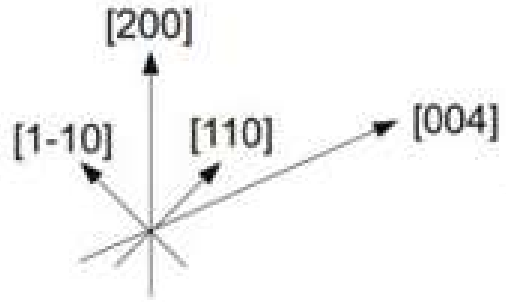

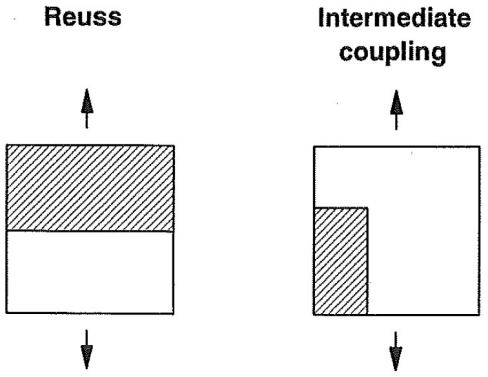

Transverse
Am and Cr in series

Longitudinal
Am and Cr in parallel

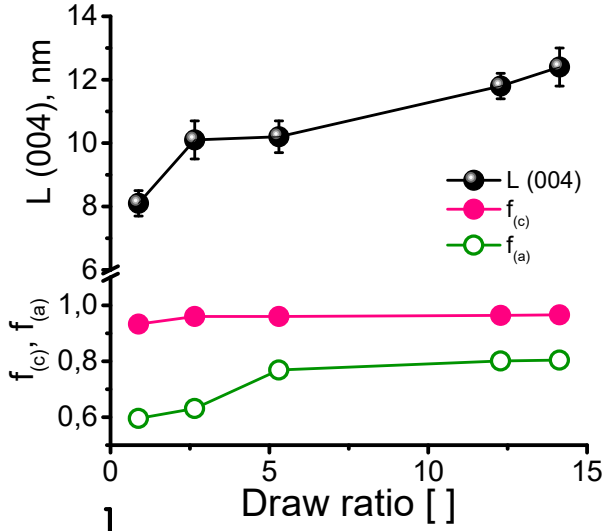

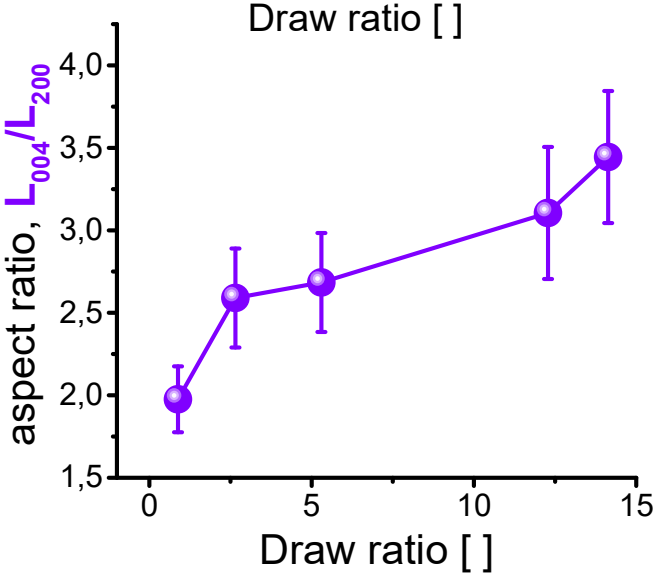

Fraatz, J. et al. ***Final BMFT report*, 1995**

Ganster, J. et al. ***Acta Polymer,* 1994**, 15, 312

Two-Phase Aggregate Model

Tsai-Halpin equation: interphase coupling, linking crystalline and amorphous phases.

E can be predicted using the crystalline aspect ratio, $L/D=L_{004}/L_{200}$

$$\overline{E} = \frac{\overline{E(R)}_a(1+\xi_{ac}\eta X_{CV})}{(1-\eta X_{CV})}$$

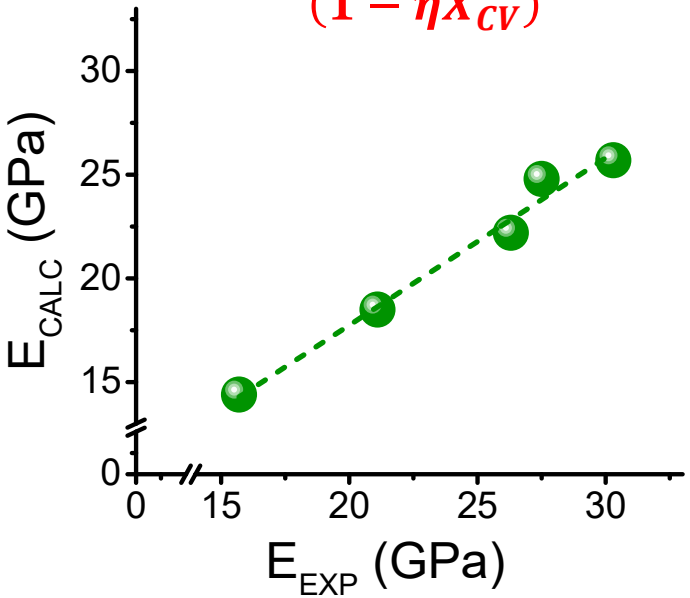

Fraatz, J. et al. ***Final BMFT report*, 1995**
Ganster, J. et al. ***Acta Polymer,* 1994**, 15, 312

π, degree of parallel mechanical coupling

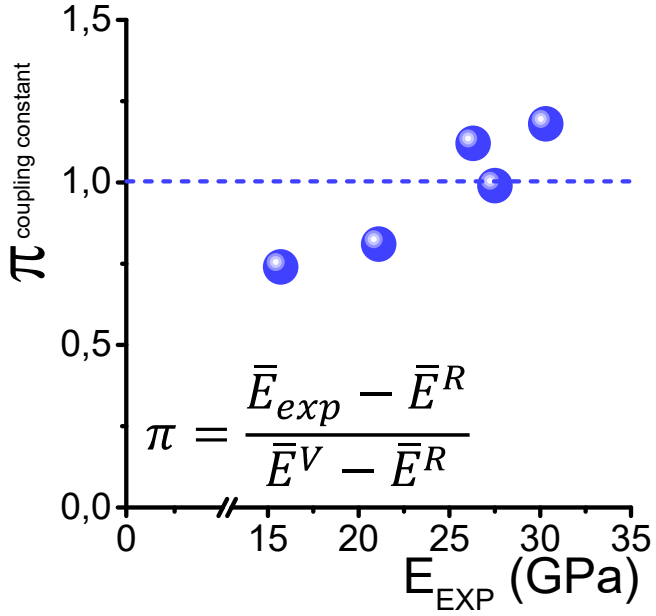

$$\pi = \frac{\bar{E}_{exp} - \bar{E}^R}{\bar{E}^V - \bar{E}^R}$$